RALOXIFENE SENSITIZES GLIOBLASTOMA CELLS TO HYPOXIA -INDUCED DEATH THROUGH INHIBITION OF STRESS GRANULE DISSOLUTION

by

Aaron Robichaud

Submitted in partial fulfillment of the requirements
for the degree of Master of Science

at

Dalhousie University
Halifax, Nova Scotia
October 2019

TABLE OF CONTENTS

LIST OF TABLES

LIST OF FIGURES

ABSTRACT

Glioblastoma multiforme (GBM) is the most common primary malignant brain tumour and carries a uniformly poor prognosis. Despite aggressive therapy, median survival is only 14 months. Death typically results from treatment failure and local recurrence. Hypoxia is a feature of the GBM microenvironment, and previous work has shown that cells residing in hypoxic regions resist treatment. Hypoxia can trigger formation of stress granules (SGs), sites of mRNA triage that promote multiple cell survival mechanisms. We hypothesize that SGs play a role in hypoxia-induced resistance to therapy. A screen of 1120 FDA-approved drugs (the Prestwick Drug Library) was conducted, and 98 candidates were identified that inhibited hypoxia-induced SG formation whereas 127 candidates inhibited SG dissolution following return to normoxia. The screen identified the selective estrogen receptor modulator raloxifene as a potent inhibitor of SG dissolution in a dose-dependent manner. When raloxifene was administered to U251 astrocytoma cells prior to hypoxia, the combination achieved synergistic killing of tumour cells that correlated with the activation of apoptosis and autophagy pathways. Taken together, this data suggests that raloxifene induces apoptotic and autophagic death in GBM cells by disrupting normal SG dynamics. As raloxifene is a currently approved drug already used in the treatment of estrogen receptor-positive breast cancer and osteoporosis, promising pre-clinical data could inform the development of a phase III clinical trial in GBM patients.

LIST OF ABBREVIATIONS

3-MA	3-methyladenine
4EBP1	eIF4E binding protein 1
ABC	ATP-binding cassette
ADCD	autophagy-dependent cell death
AKT	protein kinase B
ATCC	American Type Culture Collection
ATF4	activating transcription factor 4
ATG	autophagy-related genes
ATP	adenosine triphosphate
BART	binder of arl two
BBB	blood-brain barrier
BCL2	B-cell lymphoma 2
BSA	bovine serum albumin
BSC	biological safety cabinet
CReP	constitutive reverter of eIF2α phosphorylation
CRISPR	clustered regularly interspaced short palindromic repeats
CT	computed tomography
DMEM	Dulbecco's modified eagle medium
DMSO	dimethyl sulfoxide
DNA	deoxyribonucleic acid
DRiPs	defective ribosomal products
DYRK3	dual specificity tyrosine-phosphorylation-regulated kinase 3
EGFR	epidermal growth factor receptor
ER	endoplasmic reticulum
ERα/β	estrogen receptor α or β
ERK	extracellular signal-related kinase
eIF2α	eukaryotic translation initiation factor 2α
eIF4E	eukaryotic translation initiation factor 4E
FACS	fluorescence-activated cell sorting
FBS	fetal bovine serum

FMRP	fragile X mental retardation protein
FOXM1	forkhead box M1
G3BP	ras-GTPase-activating protein SH3-domain-binding protein
GADD34	growth arrest and DNA damage-inducible protein
GBM	glioblastoma multiforme
GCN2	general control nonderepressible 2
Glut3	neuronal glucose transporter type 3
GSC	glioma stem-like cell
GTP	guanosine triphosphate
HIF	hypoxia inducible factor
HRI	heme-regulated initiation factor 2α kinase
HRP	horseradish peroxidase
HSP	heat-shock protein
HuR	human RNA binding protein
IDH	isocitrate dehydrogenase
IF	immunofluorescence
KLC	kinesin light chain
LC3	microtubule-associated proteins 1A/1B light chain 3B
MAPK	mitogen-activated protein kinase
MGMT	O^6-methlyguanine-DNA-methyltransferase
MOMP	mitochondrial outer membrane permeabilization
MRI	magnetic resonance imaging
mRNA	messenger ribonucleic acid
mRNP	messenger ribonucleoprotein
mTOR	mammalian target of rapamycin
NF-κB	nuclear factor-κB
OR	operating room
OS	overall survival
PABP	poly-A binding protein
PARP	poly (ADP-ribose) polymerase
PB	processing body

PBS	phosphate buffered saline
PDGF(R)	platelet derived growth factor (receptor)
PERK	PKR-like endoplasmic reticulum kinase
PFA	paraformaldehyde
PFS	progression free survival
PI	propidium iodide
PI3K	phosphatidylinositol-3-kinase
PKC	protein kinase C
PKR	protein kinase R
pO_2	partial pressure of oxygen
PRC1	Polycomb repressive complex 1
PSQ	penicillin-streptomycin-glutamine
PTEN	phosphatase and tensin homolog
PTPMT1	protein tyrosine phosphatase localized to the mitochondrion 1
PVDF	polyvinylidene fluoride
RACK1	receptor of activated protein C kinase 1
RNA	ribonucleic acid
ROS	reactive oxygen species
SD	standard deviation
SDS	sodium dodecyl sulfate
SEM	standard error of the mean
SERM	selective estrogen receptor modulator
SG	stress granule
siRNA	short interfering RNA
SQSTM1	sequestosome 1, AKA p62
TCGA	The Cancer Genome Atlas
TIA-1	T cell internal antigen-1
TIAR	TIA-1 related protein
TKI	tyrosine kinase inhibitor
TP53	tumour protein 53
$tRNA_i^{Met}$	initiation transfer RNA containing methionine

TTF	tumour treating fields
UBC	University of British Columbia
USP10	ubiquitin-specific protease 10
VCP	valosin-containing protein
VEGF(R)	vascular endothelial growth factor (receptor)
WHO	World Health Organization
ZFAND1	zinc finger AN1-type containing 1
zVAD	benzoyl-Val-Ala-Asp-fluoromethyl ketone

ACKNOWLEDGEMENTS

I would like to thank Dr. Adrienne Weeks for her help in the completion of the research presented in this work, and for her availability and guidance during the writing and defense of my thesis. Additionally, Dr. Jennifer Corcoran and the members of her lab provided much assistance in experimental planning and troubleshooting during my initial time in the lab. My supervisory committee (Dr. Craig McCormick, Dr. Sultan Darvesh, Dr. Sean Christie) was also helpful in guiding my course during the research component of my Master's degree.

The Department of Surgery and the Division of Neurosurgery at Dalhousie University were instrumental in both funding me during my Master's, as well as protecting my time for research by lightening my clinical requirements during this time. I also received support from the Clinician Investigator Program, and specifically the program directory Dr. Jason Berman, at Dalhousie University. Additional personal funding was provided by Killam Scholars and the Beatrice Hunter Cancer Research Institute through the Cancer Research Training Program, and the laboratory is funded in part through the Brain Repair Center.

Finally, I would like to thank my wife, Dr. Sarah Sampson, for her patience as I delayed my clinical training to complete this research.

The results shown here are in part based upon data generated by the TCGA Research Network: https://www.cancer.gov/tcga.

CHAPTER 1: INTRODUCTION

Glioblastoma multiforme (GBM) is the most aggressive form of brain tumour, and unfortunately, diagnosis with this tumour is tantamount to a death sentence. Vast amounts of research have been done, attempting to identify novel targets for chemotherapy to help improve survival in patients receiving this diagnosis, but progress has been modest. Due to the inherent stress experienced by tumour cells as a result of their hostile microenvironment, combined with aggressive chemotherapy and radiation mechanisms, targeting the integrated stress response may sensitize these tumours to current treatments. Stress granules (SGs) develop in response to a number of different stressors encountered by GBM cells, and act as sites of messenger ribonucleic acid (mRNA) triage, allowing the cell to focus translational machinery on pro-survival transcripts during acute stress, and protecting housekeeping mRNAs within SGs for rapid release and re-initiation of translation once stress is resolved. This thesis presents the results of a drug screen identifying approved drugs interfering with SG formation and dissolution, and further research on raloxifene, an inhibitor of SG dissolution, which increases cell death in hypoxia consistent to that experienced within the tumour microenvironment. Stress granules may present a novel target for GBM chemotherapy to sensitize the tumour to chemotherapy and radiation and improve survival in patients receiving this discouraging diagnosis.

1.1 Glioblastoma Multiforme

Glioblastoma multiforme is the most common tumour to arise from brain parenchyma (Ostrom *et al.*, 2015). It is considered a grade IV glial tumour (or glioma) according to the World Health Organization (WHO) classification (International Agency for Research on Cancer, 2016), and is characterized by its rapid growth and highly invasive nature. GBM can be further differentiated based on its origin; primary GBM arises *de novo* in the brain, while secondary GBM arises from lower grade glial tumours, most commonly from tumours arising from astrocytes (astrocytoma, a subtype of glioma), the most prevalent glial cell in the brain. Grade I astrocytoma, referred to as pilocytic astrocytoma, is characterized by increased cellularity compared to normal brain, and is more benign than higher-grade counterparts. Grades II and III astrocytoma (diffuse and anaplastic, respectively) exhibit cytological atypia followed by increased

mitotic activity. Microvascular proliferation and intra-tumoural necrosis are the defining histological features of GBM. Together, grades II to IV are considered malignant astrocytoma. Regardless of origin, tumours consist of a large population of neoplastic cells maintained by a subpopulation of glioma stem-like cells (GSCs) that are capable of producing complete tumours independently (Singh *et al.*, 2004), and can be identified by a number of specific markers differentiating them from non-stem cells (Ludwig and Kornblum, 2017). Macroscopically, GBM is made up of a central necrotic core surrounded by a capsule of actively proliferating cells that take up contrast on CT or MRI (Rong *et al.*, 2006) as a result of destruction of the blood-brain barrier (BBB). Necrosis occurs as a result of tumour outgrowing its vascular supply, and active angiogenesis can be seen in this region (Holash *et al*., 1999; Zagzag *et al.*, 2000).

Classically, the WHO classified astrocytic tumours on the basis of histopathological findings, defining GBM as an astrocytic tumour with evidence of necrosis and microvascular proliferation on pathological assessment (International Agency for Research on Cancer, 2007). In the most recent classification (International Agency for Research on Cancer, 2016), GBM remains a grade IV tumour, but more emphasis is placed on tumour genetics. Primary and secondary GBM can often be differentiated based on the genetic mutations they carry (Ohgaki *et al.*, 2004). While a complete review of genetic mutations identified in GBM is beyond the scope of this work, Reifenberger and colleagues provide a comprehensive summary highlighting the clinical utility of currently identified GBM genetic alterations (Reifenberger *et al.*, 2017). Perhaps most useful is the presence of prognostic genetic markers that help clinicians predict survival of GBM. Methylation of the O^6-methylguanine-DNA-methyltransferase (MGMT) promoter turns off transcription of this DNA repair enzyme, sensitizing tumour cells to chemotherapeutic-induced death (Hegi *et al.*, 2005). Mutations in isocitrate dehydrogenase (IDH) are found in lower grade astrocytoma (WHO grade II and III) as well as secondary GBM, and are also associated with a better prognosis than IDH wildtype GBM (Hartmann *et al.*, 2010). The status of the IDH gene has been added to the definition of astrocytoma in the most recent WHO classification (International Agency for Research on Cancer, 2016), and helps to differentiate between GBM versus lower-grade astrocytoma and between primary (IDH-wildtype) versus secondary (IDH-

mutant) GBM. Finally, mutations in the epidermal growth factor receptor (EGFR), although not necessarily prognostic (Siegal, 2016), are found in tumours that are more proliferative with lower rates of apoptosis (Nagane *et al.*, 1996), and may be more resistant to radiation (Barker *et al.*, 2001).

The prognosis for patients diagnosed with GBM has been consistently dismal. Harvey Cushing, considered by many as a forefather of neurosurgery, noted that surgical removal extended patient survival from 3 months to 12 months (Bailey and Cushing, 1926). Despite a vast amount of research into GBM, including increased understanding of underlying genetics and aberrant molecular pathways, very little progress has been made in the last century. The first study to significantly impact survival over this period was published by Stupp and colleagues in the New England Journal of Medicine in 2005 (Stupp *et al.*, 2005). The authors found that the addition of temozolomide chemotherapy to radiotherapy increased survival to a median of 14.8 months from the previously quoted 12 months, and this remains as the largest gain in survival for all comers with GBM. As temozolomide kills tumour cells by alkylating DNA, patients with MGMT promoter methylation experience greater survival following chemotherapy, reaching a median of 21.7 months (Hegi *et al.*, 2005). However, overall survival is poor, with fewer than 5% surviving to 5 years (Delgado-Lopez and Corrales-Garcia, 2016). Further, GBM affects a relatively young population and thus poor survival results in a higher loss of productive life years than some other uniformly fatal cancers (Ohgaki *et al.*, 2004). Given the universally poor prognosis, many groups are actively looking for novel targets in GBM therapy in a quest to prolong survival.

1.2 Therapeutic Targets in GBM

While surgery is one of the mainstays of GBM treatment, the goal of surgery is not curative, but rather maximal safe resection to minimize tumour burden and increase the effectiveness of adjuvant treatments (Lacroix *et al.*, 2001; Hentschel and Lang, 2003). As GBM grows, it invades surrounding brain, and surgical resection is aimed at removing tumour tissue while sparing normal adjacent brain, particularly when tumours are located in or adjacent to eloquent areas (motor, sensory, language, etc.). The key to a cure lies in identifying new chemotherapeutics to more effectively kill tumour cells left behind following surgery. An increasing interest in the molecular genetics of GBM has not only

provided insight into how these tumours develop their neoplastic characteristics but has also given researchers a number of new potential targets for chemotherapy.

Mutations in EGFR, a tyrosine kinase receptor, are present in approximately 35% of primary GBM (Ohgaki *et al.*, 2004). The most common mutation, EGFRvIII, produces a constitutively active receptor which results in activation of mammalian target of rapamycin (mTOR), a well-studied oncogene known to promote growth and proliferation in a multitude of cancers (Cargnello *et al.*, 2015). Tyrosine kinase inhibitors (TKIs), such as gefitinib and erlotinib, have been tested in GBM, and although results were promising in cell culture studies (Halatsch *et al.*, 2004), these drugs have failed to demonstrate any survival advantage in early clinical trials (Rich *et al.*, 2004; Franceschi *et al.*, 2007; van den Bent *et al.*, 2009). Antibody therapies block signalling through the EGFR receptor and can also cause receptor internalization or immune system targeting to tumour cells. Antibodies against EGFR, however, have followed the same pattern as TKIs (Eller *et al.*, 2002; Neyns *et al.*, 2009; Westphal *et al.*, 2015), although some success has been seen with antibodies conjugated to radioisotopes (Li *et al.*, 2010). Finally, studies on vaccinations with peptides targeting EGFRvIII (rindopepimut) are underway, and while early studies have been promising (Heimberger *et al.*, 2006; Sampson *et al.*, 2011), a phase 3 trial failed to demonstrate improved survival in patients receiving the vaccine (Weller *et al.*, 2017). Tumour vaccines work to activate the immune system against tumour cells preferentially, theoretically allowing for increased tumour cell killing and patient survival when combined with conventional therapies. Despite disappointment with rindopepimut, a number of other GBM vaccines continue to be studied (Kong *et al.*, 2018).

Many of the mutations that are common in primary GBM act along the phosphatidylinositol-3-kinase/protein kinase B (PI3K/AKT) pathway (Amankulor and Holland, 2011). Multiple receptor tyrosine kinases (RTKs) are activated in GBM, either through direction mutation (EGFR) or by increased ligand presence as a result of other neoplastic processes (vascular endothelial growth factor receptor, VEGFR; platelet derived growth factor receptor, PDGFR). These receptors are all capable of activating the P13K pathway. The protein phosphatase and tensin homolog (PTEN) is an inhibitor of PI3K and loss of function mutations, found in up to 35% of primary GBM

(International Agency for Research on Cancer, 2016), result in a relative abundance of PI3K signalling. The main effector of this pathway is mTOR, which is involved in cell growth, proliferation, and angiogenesis. As multiple GBM mutations converge to increase mTOR, mTOR inhibitors have also been studied as a potential therapy for GBM. Rapamycin was promising in cell culture studies, demonstrating a reduction in proliferation of commercially available GBM cell lines and primary GSCs, but xenograft studies showed mixed results (Arcella *et al.*, 2013; Mendiburu-Elicabe *et al.*, 2014). In clinical trials, a number of mTOR inhibitors have been studied, but none have proven effective in improving survival (Kreisl *et al.*, 2009; Chheda *et al.*, 2015; Ma *et al.*, 2015) although studies are ongoing.

One of the defining characteristics of GBM is the necrosis found within the tumour core. The necrosis is the direct result of tumour outgrowing its vascular supply, resulting in tissue hypoxia and, subsequently, necrosis. Chronic hypoxia leads to increased levels of hypoxia inducible factor (HIF1α) and important cellular oxygen sensor (Ivan *et al*., 2001; Jaakkola *et al*., 2001), which in turn stimulates production and release of VEGF (Amankulor and Holland, 2011), encouraging angiogenesis within this hypoxic environment, thus allowing the tumour to survive and continue to grow. As discussed above, some of the tyrosine kinase inhibitors act in part on VEGFR to prevent downstream signalling, but no benefit has been seen in clinical trials to date. Sorafenib, a multikinase inhibitor with inhibitory effects on VEGFR, as well as PDGFR and the Ras pathway (also dysregulated in GBM), has been the subject of a number of studies showing little to no effect in recurrent or newly diagnosed GBM (Hainsworth *et al.*, 2010; Lee *et al.*, 2012; Galanis *et al.*, 2013; Zustovich *et al.*, 2013; Hottinger *et al.*, 2014).

The most widely studied VEGFR-targeted therapy is bevacizumab, an antibody to VEGFR that works in similar fashion to the anti-EGFR antibodies previously discussed, blocking downstream receptor signalling. Bevacizumab has been more extensively studied in recurrent GBM, often in combination with rescue chemotherapeutics. Most studies have reported only modest survival in recurrent GBM treated with bevacizumab in combination with various other drugs (Lassen *et al.*, 2013; Taal *et al.*, 2014; Field *et al.*, 2015), and a recent literature review/analysis reported a median progression free

survival (PFS) of 4.38 months on bevacizumab, with an overall survival (OS) of 8.18 months (Tipping *et al.*, 2017). Fewer studies have examined outcomes with addition of bevacizumab to conventional therapy in newly diagnosed GBM. One randomized trial found that the addition of bevacizumab to temozolomide and radiotherapy improved PFS, but did not improve OS and was associated with more adverse events (Chinot *et al.*, 2014). Another study demonstrated a modest increase in OS with a combination of bevacizumab, temozolomide and hyperfractionated stereotactic radiotherapy, quoting a median PFS of 10 months and an OS of 19 months, although only forty patients were enrolled (Omuro *et al.*, 2014). Currently, no convincing evidence exists for the use of bevacizumab as a first-line therapy.

Another therapy that is being intensively researched is the use of alternating electrical fields (tumour treating fields, TTF), which is thought to disrupt microtubule formation and thus contribute to inhibition of tumour cell migration and angiogenesis within the tumour (Kim *et al.*, 2016). In addition, improper microtubule function has been shown to cause apoptosis in mitotically active cells by preventing proper furrow formation leading to membrane rupture (Kirson *et al.*, 2004). A pilot study demonstrated increased PFS and OS using TTF in ten patients with recurrent GBM (Kirson *et al.*, 2007). More recently, an RCT of 695 patients found that patients treated with maintenance therapy of TMZ and TTF following traditional chemotherapy/radiation treatment had a PFS of 7.1 months and an OS of 20.5 months (Stupp *et al.*, 2015), an improvement on historical numbers. However, the study required that the patients maintain a shaved head and wear the device, along with a battery pack, for at least 18 hours a day indefinitely. This has caused some issues with compliance (Burri *et al.*, 2018). In addition, at a cost of approximately $30,000 (CAD) per month of treatment, there have been ongoing debates on the cost-effectiveness of the treatment given modest improvements in survival (Connock *et al.*, 2019; Guzauskas *et al.*, 2019). Taken together, these hurdles have limited the role of TTF in non-trial patients.

1.3 Mechanisms of Treatment Resistance

In order to understand treatment resistance in GBM, one must understand the role and characteristics of GBM cell types as well as the influence of tumour microenvironment on tumour cells. The majority of tumour is composed of neoplastic

cells that are maintained by a smaller number of GSCs capable of producing complete tumours when explanted into other tissues (Singh *et al.*, 2004). Treatment resistance varies between different cell types within tumour tissue, and treatment may itself select for more resistant tumour recurrence by preferentially killing cells more susceptible to treatment. The tumour microenvironment can also contribute to resistance by activating pro-survival pathways in tumour cells.

Glioblastoma arise, at their earliest moment of generation, from a single cell of origin that gives rise to a population of GSCs. These stem cells can then produce populations of tumour cells and other GSCs with different genetic or epigenetic signatures. A recent review has summarized the genetic differences separating GSCs from non-stem cells (Osuka and Van Meir, 2017). The cell of origin may be a neural stem cell or a differentiated glial cell that has acquired stem-like properties. As cells replicate and acquire further mutations, the result is a tumour consisting of several clonal populations, with genetically similar cells clustered more closely together according to the temporal sequence of their generation. GSCs are scattered throughout the cell mass, and these too may be genetically dissimilar based on their location within the tumour. Both stromal tumour cells and GSCs may differ spatially in their ability to survive microenvironment or treatment-associated stress.

GBM cells have utilized a number of mechanisms to evade commonly used treatments. Firstly, the BBB acts as a physical barrier for some chemotherapeutics (Wang *et al.*, 2014), limiting their effectiveness against tumour cells located outside the tumour core where the BBB has been broken down. As previously mentioned, MGMT is involved in DNA repair, and populations of GBM expressing this enzyme are capable of repairing TMZ-associated DNA damage. TMZ treatment can induce expression of MGMT so that cells surviving initial treatments are more resistant to subsequent treatment (Hegi *et al.*, 2005). Prior to the discovery of increased survival with TMZ, RTK inhibitors were commonly used as chemotherapeutics. However, GBM resisted treatment with RTK inhibitors, accomplished in part through co-activation of multiple RTKs converging on a single downstream pathway (for example, both EGFR and PDGFR), adding redundancy to mTOR expression and thus evading monotherapy regimens (Stommel *et al.*, 2007). To counteract the effects of anti-VEGF therapies,

tumour cells are capable of taking on endothelial-like properties and forming channels that mimic vasculature to aid in the delivery of nutrients and oxygen to ischemic tumour tissues (Angara *et al.*, 2017). Finally, GBM cells express membrane efflux pumps as well as small proteins capable of inactivating a number of different drugs, and are also capable of changing the structure of intended chemotherapeutic targets to evade drug treatments (Tews *et al.*, 2000). These adaptations have contributed to resistance of tumour cells to current and previous treatments, and to the survival of tumour cells within the hypoxic tumour microenvironment.

The tumour cells most resistant to therapy are the GSCs responsible for tumour generation. These cells utilize a number of mechanisms to avoid death following treatment with radiation and chemotherapy (Lathia *et al.*, 2015). A number of pro-survival pathways have been found to be constitutively activated in GSCs (Bao *et al.*, 2006; Wang *et al.*, 2010; Venere *et al.*, 2014; Kim *et al.*, 2015). Some of these pathways are involved in the repair of DNA damage following chemotherapy, and others are responsible for increasing the invasiveness and replication of GSCs. As these cells are more resistant than non-stem cells, treatment not only selects for a more aggressive tumour by activating tumourigenicity, but also by increasing the relative number of GSCs by killing off non-resistant cells.

In addition to their ability to survive following treatment, GSCs are also more adapted to survival in the harsh conditions of the tumour microenvironment. As the tumour outgrows its blood supply, the core of the tumour becomes hypoxic and relatively nutrient-poor. Upregulation of neuronal glucose transporter type 3 (Glut3) in GSCs leads to increased glucose uptake in these cells, selecting for their preferential survival in starvation (Flavahan *et al.*, 2013). An acidic pH is also present in GBM and is associated with hypoxia and anaerobic metabolism present in these tumours. Low pH is independently capable of upregulating VEGF to counteract hypoxia and nutrient starvation (Fukumura *et al.*, 2001), and has also been shown to increase resistance to a number of chemotherapeutics (Reichert *et al.*, 2002). While the brain is an immune-privileged site, GBM causes breakdown of the BBB, thus theoretically allowing access by the immune system. However, GBM, and specifically GSCs, have adapted several mechanisms that allow them to evade the immune system and survive subsequent self-

regulated destruction, using mechanisms such as secretion of immunosuppressive signalling factors and expression of immune inhibitory ligands, among others (Razavi *et al.*, 2016; Silver *et al.*, 2016).

Hypoxia is a prevalent component of the tumour microenvironment and contributes to a number of the survival mechanisms already discussed. While GBM is typically thought of as having a hypoxic core, the exact partial pressure of oxygen (pO_2) within the tumour is highly variable spatially (Patel *et al.*, 2014). Studies measuring oxygen pressures in patients with GBM have consistently demonstrated lower pO_2 within tumour compared to surrounding brain under a number of conditions (Beppu *et al.*, 2002; Chakhoyan *et al.*, 2017). Additionally, hypoxia is not consistent in any region of tumour, but rather cycles both acutely and on a more chronic basis (Dewhirst *et al.*, 2008). This cycling is the result of tumour outgrowing blood supply, which lowers core oxygen levels, followed by cell death, which in turn decreases oxygen consumption and leads to a relative increase in pO_2. On a more chronic level, hypoxia triggers the release of VEGF, mediated by HIF1α, leading to angiogenesis and raised pO_2. In addition to directly contributing to tumour invasiveness by encouraging cell migration away from the hypoxic core (Martinez-Gonzalez *et al.*, 2012), hypoxia is an important contributor to treatment resistance in GBM.

Glioma stem-like cells exhibit higher treatment resistance than the remainder of tumour cells, and one of the main ways in which hypoxia encourages treatment resistance is through induction and maintenance of a stem cell state. When observing the characteristics of tumour cells in GBM, GSCs are more prominent in hypoxic regions (the tumour core) with more differentiated cells located at the vascular tumour periphery (Pistollato *et al.*, 2010). Hypoxia induces the expression of HIF2α, which, in addition to the action of HIF1α, upregulates stem cell markers in non-stem astrocytoma cells, and promotes self-renewal of tumour cells (Heddleston *et al.*, 2009). The HIF transcription factors (particularly HIF2α) co-localize with stem cell markers (Li *et al.*, 2009), suggesting that GSCs are disproportionately responsible for tumour angiogenesis. Hypoxia also induces the expression of multiple stem cell markers in non-stem cells in a HIF1α-dependent manner, with subsequent increase in cellular proliferation and apoptosis resistance (Wang *et al.*, 2017). These studies, taken together, demonstrate that

hypoxia induces a stem cell fate in GBM cells by increasing expression of HIF transcription factors, resulting in the generation of GSCs that are more tumourigenic than non-stem or non-hypoxic tumour cells.

It is clear that hypoxia is an important driver of stemness in GBM cells, and that GSC state confers increased tumourigenicity and treatment resistance to tumour cells. As outlined, there are several mechanisms that seem to contribute to this increased resistance in hypoxia, and HIF seems to be a major player. In addition to HIF signalling, some early evidence suggests that GBM cells may be able to adapt to hypoxic stress through generation of cytoplasmic RNA stress granules (SGs), a component of the integrated stress response (Vilas-Boas Fde *et al.*, 2016; Weeks *et al.*, 2016). These granules are hypothesized to be sites of mRNA triage under a number of different cellular stresses (Anderson and Kedersha, 2009), and studies have linked the formation and dissolution of these granules to altered levels of HIF expression in a hypoxic setting. Aggregation of SGs in hypoxia decrease levels of expression (Gottschald *et al.*, 2010), while re-oxygenation following radiation therapy leads to increased HIF activity coincident with rates of granule dissolution (Moeller *et al.*, 2004). Thus, we hypothesize that SGs may play a role in HIF regulation and GBM cell survival in hypoxia, as well as the initiation of a "pro-survival" and treatment-resistant phenotype in surviving cells.

1.4 Cytoplasmic RNA Stress Granules

In non-stressed conditions, cells carry out a multitude of processes related to their tissue-specific functions and the maintenance of homeostasis. As such, many variable mRNAs are being translated by multiple ribosomes (polysomes) within the cytoplasm. This highly efficient process consumes large amounts of energy and is responsible for a large portion of resting energy consumption. When cells become stressed, energy conservation becomes important as cells must focus energy expenditure on a small number of key processes that ensure survival and allow the resumption of homeostasis once stress is relieved (Kawai *et al.*, 2004). The formation of cytoplasmic RNA stress granules is one way that a cell accomplishes this energy reorganization through the global dampening of cellular translation (**Fig 1.1**).

The initial step in the formation of SGs is the phosphorylation of eukaryotic initiation factor 2α (eIF2α) by a stress-specific kinase (Kedersha *et al.*, 1999).

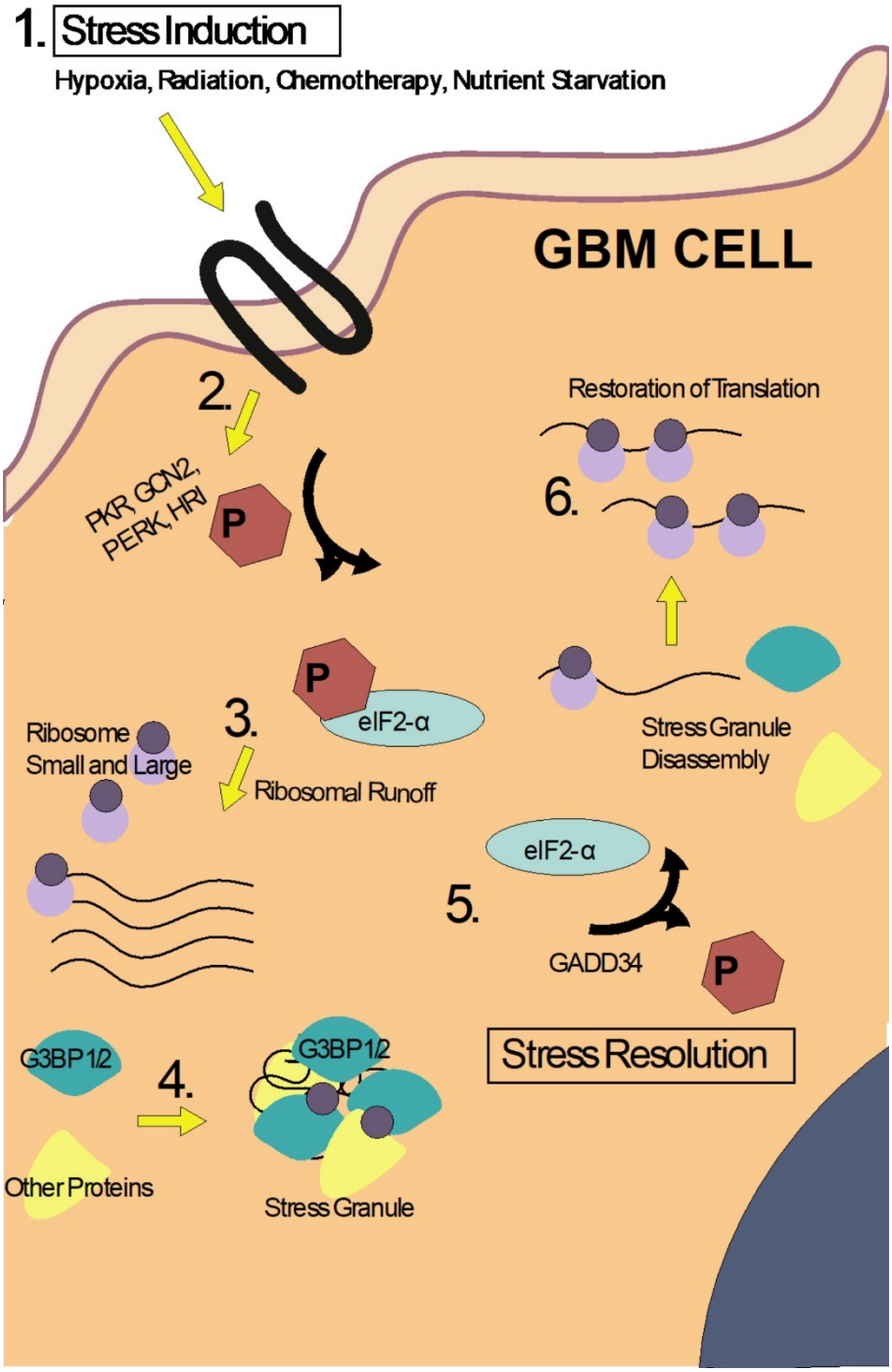

Figure 1.1. Graphic representation of SG dynamics. Stressors such as hypoxia, nutrient starvation, UV radiation and certain drugs (**1**) lead to the activation of stress-associated kinases (PKR, GCN2, PERK, HRI) (**2**) and the resulting phosphorylation of eIF2α (**3**). This leads to ribosomal run-off, diminished overall translation, and ultimately the aggregation of translationally stalled mRNAs with proteins such as G3BP1/2 and

TIAR into SGs (**4**). Stress resolution results in the dephosphorylation of eIF2α by the phosphatase GADD34 (**5**), SG disassembly and the restoration of normal translation from packaged mRNA (**6**).

Phosphorylation prevents further initiation of translation by preventing the formation of the ternary complex of eIF2α, guanosine triphosphate, and transfer RNA (eIF2-GTP-$tRNA_i^{Met}$) responsible for initiation, allowing ribosomes currently on the mRNA to "run off", leaving an exposed mRNA (Anderson and Kedersha, 2008). Exposed mRNAs are then bound by a number of mRNA-binding proteins, including T cell internal antigen-1 (TIA-1) or TIA-1 related (TIAR), ras-GTPase-activating protein SH3-domain-binding protein (G3BP), and fragile X mental retardation protein (FMRP) (Mazroui *et al.*, 2002; Tourriere *et al.*, 2003; Gilks *et al.,* 2004). These mRNA-binding proteins are also capable of protein-protein interactions via prion-like domains (Tian *et al.*, 1991; Kedersha *et al.*, 1999), allowing the formation of progressively larger messenger ribonucleoproteins (mRNPs) within the cytoplasm as smaller aggregations fuse (Kedersha *et al.*, 2000). Pre-initiation machinery and the small ribosomal subunit remain bound to mRNA as granules assemble, thus ensuring availability for re-initiation of translation once granules dissolve (Anderson and Kedersha, 2008).

Although phosphorylation of eIF2α is the inciting event for SG nucleation, this phosphorylation represents the final convergent step of multiple pathways activated by a variety of stressors. Protein kinase R (PKR) is activated by double-stranded RNA and phosphorylates eIF2α to activate the stress response following viral infection (Der and Lau, 1995; Srivastava *et al.*, 1998), and can also respond to UV irradiation and heat shock (Anderson and Kedersha, 2008). The kinase general control nonderepressible 2 (GCN2) senses deficiency of a number of amino acids as a trigger for eIF2α phosphorylation (Wek *et al.*, 1995). PKR-like endoplasmic reticulum kinase (PERK) phosphorylates eIF2α as part of the unfolded protein response (Harding *et al.*, 2000a), where an excess of unfolded proteins generates endoplasmic reticulum (ER) stress. PERK is also involved in the formation of SGs in response to hypoxia as cells deficient of PERK are unable to form SGs under these conditions (Gardner, 2008). Finally, heme-regulated initiation factor 2α kinase (HRI) becomes activated during oxidative stress and induces the formation of SGs (McEwen *et al.*, 2005). In addition to eIF2α phosphorylation, SGs have also been reported to form via a non-canonical pathway mediated by inhibition of eukaryotic translation initiation factor 4E (eIF4E) by eIF4E-binding protein 1 (4EBP1), which also results in a decrease in translation (Fujimura *et al.*,

2012). Type 2 stressors (for example, ionizing radiation or genotoxic drugs) do not induce SG formation and are typically more likely to result in apoptotic cell death (Arimoto *et al.*, 2008).

Originally, SGs were thought to simply be sites of mRNA storage during stress, but evidence that a relatively low percentage of cellular mRNAs were actually contained within SGs, coupled with the fact that mRNA shuttling between SGs and the cytoplasm is fairly rapid, encouraged the hypothesis of SGs as sites of mRNA triage (Kedersha *et al.*, 1999; Kedersha *et al.*, 2000; Zurla *et al.*, 2011). The presence of mRNA-stabilizing proteins, such as poly-A binding protein (PABP) and human RNA binding protein (HuR), in SGs suggests that some mRNAs are indeed stabilized within granules (Kedersha *et al.*, 1999; Gallouzi *et al.*, 2000), and the presence of translational machinery (Kimball *et al.*, 2003) allows for rapid resumption of translation once stress is relieved (Cherkasov *et al.*, 2013). However, certain mRNAs are exempt from SGs and undergo continued translation during stress. For the most part, mRNA involved in the stress response, like the heat-shock proteins (HSP) and activating transcription factor 4 (ATF4), undergo continued translation (Harding *et al.*, 2000b; Kedersha and Anderson, 2002), allowing the cell to survive under acute stress. In addition, SGs also interact transiently with processing bodies (PBs), which are sites of mRNA degradation, allowing efficient shuttling of non-necessary mRNA to PBs for destruction (Kedersha *et al.*, 2005). Thus, the current understanding is that SGs are acting as sites of mRNA triage, determining which mRNAs will be degraded, which will continue to be translated, and which will in fact be stored and protected for continuation of translation once stress is relieved.

In addition to mRNA, some non-RNA binding proteins also aggregate into SGs, and are thought to play a role in the control of various other cellular processes while the cell is stressed. Recruitment of several mTOR-regulating proteins within SGs inhibits mTOR-dependent apoptosis under conditions of oxidative stress (Heberle *et al.*, 2015). Stress granules formed from type 1 stressors further inhibit apoptosis by sequestering the scaffolding protein receptor of activated protein C kinase 1 (RACK1), an important activator of mitogen-activated protein kinase (MAPK) and subsequent apoptosis in response to type 2 stress (Arimoto *et al.*, 2008). Cells that have been exposed to stress and formed SGs have also been shown to be more resistant to further stressors, and this is

in part due to inhibition of nuclear factor-κB (NF-κB)-mediated inflammation through selective binding of upstream regulatory proteins in SGs during stress (Kim *et al.*, 2005). Thus, in addition to their role in mRNA triage, binding of certain regulatory proteins in SGs seems to also confer a survival advantage on stressed cells.

Once a cell is released from stress, it must restore normal cellular function to continue survival. In order to accomplish this, the cell must dissolve SGs to access the mRNA and protein contained within. While the mechanisms of SG assembly are understood in some detail, very little is known regarding the mechanisms of SG disassembly. Even when SGs are fully formed in the cytoplasm, there is in fact a homeostasis between formation and dissolution as shown by rapid fluorescence recovery following photobleaching of fluorescence-tagged SG proteins (Kedersha *et al.*, 2000). Microtubules are involved in both the formation and dissolution of SGs, and SGs can be seen as aggregates of progressively smaller granules that move along microtubules to either fuse or break apart, depending on the stress state of the cell (Ivanov *et al.*, 2003; Nadezhdina *et al.*, 2010). Furthermore, autophagy-mediated SG clearance (granulophagy) seems to play a role in SG dissolution as SG components are abundant in autophagic vacuoles when autophagic vesicle breakdown is inhibited in yeast, and blockade of autophagy initiation by depletion of the ATPase valosin-containing protein (VCP, a participant in granulophagy activation) in mammalian cells leads to an accumulation of SGs in the cytoplasm (Buchan *et al.*, 2013). Additionally, certain proteins sequestered in SGs in response to stress have been shown to automatically activate autophagic SG clearance (Krisenko *et al.*, 2015). Finally, the phosphorylation status of eIF2α must also be considered; the phosphatases constitutive reverter of eIF2α phosphorylation (CReP) and growth arrest and DNA damage-inducible protein (GADD34) are responsible for constitutive and inducible dephosphorylation of eIF2α respectively. Regulation of GADD34 during stress in particular is in part responsible for SG clearance and may blunt subsequent SG responses to stress (Shelkovnikova *et al.*, 2017). This mechanism suggests that SG clearance following release from stress might in fact be the result of a changing balance between stress-induced eIF2α phosphorylation, dephosphorylation by CReP/GADD34, and ongoing autophagic SG clearance. However, the exact mechanisms by which this balance occurs are still being investigated.

The closest example of a unifying theory on the mechanisms responsible for SG dissolution was recently proposed in a review by Alberti and colleagues (Alberti *et al.*, 2017). This theory differentiates between physiologic SGs, which exist in a dense liquid state and are cleared with the assistance of molecular chaperones, and aberrant or persistent SGs that co-aggregate with defective ribosomal products (DRiPs), taking on a more solid state and requiring activation of autophagy for their clearance. This model is based on earlier studies that demonstrated the necessity of chaperones in SG surveillance and maintenance of normal SG dynamics, with only a minority of SGs requiring autophagy for clearance (Ganassi *et al.*, 2016). In cases of impaired chaperone function, the accumulation of DRiPs within SGs triggers a phase transition, leading to solid state granules and subsequent degradation by autophagy (Mateju *et al.*, 2017). Thus, under most physiologic conditions, the protein quality control (PQC) machinery clears SGs, and autophagic mechanisms, as discussed above, are only utilized when the PQC mechanisms are not functioning sufficiently. The balance between phosphorylation and dephosphorylation states of eIF2α (mediated by CReP/GADD34) would act as a switch in either circumstance, promoting or preventing further SG formation.

Given their role in cell survival under stressful conditions, SGs have been hypothesized to play a role in several diseases. As previously mentioned, SGs form in response to viral infection through activation of PKR. However, many viruses are able to manipulate SG dynamics to either dampen the host cell adaptive response, or hijack SG machinery to aid in viral replication (Lloyd, 2013). Stress granules, either directly or through interactions with other mRNP granules, are also dysregulated in a number of neuronal and neurodegenerative diseases (Liu-Yesucevitz *et al.*, 2011; Ghosh and Geahlen, 2015; Mackenzie *et al.*, 2017). Finally, SGs play an important role in cancer cell survival in response to therapeutic and microenvironment-induced stress, and their role in a number of different cancers is an active area of research (Anderson *et al.*, 2015).

1.5 Stress Granules in Cancer

Stress granules assist cell survival in many different stressful conditions. While cellular stress is an exception for most healthy tissues, diseased tissue can be exposed to many different stressors, and cancer in particular presents a stressful environment. Rapid tumour growth carries with it many environmental stressors (hypoxia, nutrient starvation,

etc) that tumour cells must overcome to continue proliferation. In addition, chemotherapy and radiation can also cause stress to tumour cells, and the high recurrence rate of some solid tumours indicates that they have adaptive mechanisms to help them resist treatment and survive. Stress granules likely play a role in tumour cell survival, and many studies have shown a link between SG formation and cancer development or survival following treatment. These studies have been reviewed in depth elsewhere (Anderson *et al.*, 2015), but an abridged summary is provided.

As previously discussed, one feature of most solid tumours is rapid cell proliferation, resulting in tumour growth disproportionate to rates of angiogenesis and a hypoxic tumour core. As SGs form in response to hypoxia, they may play a role in the survival of tumour cells within this hypoxic environment. In addition, the lack of adequate vasculature also means that cells within this region are relatively nutrient starved; this is another SG trigger, mediated by the kinase GCN2. The combination of rapid proliferation and amino acid starvation leads to inefficient protein folding, generating ER stress (Clarke *et al.*, 2014), yet another SG trigger. Finally, adaptation to the harsh microenvironment involves the decoupling of glycolysis from oxidative phosphorylation, leading to the production of reactive oxygen species (ROS), increasing cellular oxidative stress. Thus, the tumour microenvironment alone provides many stimuli for SG formation.

Biochemically, SGs may play a role in increased cancer cell proliferation and invasiveness. It has been demonstrated that mTOR signalling is increased in many different cancers, through a number of mechanisms, and this increases the proliferation of tumour cells. However, chronic mTOR activation promotes apoptosis, in part through inhibition of ER stress sensor PERK (Appenzeller-Herzog and Hall, 2012), a kinase involved in SG formation. In addition, mTOR has inhibitory effects on autophagy which can be counter-productive in advanced cancer (Paquette *et al.*, 2018). Therefore, cancer cells must regulate mTOR signalling in order to survive and continue proliferating. Stress granules have been shown to regulate mTOR signalling (Wippich *et al.*, 2013), and SG-mediated inhibition of mTOR in cancer prevents apoptosis (Thedieck *et al.*, 2013). Sequestration of mTOR components also allows for the activation of autophagy, and SG formation itself has been shown to induce autophagy and subsequent SG clearance, as

discussed above. Thus, SGs represent a means of regulating the competing interests of mTOR and autophagy in cancer cells.

Separate from their possible role in mTOR signalling, SGs are also regulators of hypoxia-induced angiogenesis via their effect on HIF1 signalling. Under acutely hypoxic conditions, the SG nucleating protein TIAR/TIA-1 binds HIF-1α mRNA leading to a decrease in HIF signalling (Gottschald *et al.*, 2010). This allows hypoxic cells to conserve the energy associated with activation of the numerous downstream transcription factors regulated by HIF under acute hypoxic conditions. As hypoxia in solid tumours is cycling due to microvessel remodelling (Dewhirst *et al.*, 2008), HIF expression will also cycle in tandem with SG formation and dissolution. Reoxygenation causes a release of HIF mRNA as SGs dissolve, leading to a rise in HIF signalling (Moeller *et al.*, 2004) and subsequent downstream effects such as angiogenesis and enhanced glycolysis. Radiation can also trigger reoxygenation and HIF activation through tumour cell killing, thereby decreasing oxygen consumption in hypoxic regions, raising relative oxygen partial pressures. Through their effects on HIF expression, SGs regulate tumour metabolism and angiogenesis, and as discussed above, HIF expression can have direct effects on tumorigenicity and treatment resistance (Moeller and Dewhirst, 2004).

Further to their role in regulating tumorigenicity, SGs have been shown to play a role in interactions beyond the cell membrane. Studies using pancreatic cancer cell lines demonstrated that G3BP interacts with and degrades microtubule regulator binder of arl two (BART) in SGs (Taniuchi *et al.*, 2011). BART typically functions to stabilize cell adhesions, and its degradation leads to increased invasion and metastasis in mouse xenograft models. In keeping with this observation, Somasekharan and colleagues found that down-regulation of G3BP1 in sarcoma xenografts prevented SG formation, tumour invasion and metastasis (Somasekharan *et al.*, 2015). Recently, a group reported that pancreatic cancer cells with a mutant KRAS gene demonstrated upregulation of SGs in response to stress stimuli, and in addition, KRAS-mediated secretion of prostaglandins was sufficient to induce SG formation in nearby cells, indicating that SGs can be induced in a paracrine fashion within tumours to promote resistance to treatment and tumour cell survival (Grabocka and Bar-Sagi, 2016). This illustrates the complex interplay between

the effects of tumour genetics and microenvironment on SGs, and the effects that SGs have on the tumour cell and its environment to regulate cell survival.

Many studies have demonstrated the benefits of SG formation on cell survival in the stressful conditions such as those present in the tumour microenvironment. However, tumour treatment can also provide stressors that are capable of inducing SG formation. The role of radiation therapy in tumour reoxygenation and release of HIF from SGs has already been discussed (Moeller *et al.*, 2004). Additionally, multiple chemotherapeutics induce SGs, which may be one way in which tumours evade these therapies. The earliest study to form a link between SG formation and treatment resistance showed that bortezomib, a proteasome inhibitor, strongly induced SG formation; blockage of HRI (the kinase activated by bortezomib-induced stress) increased bortezomib-mediated apoptosis in a number of different cancer cell lines (Fournier *et al.*, 2010). Vinca alkaloids are a class of chemotherapeutics that act by interfering with mitosis through either stabilizing or destabilizing effects on microtubules. They induce SG formation via both canonical and non-canonical pathways, and inhibition of SG formation by specific blockade of these pathways concomitant with drug treatment increased rates of apoptosis with a subsequent decrease in tumour cell viability (Szaflarski *et al.*, 2016). Finally, sorafenib, a multi-kinase inhibitor being studied in a number of cancers (including GBM) induces SGs in hepatocellular carcinoma (HCC) cell lines, and contributes to resistance in a number of cancer cell lines (Adjibade *et al.*, 2015). Taken together, these studies demonstrate that SGs promote increased tumour cell survival in a number of cancers exposed to treatment-related stress.

Stress granules have been implicated in several different cancers since their discovery. Some of the research regarding their roles in osteosarcoma and pancreatic cancer has been discussed above. A recent study on breast cancer cell lines suggested a role for SG-mediated translational control as a positive regulator of cell proliferation and invasion by co-localizing a number of important regulatory proteins (Morettin *et al.*, 2017). Another group showed that high levels of ubiquitin-specific protease 10 (USP10) in prostate cancer enhances the inhibitory effects of G3BP2 on p53, and is associated with a poor prognosis (Takayama *et al.*, 2018). Stress granule formation has also been noted in some non-solid tumours, although in these cases they have been shown to be

both pro- and anti-neoplastic (Podszywalow-Bartnicka *et al.*, 2014; Yeomans *et al.*, 2016). So far, studies on SGs and their contribution to tumorigenicity have been limited to a few studies in any one tumour type, and research on the role of SGs in GBM is in its infancy (Vilas-Boas Fde *et al.*, 2016; Weeks *et al.*, 2016; Bittencourt *et al.*, 2019).

To date, only a handful of studies have been published linking SGs to GBM. Aberrant mTOR and HIF signalling has been noted in GBM, so SG effects previously discussed likely play a role in GBM as well. However, specific studies in GBM cell lines are lacking. The first published study examining SGs in GBM showed that inhibition of eIF2α phosphorylation increased the sensitivity of U87 astrocytoma cell lines to a number of chemotherapeutics (Vilas-Boas Fde *et al.*, 2016). However, dominant-negative inhibition of eIF2α phosphorylation, as employed in that study, is expected to have widespread effects on translational control and the results are difficult to attribute to SG effects. In addition, the chemotherapeutics tested by Vilas-Boas and colleagues are not typically used to treat GBM, bringing clinical relevance into question. Another study investigating SGs in GBM showed that multiple mRNA involved in a number of astrocytoma signalling pathways, such as cytoskeletal remodelling and apoptosis signalling, were harboured in SGs formed in response to stress with sodium arsenite, providing evidence that SGs are involved in GBM biology (Weeks *et al.*, 2016). Finally, a recent study showed that inhibition of SG formation through knockdown of G3BP1 sensitized astrocytoma cells to treatment with bortezomib (Bittencourt *et al.*, 2019).

Given the role of SGs in cell survival under a number of different stressors, including hypoxia, we hypothesize that they contribute to GBM cell survival within the hypoxic tumour microenvironment. As discussed, SG formation and dissolution are both important in cell survival, as SG formation allows cells to survive acute stress, while effective SG dissolution is necessary for return to homeostasis following release from stress. A recent study demonstrated that SGs are indeed a druggable target, and pharmacologic induction of SG formation blocked influenza A virus replication in multiple cell lines (Slaine *et al.*, 2017). The current project identifies drugs that inhibit SG formation or dissolution in GBM cells and shows that inhibition of SG dissolution correlates with increased tumour cell death in hypoxia. Stress granules may prove a

novel target in GBM and provide some hope for patients diagnosed with this unfortunate disease.

CHAPTER 2: MATERIALS & METHODS

2.1 Cell and Tissue Culture

All cell culture experiments were carried out on U251 human astrocytoma cells provided as a generous gift from Dr. James Rutka, originally purchased from American Type Culture Collection (ATCC). U251 cells were cultured in Dulbecco's modified Eagle's medium (DMEM) supplemented with 10% fetal bovine serum (FBS) and 1% penicillin/streptomycin/glutamine (Thermo Fisher Scientific) at 37 ºC and 5% CO_2. Human tissue stained for SGs was obtained directly from the operating room (OR) after obtaining consent from patients to participate in brain tumour tissue banking, as approved by the Dalhousie University ethics review board. Tissue was transported in ice-cold phosphate buffered saline (PBS) to the lab and immediately embedded in paraffin wax for tissue slice preparation. Tissue slices were maintained in DMEM at 37 ºC and 5% CO_2 until ready for staining, which always occurred within 24 hours of obtaining tissue.

2.2 Immunofluorescence

U251 cells were seeded onto glass coverslips so that they would be at a confluency of 70-80% the next day. On the day of analysis, following experimentation, cells were washed briefly with PBS and fixed in 4% paraformaldehyde (PFA, Electron Microscopy Sciences) for 10 minutes at room temperature. Coverslips were washed briefly in PBS 3 times and then permeabilized in 0.1% Triton X-100 (Sigma-Aldrich) for 10 minutes and washed again 3 times in PBS. Cells were blocked in 8% bovine serum albumin (BSA, Sigma-Aldrich) in PBS for 1 hour followed by a 1 hour incubation with antibodies specific for SG components (see **Table 2.1**) diluted in 1% BSA in PBS. Following incubation with the primary antibody, cells were washed 3 times in PBS and incubated for 1 hour with Alexa-Fluor conjugated secondary antibodies (see **Table 2.1**) diluted in 1% BSA in PBS. Cells were washed again 3 times in PBS and nuclei were stained with either DRAQ5 (1,5-bis{[2-(dimethylamino)ethyl]amino}-4,8-dihydroxyanthracene-9,10-dione, Cell Signalling), DAPI (2-(4-amidinophenyl)-1H-indole-6-carboxamidine, Thermo Fisher) or Hoescht nuclear stain (Sigma-Aldrich) depending on the experiment. Coverslips were mounted on frosted glass microscope slides using either ProLong Gold antifade reagent (Life Technologies) or Dako fluorescence mounting medium (Dako Canada Inc., Cedarlane).

Table 2.1. **Antibodies used in U251 IF experiments.**

Antibody	**Concentration**	**Supplier**
Purified mouse anti-TIAR	1:200 (1:400)	BD Transduction Laboratories
FMRP rabbit mAb	1:400	Cell Signaling
Alexa-Fluor 488 nm chicken anti-mouse	1:500	Life Technologies
Alexa-Fluor 488 nm goat anti-mouse	1:1000	Life Technologies
Alexa-Fluor 555 nm donkey anti-rabbit	1:500	Life Technologies

Immunofluorescence staining during the drug screen followed a different protocol. As it was a screening test, and cells were being visualized mechanically, the protocol was less stringent. Cells were in 96-well plates seeded the day before experimentation. Following our experiments, a mixture containing 0.3% Triton X-100 and 0.015% Hoescht stain in 3% PFA was added to each well to simultaneously fix, permeabilize and stain cell nuclei. Cells were incubated in this mixture for 20 minutes, then washed in PBS after aspiration of the mixture. For blocking, 3% BSA was added to each well for 1 hour. Only TIAR primary antibody was used in the screen, and at a reduced concentration (1:400). Antibodies were diluted in 3% BSA, followed by an hour-long incubation. Primary antibody was then removed, and cells were washed in PBS one time, followed by addition of goat anti-mouse secondary antibody for 1 hour. Cells were washed a final time in PBS after secondary antibody removal, then stored in the dark in PBS at 4 ºC until visualized.

2.3 Glioblastoma Tissue Slice Immunofluorescence

Multiple brain tissue samples from a single patient were maintained in DMEM as outlined above. Gross tissue was immobilized in agar (Sigma-Aldrich) and sliced using a Campden Instruments Inc. 7000 SMZ-2 vibratome. Slices were stained in 6-well plates on Millicell tissue culture inserts (Merck Millipore). The tissue staining protocol was adapted from the protocol published by Gogolla and colleagues (Gogolla *et al.*, 2006). All solutions were added by pipetting 1 mL above and 1 mL below the tissue culture insert membrane, as outlined in the protocol. After tissue slice preparation, tissue was fixed with 4% PFA and incubated for 10 minutes at 4 ºC. After removal of PFA, cells were washed in cold PBS by application and immediate removal. Following removal, 20% methanol (in PBS) was added to tissue and incubated at 4 ºC for 10 minutes. Methanol was then removed, followed by another PBS wash. Finally, 0.1% triton X-100 (in PBS) was added to the tissue, and slices were then incubated overnight at 4 ºC.

The following day, Triton was removed from tissue, and the tissue was then washed in cold PBS. For blocking, 20% BSA (in PBS) was added to the slices, which were then incubated for three days at 4 ºC.

Once blocking was complete, BSA was removed. Sections of membrane containing the tissue slices were excised with a razor and transferred into a large culture

dish. TIAR primary antibody (see **Table 2.1**), diluted in 5% BSA, was added to the tissue slices. The culture dish was then placed in a humidity chamber and incubated at 4 ºC for 24 hours.

Following incubation in primary antibody, tissue slices were transferred to a 12 well plate and washed 3 times for 10 minutes per wash in 5% BSA and then incubated with secondary antibody (diluted 1:400 in 5% BSA) for 4 hours at room temperature. This was followed by 3 additional 5% BSA washes. Once staining was complete, slices were mounted onto frosted glass slides with ProLong Gold and then stored at 4 ºC until ready for visualization.

2.4 Western Blotting

Cells were scraped in DMEM and centrifuged at 300 x g for 5 minutes at 4 ºC. Cell pellets were resuspended in RIPA lysis buffer (150 mM NaCl, 1% nonidet P-40, 0.5% deoxycholate, 0,1% sodium dodecyl sulfate [SDS], 25 mM Tris in ddH_2O) with 1X protease inhibitor (cOmplete ULTRA tablets), 1 mM sodium orthovanadate and 10 mM sodium fluoride (Sigma-Aldrich). Cell lysates were then centrifuged at 17,900 x g for 30 minutes at 4 ºC with the supernatant being quantified by the colorimetric DC protein assay (Bio-Rad) according to manufacturer's protocol. Following quantification, samples were diluted to a concentration of 1 µg/µL in cold RIPA and 4X sample buffer (40% glycerol, 200 mM Tris, 8% SDS, 0.2% bromophenol blue, 20% β-mercaptoethanol in ddH_2O). Following dilution, samples were boiled to 95 ºC for 5 minutes.

Protein lysates were separated in 12% TGX Stain-Free acrylamide gels (Bio-Rad). A total of 10 µg of protein was loaded into each well along with 5 µg of BluELF prestained ladder (FroggaBio). Gels were run in 1X SDS running buffer (diluted from 10X SDS buffer; 25 mM Tris, 192 mM glycine, 0.1% SDS in ddH_2O; Sigma-Aldrich) and initially run at 50 V for 10 min before being increased to 100 V for 1-2 hours. Following SDS-electrophoresis, gels were activated with UV light in the ChemiDoc Touch imaging system (Bio-Rad) for 45 seconds then transferred to polyvinylidene fluoride (PVDF) membranes using the Trans-Blot Turbo transfer system and imaged with the ChemiDoc Touch imaging system (2.5 amps, 25 V, 7 minutes). Membranes were then blocked in either 5% BSA or fat free skim milk in TBS-T (50 mM Tris, 150 mM NaCl, 0.1 – 0.2% Tween-20) for 1 hour at room temperature followed by an overnight incubation at 4 ºC

with primary antibody (see **Table 2.2**). Membranes were then washed 3 times (5 min per wash) in TBS-T, followed by a 1-hour incubation with horseradish peroxidase (HRP) conjugated secondary antibody (see **Table 2.2**) and 3 TBS-T washes (5 min per wash). Detection was performed with Clarity Western ECL substrate (Bio-Rad) and imaged on the Chemidoc. Images were analyzed with ImageLab software (Biorad). The stain free membrane image was used to quantify total lane protein, and then individual protein bands were normalized to this value. Data was exported to Microsoft Excel, which was then used to calculate fold change relative to control or protein band ratios depending on the experiment being conducted.

2.5 Screen for Drugs Affecting Stress Granule Dynamics

The drug screen was conducted in the laboratory of Dr. Michel Roberge at the University of British Columbia (UBC) using the Prestwick chemical library (Prestwick Chemical), a collection of 1120 drugs, 95% of which are approved for use in humans. The library is arranged in 96-well plates with the first and 12th column containing empty wells to serve as negative controls. Each intervening well contains a single drug dissolved in dimethyl sulfoxide (DMSO) at a concentration of 10 mM. The protocol for the drug screen experiments is shown in **Figure 2.1**.

Cells were seeded the day prior to drug introduction at 7500 cells/well in 96-well plates. The morning of drug addition, fresh DMEM was added to each well. Drug plates were spun to settle contents. A final drug concentration of 30 μM was introduced into each well using the Biorobotics Biogrid II robot equipped with 0.7mm pins. Cells were then incubated for 1 hour at 37ºC to allow the drug to become active. Hypoxia (<1% O_2) was achieved by incubating cells in a hypoxic incubation chamber (STEMCELL Technologies) flushed with high purity (99.9%) nitrogen gas at 2 psi for 10 minutes. The chamber was then sealed and incubated at 37 °C for 50 minutes, followed by a second 10 minute nitrogen flush to remove any oxygen initially dissolved in the DMEM that had re-equilibrated within the chamber, and a 1 hour incubation at 37°C (for a total of 2 h of hypoxia).

Following release from hypoxia, cells were fixed and labelled using immunofluorescence (see Section 2.2) to identify drugs interfering with SG formation or

Table 2.2. Antibodies used in western blotting experiments.

Antibody	Concentration	Solvent	Supplier
Cleaved PARP (human specific) rabbit Ab	1:1000	5% BSA	Cell Signaling
Caspase 3 rabbit mAb	1:1000	5% skim milk	Cell Signaling
LC3B antibody (rabbit)	1:1000	5% BSA	Novus Biologicals
SQSTM1/p62 rabbit mAb	1:1000	5% BSA	Cell Signaling
Anti-rabbit IgG, HRP-linked	1:2000	Same as primary	Cell Signaling

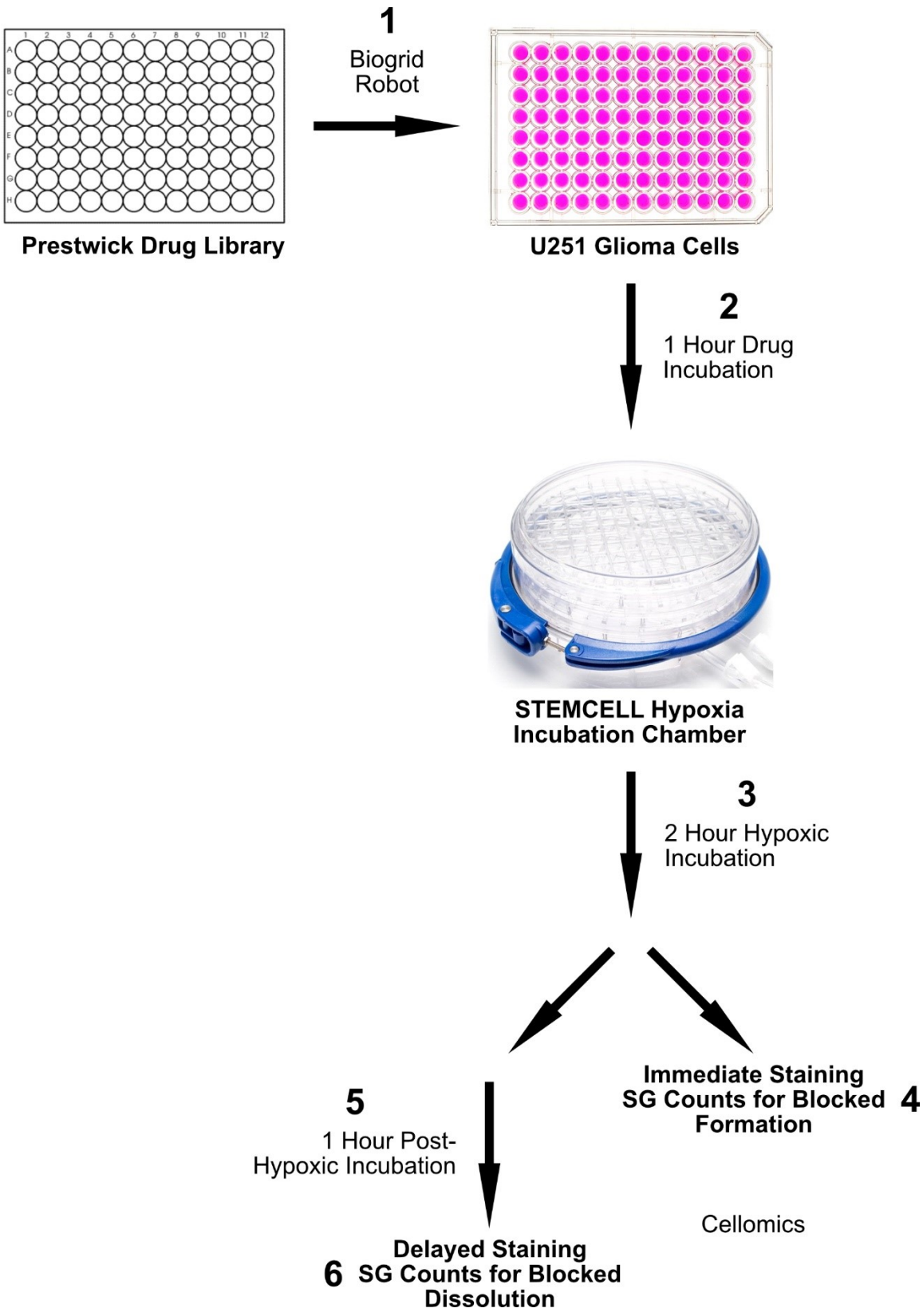
1
Biogrid
Robot
Prestwick Drug Library
U251 Glioma Cells
2
1 Hour Drug
Incubation
STEMCELL Hypoxia
Incubation Chamber
3
2 Hour Hypoxic
Incubation
Immediate Staining
SG Counts for Blocked
Formation
4
5
1 Hour Post-
Hypoxic Incubation
Cellomics
Delayed Staining
6 SG Counts for Blocked
Dissolution

Figure 2.1. Work flow for the Prestwick library drug screen. The Prestwick drug library consists of 1120 drugs arranged in 96-well plates, with each well containing a different drug. Columns 1 and 12 are empty to serve as negative controls. The Biogrid robot was used to introduce drug (30 μM) onto U251 astrocytoma cells cultured in DMEM in separate 96-well plates (**1**), and the cells were then incubated for 1 hour to allow the drug to take effect (**2**). Cells were then incubated in the hypoxia chamber for 2 hours (**3**). Upon release from hypoxia, cells were either fixed and stained immediately to asses for drug effects on SG formation (**4**) or incubated for an additional hour (**5**) then fixed and stained to assess for drug effects on SG dissolution (**6**). The SG response in all cells was assessed using high throughput cellomics.

dissolution. One complete library screen was fixed and stained immediately following release from hypoxia to investigate the role of the drugs on SG formation. Cells exposed to drugs preventing SG formation would be expected to have fewer granules following hypoxia than cells in the control wells. Conversely, cells exposed to drugs promoting SG formation would have more granules than the control cells. A second complete library screen was incubated at 37 ^{o}C for one hour following release from hypoxia and then fixed and stained to investigate the role of drugs on SG dissolution. Cell exposed to drugs preventing SG dissolution would be expected to have more granules at one hour after release from hypoxia compared to cells in control wells as more granules in control cells would have dissolved over the hour following release from hypoxia. Conversely, drugs that enhance SG dissolution would contain fewer granules than control cells. Finally, a third complete library was added to cells and incubated for 4 hours at 37 ^{o}C without any hypoxic incubation to identify drugs that directly cause SG formation. Plates were scanned using the Cellomics Arrayscan V^{TI} automated fluorescence imager using the Hoescht and GFP channels. Images were analyzed with Arrayscan software (Carl Zeiss) and data was exported to and analyzed with Microsoft Excel.

The Arrayscan software was used to count the average number of granules per cell in each of the wells, averaging across 20 high powered fields. Drugs were considered positive hits if the mean number of granules per cell was two standard deviations (SD) greater or less than the mean of control wells. To narrow down positive hits, drugs that increased SG numbers in the immediate fixation experiments and the non-hypoxic screen were removed from the list of drugs inhibiting dissolution as it was possible these drugs were in fact causing SGs to form rather than inhibiting SG dissolution. Likewise, drugs that resulted in fewer granules than control wells in the delayed fixation experiments were removed from the list of drugs preventing SG formation as it was possible these drugs were promoting SG dissolution rather than blocking formation.

The top ten drugs in each category (as determined by the degree of deviation off the control mean) were searched on PubMed for papers linking them to glioblastoma, hypoxia/oxidative stress, or SGs. Three drugs in each category were then selected for further testing with dose response curves. Final drug selection was based on a

combination of deviation from control mean SGs per cell and literature linking them to either glioblastoma treatment or a role in oxidative stress. Alexidine was also tested further despite a lack of literature linking it to either SGs, GBM or oxidative stress based on the magnitude of response in the initial screen. None of the top candidate drugs were linked to SGs prior to our selection.

2.6 Dose Response for Drug Effects on Stress Granule Dynamics

Cells were seeded onto coverslips so that they would be 70-80% confluent the following day. Drugs (see **Table 2.3**) were added to cells one hour prior to the administration of hypoxia to allow the drug to take effect. Dosages ranged from 0 to 60 μM in 10 μM increments. Two experimental plates were set up, one to receive drug and hypoxic incubation, and one to receive only drug without hypoxic incubation. In addition one well (or two wells for dissolution experiments) was given no treatment apart from hypoxia, and one well was completely untreated (no drug, no solvent, no hypoxia).

After an hour incubation in drug/solvent, cells were subject to two hours of hypoxia (see protocol in Section 2.5). If SG formation was being investigated, cells were immediately fixed for immunofluorescence, with the hypoxia-only well serving as a 0 μM drug control. If SG dissolution was being investigated, one of the hypoxia-only wells was fixed immediately to confirm SG presence within the current experiment. All other wells were incubated for an additional hour and then fixed for immunofluorescence with the second hypoxia-only well serving as a 0 μM drug control.

Following staining, cells were visualized on the EVOS FL cell imaging system (Thermo Fisher Scientific) to confirm drugs had the same effect on SGs as observed in the initial drug screen. Any drug considered to be a false positive was not investigated further. Coverslips for drugs in which SG effects were confirmed were further visualized on the Zeiss LSM 510 META laser scanning confocal microscope. At each drug dose, the percentage of cells containing SGs was estimated by counting the number of cells containing and not containing SGs in ten high powered fields (60x magnification). Cells containing five or more SGs were considered positive for granules. The percentage of cells containing SGs was counted for all drug doses from 0 to 60 μM for both hypoxic and non-hypoxic experiments. The experiment was repeated for a total of three

Table 2.3. Drugs screened for effects on stress granule dynamics.

Drug	Solvent	Supplier
Raloxifene	DMSO	Cayman Chemical Company
Thonzonium bromide	DMSO	Sigma-Aldrich
Parthenolide	Chloroform	Sigma-Aldrich
Amphotericin B	ddH_2O	Sigma-Aldrich
Niclosamide	1:1 methanol/acetone	Sigma-Aldrich
Proscillaridin	DMSO	Sigma-Aldrich
Alexidine	DMSO	Sigma-Aldrich

biological replicates, with a new set of cells split prior to each experiment from cells maintained at low passage.

2.7 Stress Granule Dissolution Rates with Raloxifene Treatment

Cells were seeded onto coverslips so that they would be 70-80% confluent on the day of experimentation. Raloxifene was added to cells at a dosage of 40 μM an hour prior to hypoxic incubation. A second plate of cells received no raloxifene prior to hypoxic incubation. After incubation in raloxifene, cells were incubated in hypoxia for 2 hours as previously described, along with the cells that had not received raloxifene. Following hypoxia, cells were fixed for immunofluorescent staining at 15-minute intervals up to two hours following release. Cells were then visualized on the confocal microscope, and the percentage of cells containing SGs at each time point was determined as previously described for both the cells receiving raloxifene and those receiving only hypoxia. Three biological replicates were completed and analyzed to produce mean SG dissolution rates.

2.8 Determining Cell Death Rates in Combined Raloxifene and Hypoxia

To investigate the effects of hypoxia, raloxifene or a combination of the two on astrocytoma cell death rates, hypoxia was administered for a longer period (12 h) to mimic the chronic hypoxia experienced by these cells within the tumour microenvironment. Cell death was estimated both by counting the number of viable cells following each treatment, and by estimating cell viability using Presto Blue cell viability reagent (Thermo Fisher Scientific). Presto Blue has been used as a measure of cell survival in other studies, including those investigating cancer cell survival, astrocyte survival and in the setting of oxidative stress (Ayyagari *et al.*, 2017; Terrasso *et al.*, 2017).

For cell viability assays cells were seeded so that they would be 70-80% confluent the following day. Cells were treated for 1 hour with either 40 μM raloxifene or DMSO vehicle control, or alternatively received no treatment. Cells were then subjected to hypoxia by flushing the hypoxia chamber with nitrogen for 10 minutes, followed by a 50 minute incubation, a second 10 minute nitrogen flush followed by a final 11 hour incubation (for a total of 12 h hypoxia). A secondary set of cells was treated identically

but remained at normoxia for 12 hours. Hypoxic induction of SGs was subsequently confirmed by immunofluorescent staining for SG markers.

Immediately following hypoxia, cells were trypsinized, washed in PBS and pelleted at 300 x g for 5 minutes. Cell pellets were resuspended in PBS and counted using a conventional light microscope (Olympus CKX53) and a hemacytometer. Three biological replicates were done to provide mean cell viability rates following treatment.

The Presto Blue assay was conducted in a similar manner to the cell counting experiments. However, cells were instead split into 96-well plates (at 8000 cells/well) the day prior to experimentation, with three wells designated to each treatment. In addition, a standard curve was prepared by serially diluting cells. On the day of experimentation, raloxifene and DMSO were added to wells as above, but each treatment was repeated in triplicate. The plate with the standard curve (also containing 3 wells of untreated cells, 3 wells treated with 40 μM raloxifene, and 3 wells treated with DMSO) was incubated in the normoxia for 12 hours. The other plate (similar except for the lack of a standard curve) was incubated in the hypoxia chamber as above.

Following hypoxia cells were washed in PBS and then incubated for 1 hour at 37 ºC with 10% Presto Blue (diluted in DMEM). Absorbance at 570 and 600 nm was read using the Tecan M200 plate reader and associated software. Data was exported to Microsoft Excel for analysis.

Data from the Presto Blue assay was reported as percent reduction of Presto Blue reagent. This was calculated using the following equation:

$$\frac{(O_2 x A_1) - (O_1 x A_2)}{(R_1 x N_2) - (R_2 x N_1)} x100$$

where O_1 is the molar extinction coefficient of oxidized Presto Blue at 570 nm (80,586), O_2 is the molar extinction coefficient of Presto Blue at 600 nm (117,216), R_1 is the molar extinction coefficient of reduced Presto Blue at 570 nm (155,671), R_2 is the molar extinction coefficient of reduced Presto Blue at 600 nm (14,652), A_1 is absorbance of test well at 570 nm, A_2 is absorbance of test well at 600 nm, N_1 is absorbance of media-only well at 570 nm, and N_2 is absorbance of media-only well at 600 nm. The percent

reduction was calculated independently for each well, and the average of the triplicates was used as the percent reduction for each treatment. This experiment was repeated for a total of three biological replicates.

2.9 Determining Mechanisms of Cell Death

To determine mechanisms of cell death, cells were once again subject to 12 hours of hypoxia to mimic the more chronic hypoxia of the tumour microenvironment. Apoptosis and autophagy were investigated by western blot analysis of key proteins in each of the pathways. Western blotting against cleaved poly (ADP-ribose) polymerase (PARP) and caspase 3 was used to investigate apoptosis. Western blotting against microtubule-associated proteins 1A/1B light chain 3B (LC3) and p62 was used to investigate autophagy. A list of antibodies used in these experiments is provided in **Table 2.2**.

Cells were seeded so that they would be 70-80% confluent on the day of experimentation. Cells were treated for 1 hour with 40 μM raloxifene or DMSO vehicle control, or remained untreated. Following an hour of drug incubation, cells were made hypoxic for 12 hours as previously described (see section 2.5). One well each treated with raloxifene and DMSO were incubated in normoxia for 12 hours to investigate drug-only treatment. Immediately post-hypoxia cells were lysed, protein was harvested, and subsequently blotted for relevant enzymes previously described (see section 2.4). Cell treatment was repeated on three separate sets of cells to calculate average protein levels.

2.10 Imaging Analysis

All cells stained with immunofluorescence were imaged using the Zeiss LSM 510 META laser scanning confocal microscope. For all experiments, three coverslips served as imaging controls; one containing cells that had received primary but not secondary antibody, on containing cells that had received secondary but not primary antibody, and one containing cells that had received no antibody. These coverslips were used to rule out antibody or cellular autofluorescence within any given experiment. For each analysis, thresholds for red, green and far red fluorescence were set using a coverslip containing cells that were stained immediately following release from hypoxia, thus representing the most robust SG response. All subsequent coverslips within a single experiment were imaged using the same thresholds to provide internal consistency.

Thresholds were set to maximize SG appearance without saturating the signal, and to minimize any background fluorescence.

2.11 Statistics and Data Representation

The Cancer Genome Atlas (TCGA) database was used to provide correlation between SG-associated mRNA expression and human astrocytoma samples. Statistical analysis was done using Tukey's Honest Significant Difference performed on GlioVis with the assistance of Dr. Adrienne Weeks.

GraphPad Prism 8 was used to analyze all data (except data from the drug screen) and generate line and bar graph figures. T ratios and P values were calculated using unpaired t tests (Holm Sidak method, $\alpha = 0.05$). The Holm Sidak method can be used to perform multiple t tests at once and is the recommended test for multiple comparisons when using GraphPad software. The drug screen data was analyzed and graphed with the help of Dr. David Brandman. Z statistics were calculated for the top 100 drugs inhibiting SG dissolution and formation using MATLAB (Mathworks), and R (v3.4.4) was used to generate the bar charts. Final figures were prepared using Affinity Designer (v1.7.1.404).

CHAPTER 3: RESULTS

3.1 Stress Granule-like Structures are Present in Glioblastoma Derived from Human Samples

In order to posit that SGs play a role in GBM cell survival and treatment resistance, SGs should be identified in human GBM tissue. To accomplish this, surgical human GBM samples were stained for the key SG nucleating protein TIAR (**Fig 3.1**). For this experiment, multiple samples were taken from a single patient. The majority of the tumour tissue demonstrated homogenous cytoplasmic and nuclear staining for TIAR across the samples taken. However, there were a few small regions of tissue in one of the samples where granular staining was present in the cytoplasm and absent in the nuclear region suggesting a possible SG response. This is a novel finding as, at the time of writing, no publication has demonstrated SGs in human tissue *in vivo*.

3.2 Expression of Stress Granule-Associated mRNA is Correlated with Glioblastoma Tumorigenicity

After confirming that SG-like structures do indeed form in human GBM tissue, the TCGA database was searched to determine whether expression of SG-related mRNA correlated with astrocytoma tumour grade. The TCGA database contains molecular characterization of over 20,000 primary tumours, including astrocytoma. The expression of genes involved in initiation of the SG response, SG nucleation, and eIF2α dephosphorylation/SG dissolution was investigated across astrocytoma from grade II to grade IV (GBM). The results of this analysis are shown in **Figure 3.2**. Two of the key stress-sensing kinases involved in initiation of the SG response show increased expression with increasing tumour grade. G3BP1, one of the key SG-nucleating proteins, also shows this response. The phosphatase known as growth arrest and DNA damage-inducible protein (GADD34) dephosphorylates eIF2α and is therefore involved in regulating the SG response (Shelkovnikova *et al.*, 2017); expression of this phosphatase is also increased in higher grade tumours. Taken together, the presence of SG-like structures in human GBM tissue on IF staining and a demonstrated increased expression of key SG-associated genes in higher grade astrocytoma lend evidence to support the hypothesis that SGs may contribute to GBM tumourigenicity.

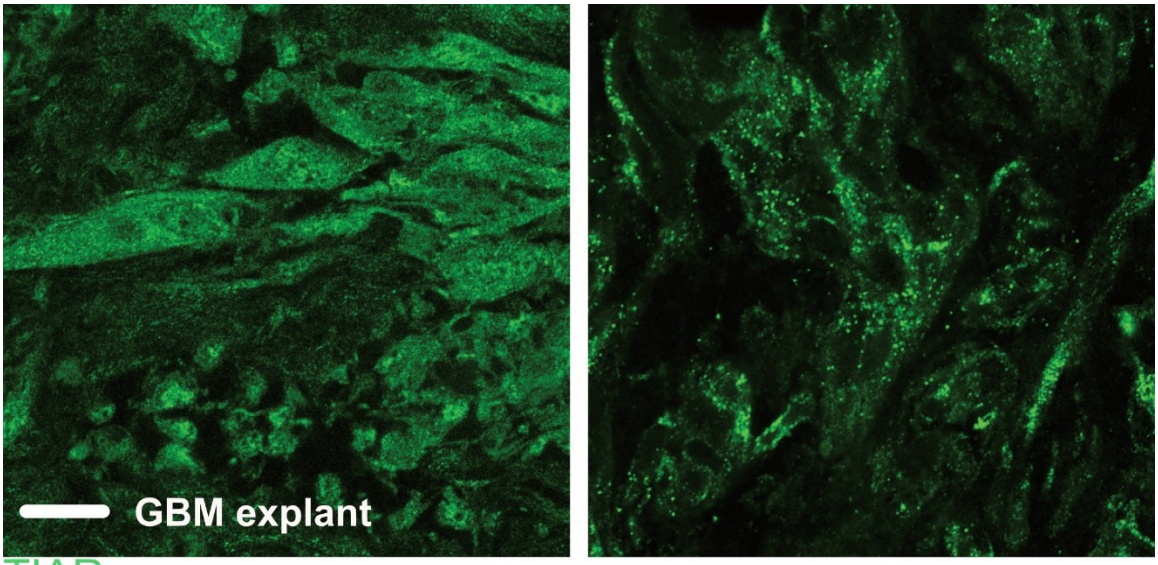

Figure 3.1. Human GBM tissue forms SGs *in vivo*. Two different sections of explanted GBM tissue from a single patient. Tissue was taken directly from the OR, sliced on a vibratome, and then fixed and immunofluorescently labelled against TIAR. The explant seen on the left shows diffuse cytoplasmic and nuclear staining. The explant seen on the right shows TIAR puncta in the cytoplasm with a lack of nuclear staining, consistent with the presence of SGs. Scale bar = 40 μm.

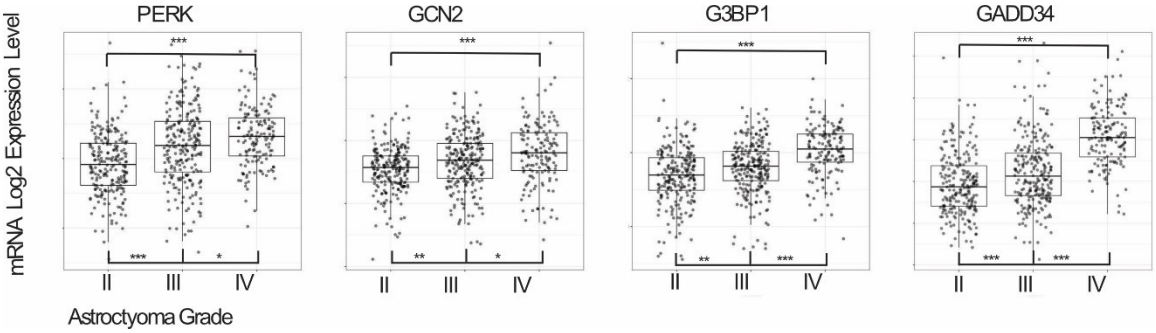

Figure 3.2. Expression of SG-associated mRNA correlates with GBM grade. The TCGA database was queried for expression of mRNA (via RNA-seq) involved in stress sensing (PERK, GCN2), SG nucleation (G3BP1) and dephosphorylation of eIF2α/SG dissolution (GADD34). This demonstrates increased mRNA expression in correlation with increased astrocytoma grade/tumourigenicity. Statistical analysis using Tukey's Honest Significant Difference, performed on GlioVis. ***p<0.001, **p<0.01, *p<0.05.

3.3 Multiple Drug Classes Interfere with Stress Granule Dynamics

Following evidence that SGs are present and play a role in human GBM, focus shifted to finding drugs capable of blocking the formation or dissolution of SGs. The Prestwick Drug Library contains 1120 drugs, the majority of which are already approved for use in humans. Hypoxia was used to induce SGs as this is a stressor commonly experienced by GBM tumour cells *in situ*. The library was screened for drugs interfering with SG formation or dissolution using high throughput cellomics conducted in the laboratory of Dr. Michel Roberge at UBC. Three separate screens were done: one screen to identify drugs inhibiting the formation of hypoxia-induced SGs, one screen to identify drugs inhibiting the dissolution of hypoxia-induced SGs, and a final screen of the drugs without a hypoxic incubation to identify any drugs that independently caused SGs to form.

Initially, 98 drugs resulted in fewer SGs on the formation screen (preventing formation), and 127 drugs resulted in more SGs on the dissolution screen (preventing dissolution). Drugs that caused cells to form fewer SGs in the dissolution screen were removed from the formation list as possible false positives under the assumption that the drug might be enhancing dissolution rather than preventing formation. Likewise, drugs that caused cells to form more SGs in the formation screen, or that elicited an SG response in the non-hypoxic screen, were removed from the dissolution list under the similar assumption that the increased SG numbers observed may be the result of enhanced SG formation rather than inhibition of SG dissolution. This left 73 drugs that interfered with SG formation and 92 drugs that interfered with SG dissolution. Three drugs were selected from each category for further testing based on a literature review. The algorithm for final drug selection is shown in **Figure 3.3**.

Z scores were calculated for the top 100 drugs interfering with SG dissolution (**Fig 3.4**). Multiple drug classes were found to inhibit SG dissolution. However, of the top 100 drugs, the majority (55%) belonged to classes of drugs interfering with monoamine metabolism. Guanabenz, a known inhibitor of SG dissolution, was also in the top 100 drugs. Two selective estrogen receptor modulators (SERMs), raloxifene and clomiphene, also screened positive for inhibition of SG dissolution. Similar statistics were compiled for the 98 drugs inhibiting SG formation (**Fig 3.5**). No obvious trends

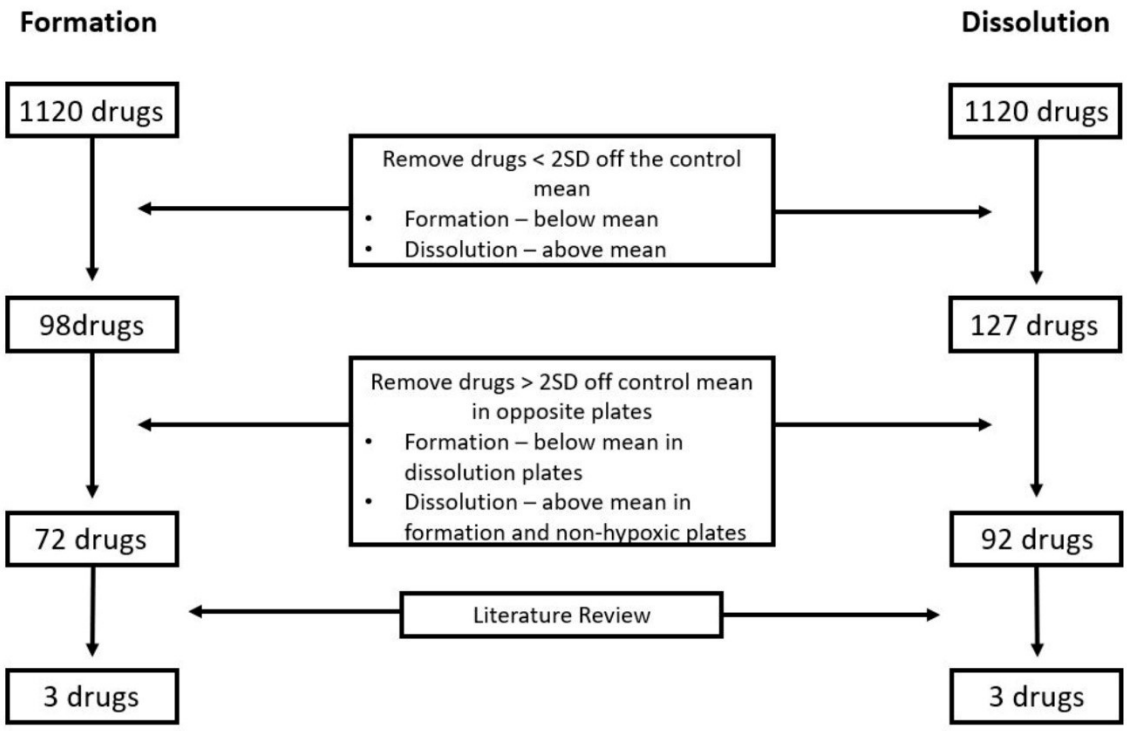

Figure 3.3. Candidate drug selection algorithm. The initial drug screen identified drugs interfering with SG formation and dissolution. This drug list was pared down by removing drugs that were likely to be false positive findings. Three drugs in each category were then selected based on statistical significance of effect and literature review.

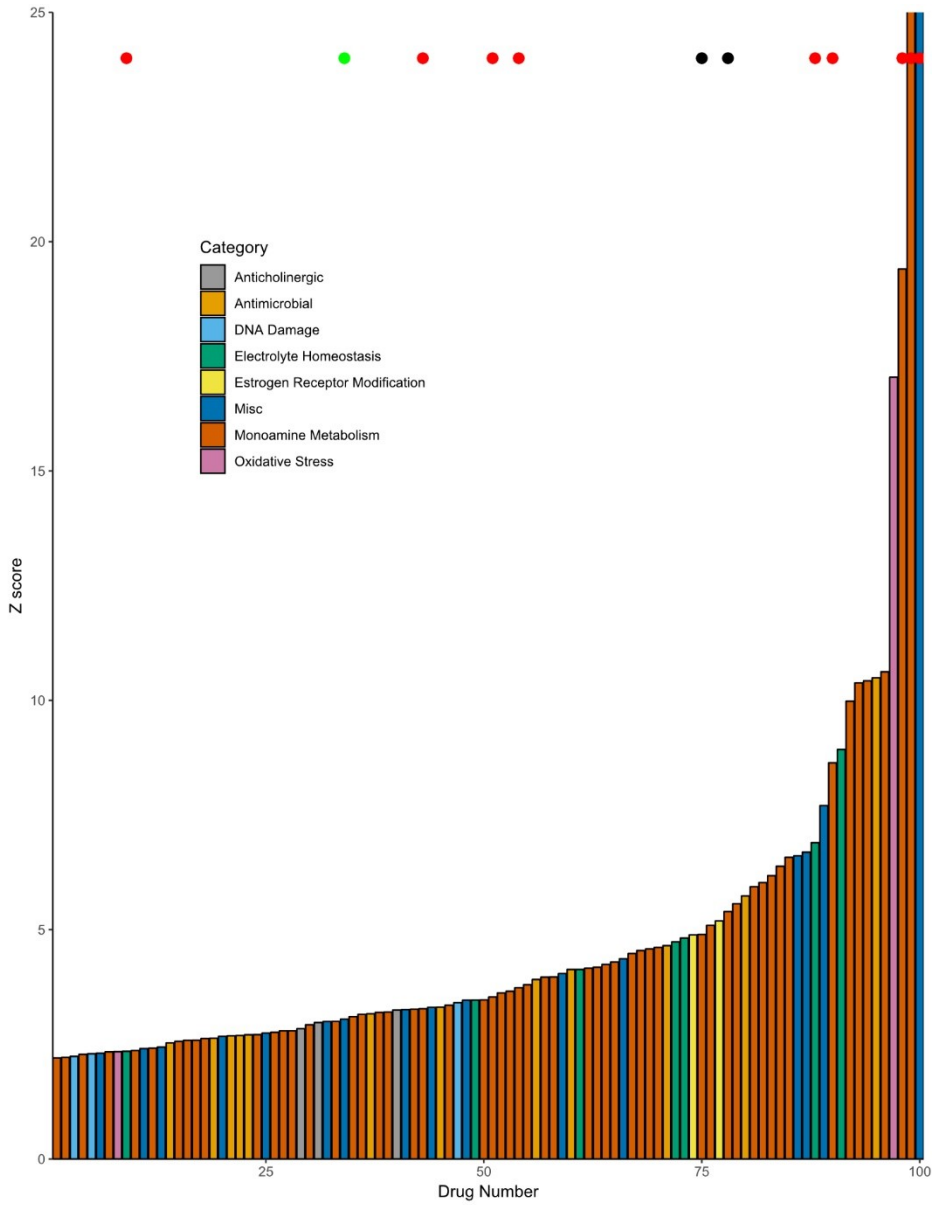

Figure 3.4. Top 100 screened drugs inhibiting SG dissolution. Drugs are displayed in order of ascending effect as determined by Z score, and bars are colour-coded by drug class. Red dots denote drugs having a high likelihood of being false positive on the initial screen based on cross referencing with the formation and non-hypoxic screen. The green dot represents guanabenz, a known inhibitor of SG dissolution (positive control). Black dots represent the SERMs raloxifene and clomiphene.

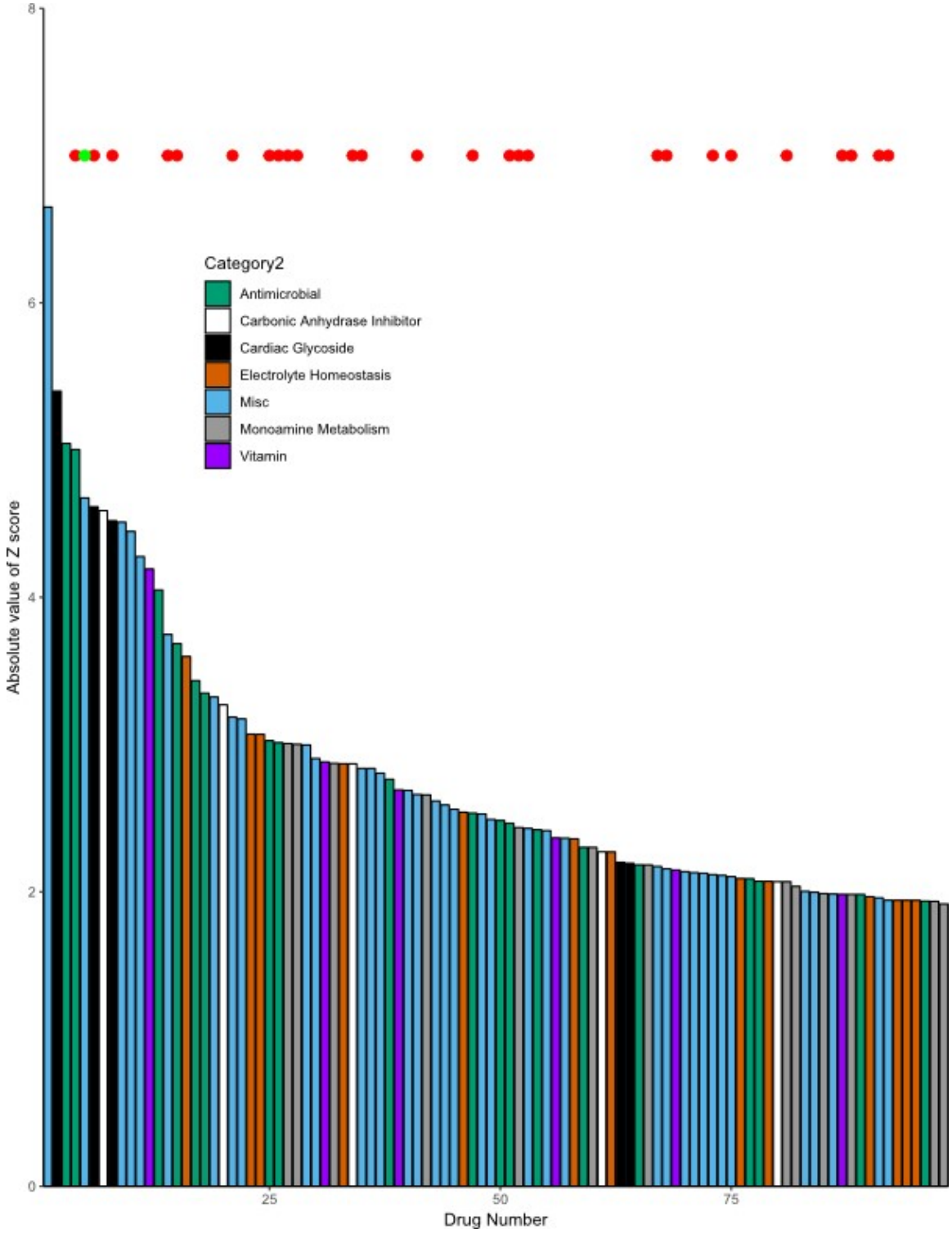

Figure 3.5. Top 98 screened drugs inhibiting SG formation. Drugs are displayed in order of descending effect by Z score, and bars are colour-coded by drug class. Data is displayed as absolute value of Z score as these drugs resulted in negative Z scores due to

the presence of fewer granules compared to control wells. Red dots denote drugs having a high likelihood of being false positive on the initial screen based on cross referencing with the dissolution screen. The green dot represents cycloheximide, a known inhibitor of SG formation (positive control).

were apparent regarding specific drug classes. Alexidine dihydrochloride was a potent inhibitor of SG formation, with complete absence of SGs during screening, correlated with a large decrease in cell viability. Cycloheximide, a known inhibitor of SG formation, was included in the drugs that screened positive. A complete list of the top 100 drugs inhibiting dissolution and the 98 drugs that inhibited SG formation can be found in **Appendix 1.**

3.4 Raloxifene Prevents Stress Granule Dissolution Following Hypoxia

Three drugs from both the formation and dissolution screens were selected to confirm their observed effects on SGs (selected as shown in **Figure 3.3**). None of the drugs selected for additional testing in the formation screen prevented SG formation at the selected screening doses. Alexidine continued to exhibit a strong inhibitory effect on SG formation, but most of the cells failed to survive treatment at the screening doses; further testing at a lower dose range is needed. For dissolution candidates, two of the drugs also failed to prevent SG dissolution on further testing. The SERM raloxifene, however, did prevent SG dissolution following hypoxia.

To test the effects of raloxifene on SG dissolution, U251 cells were treated with raloxifene for one hour prior to a two-hour incubation in hypoxia, and then allowed to recover for one hour following release from hypoxia before being fixed and stained for SG components. Raloxifene was administered at doses ranging from 0 to 60 μM in 10 μM intervals. A second set of cells received raloxifene across the same range of doses for the same time period, but instead of a two-hour hypoxia incubation, were instead incubated in normoxia. This second set served as a control for the isolated effects of raloxifene on the U251 cells. In each hypoxic treatment group, some cells were fixed and stained immediately to confirm that hypoxia had indeed induced SGs.

Following release from short-term hypoxia, SGs are present in U251 cells that are immediately fixed and stained for key SG components TIAR and FMRP. However, at one hour post-release, SGs have dissolved. With the addition of raloxifene at the screening dose (30 μM), SGs persist in the cytoplasm at one hour following hypoxic release, and this finding is amplified with a 60 μM dose (**Fig 3.6A**). When comparing cells stained at one hour following release from hypoxia in the presence or absence of raloxifene, the increase in percentage of cells that remain positive for SGs reaches

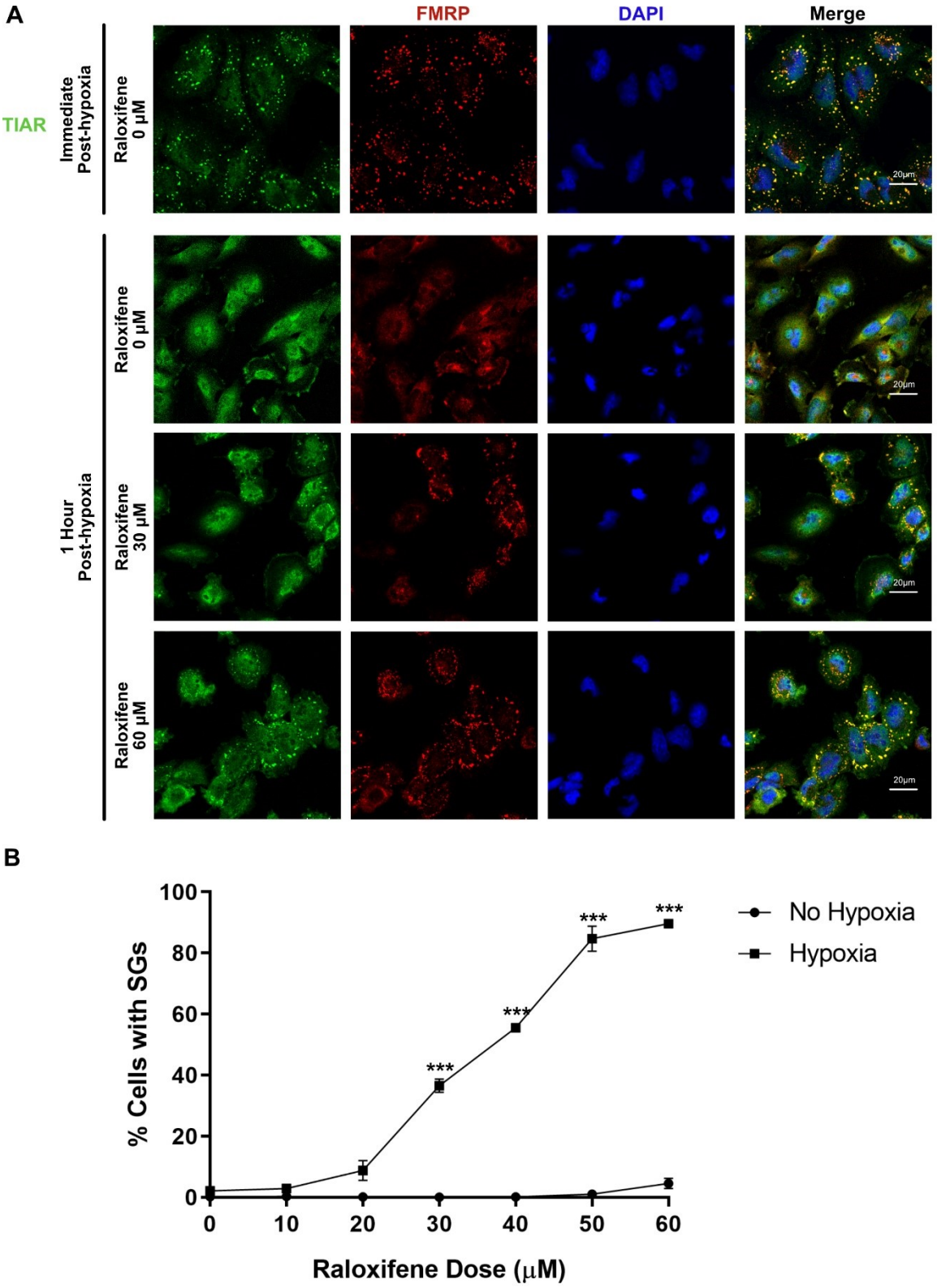

Figure 3.6. Raloxifene inhibits dissolution of hypoxia-induced SGs in a dose-dependent manner. U251 cells were treated with raloxifene at doses ranging from 0 to

60 μM for one hour prior to a two-hour hypoxic incubation. Cells were then recovered for one hour, and then fixed and stained for TIAR and FMRP. A second set of cells were administered raloxifene but were not incubated in hypoxia to assess for the isolated effects of raloxifene. **(A)** U251 cells examined by immunofluorescence against SG nucleating proteins TIAR and FMRP. Cells were stained immediately following release from hypoxia to demonstrate the normal SG response. Cells were also stained at one hour following release from hypoxia with varying doses of raloxifene to assess for inhibition of SG dissolution. **(B)** Quantification of data in (A), with additional raloxifene doses at 10 μM intervals. Comparison is made to cells treated with raloxifene in a non-hypoxic environment. Statistical analysis using the Holm Sidak method, performed on Prism8. Data presented as mean ± SEM (N=3 biological replicates). ***$p<0.001$.

statistical significance at the screening dose of 30 μM, and the effect increases with increasing drug dose to reach a relative plateau around the 50 μM dose (**Fig 3.6B**). A dose of 40 μM was selected for subsequent testing as it elicited a significant SG response, but remains on the upwards curve, allowing for easier detection of differences between various treatments. Additionally, 40 μM likely approximates the dose at which there is a 50% inhibitory response (IC_{50}) on SG dissolution based on **Figure 3.6B**.

After confirming that raloxifene prevented the dissolution of SGs formed in hypoxia, we were interested in characterizing the difference in the dynamics of SG dissolution following release from hypoxia in the presence and absence of raloxifene. To accomplish this, cells were once again subjected to hypoxia for two hours, and then fixed and stained at 15-minute intervals following release from hypoxia to a maximum of two hours. One set of cells was pre-treated for one hour prior to hypoxia with raloxifene (40 μM), and another set did not receive the drug. The rate of SG dissolution following hypoxia was significantly slower in cells pre-treated with raloxifene (**Fig 3.7**). Immediately following release, cells exhibit a robust SG response irrespective of the presence of raloxifene. However, at every following time point, the percentage of cells with SGs is significantly higher in raloxifene-treated cells. Stress granules have completely dissolved by 30 minutes following release in untreated cells while 71.0 ± 14.4% (mean ± SEM) still have SGs at two hours following release in cells treated with raloxifene.

3.5 Combination Raloxifene and Hypoxia Causes Synergistic Killing of Astrocytoma Cells

Further testing confirmed that raloxifene inhibits the dissolution of hypoxia-induced SGs; if SGs are indeed a targetable pathway for GBM treatment, then administration of raloxifene in a hypoxic setting should increase astrocytoma cell death. A prolonged course of hypoxia (12 hours) was used to mimic chronic tumour hypoxia. Two different methods were used to assess cell viability: direct cell viability counts and reduction of Presto Blue following treatment protocols. The only alteration in treatment protocols between earlier dose-response and dissolution rate experiments was lengthening of the period of hypoxia – raloxifene was dosed at 40 μM for a one-hour pre-hypoxia incubation and remained on cells until they were analyzed following release

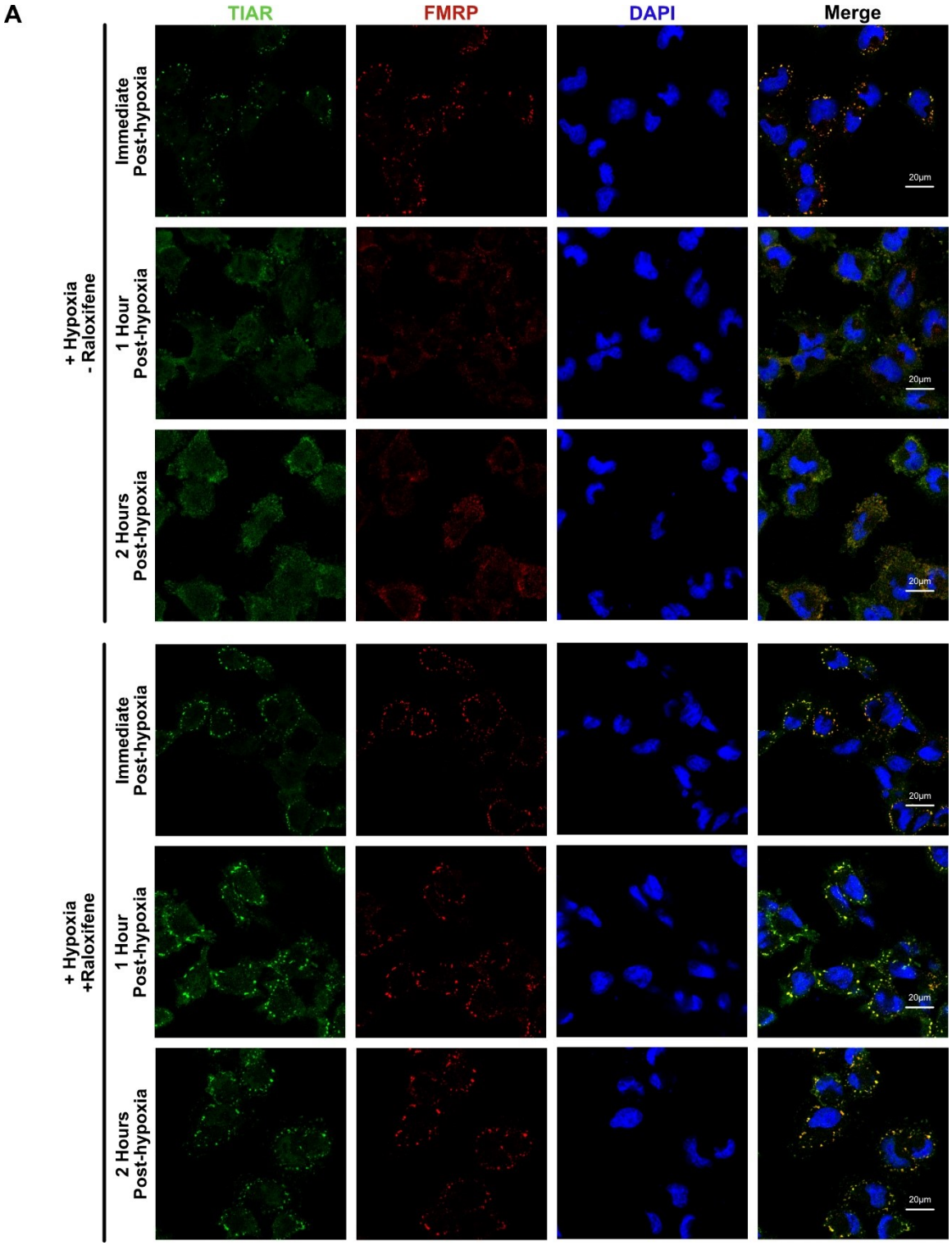
A
TIAR
FMRP
DAPI
Merge
+ Hypoxia
- Raloxifene
Immediate
Post-hypoxia
1 Hour
Post-hypoxia
2 Hours
Post-hypoxia
+ Hypoxia
+Raloxifene
Immediate
Post-hypoxia
1 Hour
Post-hypoxia
2 Hours
Post-hypoxia
20µm

B

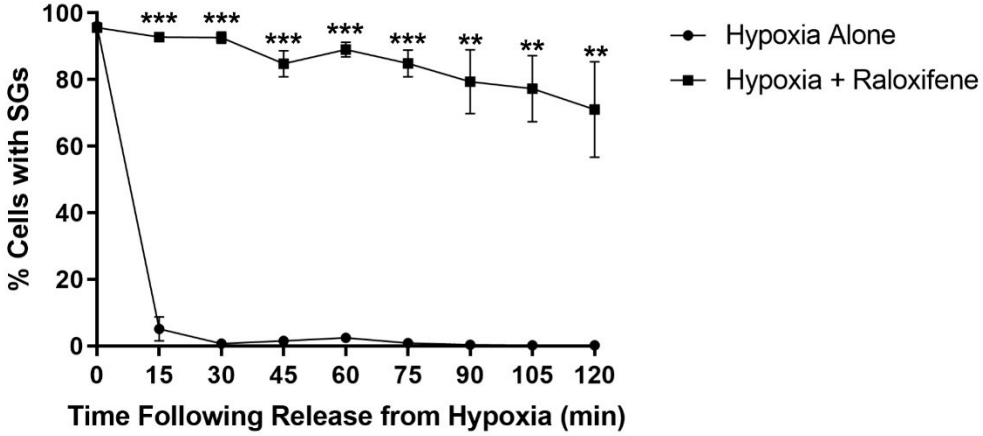

Figure 3.7. SGs persist for up to two hours following release from hypoxia in raloxifene-treated cells. U251 cells were incubated in hypoxia for two hours, and then fixed and stained for TIAR and FMRP at 15-minute intervals to observe rates of SG dissolution. One set of cells received raloxifene (40 μM) for one hour prior to hypoxic incubation to assess the effects of raloxifene on SG dissolution rates following release from hypoxia. **(A)** U251 cells examined by immunofluorescence against SG nucleating proteins TIAR and FMRP. Cells were fixed at 15-minute intervals following release from hypoxia (2 hours) with or without pre-treatment with raloxifene (40 μM). **(B)** Quantification of data in (A) for all time points up to 2 hours. Statistical analysis using the Holm Sidak method, performed on Prism8. Data presented as mean ± SEM (N=3 biological replicates). ***$p<0.001$, **$p<0.01$.

from hypoxia. Cells were analyzed immediately following release from hypoxia, either by counting viable cells using a hemacytometer, or by addition of Presto Blue reagent. Cells that were treated with hypoxia or raloxifene independently had post-treatment viability rates of 53.2 ± 6.5% (mean ± SD) and 48.4 ± 6.1% respectively (**Fig 3.8A,B**). However, pre-treatment of hypoxic cells with raloxifene resulted in a marked drop in post-treatment viability, with only 11.7 ± 2.3% of cells remaining viable. This represents a synergistic effect with combination treatment and was statistically significant when comparing combination treatment to each individual treatment alone ($p = 5 \times 10^{-4}$ for hypoxia, $p = 6 \times 10^{-4}$ for raloxifene). Viability in cells treated with DMSO (vehicle) prior to hypoxia was 43.7 ± 0.7%, and this was statistically different from combination treatment ($p = 2 \times 10^{-5}$), but not hypoxia alone ($p = 0.07$), suggesting the effect is from raloxifene and not the DMSO in which it was dissolved.

To confirm the effect of raloxifene on cell death in hypoxia, the Presto Blue assay demonstrated lower rates of Presto Blue reduction in combination treatment (29.4 ± 2.1%) than either hypoxia (45.0 ± 5.5%) or raloxifene (39.3 ± 7.0%) alone (**Fig 3.8C**). The difference between combination treatment and hypoxia alone was statistically significant ($p = 0.01$), but the difference between raloxifene alone and combination treatment only trended towards positivity ($p = 0.08$), unlike the viability data. The hypoxic DMSO treated cells had a 46.5 ± 5.3% reduction is Presto Blue, which was again statistically different from combination treatment ($p = 0.007$), but not hypoxia alone ($p = 0.23$). Taken together, the cell death assays performed provide evidence for increased cell killing by combination treatment, with a synergistic effect noted in direct cell viability assessment.

3.6 Apoptosis and Autophagy are Activated in Combination Treatment

The preceding experiments have shown that raloxifene can prevent the dissolution of SGs following release from hypoxia, and that the combination of raloxifene and hypoxia increases cell death in chronic hypoxia. The final question investigated were mechanisms of cell death in experimental conditions. Apoptosis and autophagy are two prominent mechanisms by which chemotherapeutics cause non-necrotic cell death and are amenable to experimental detection; therefore, we chose to investigate these mechanisms.

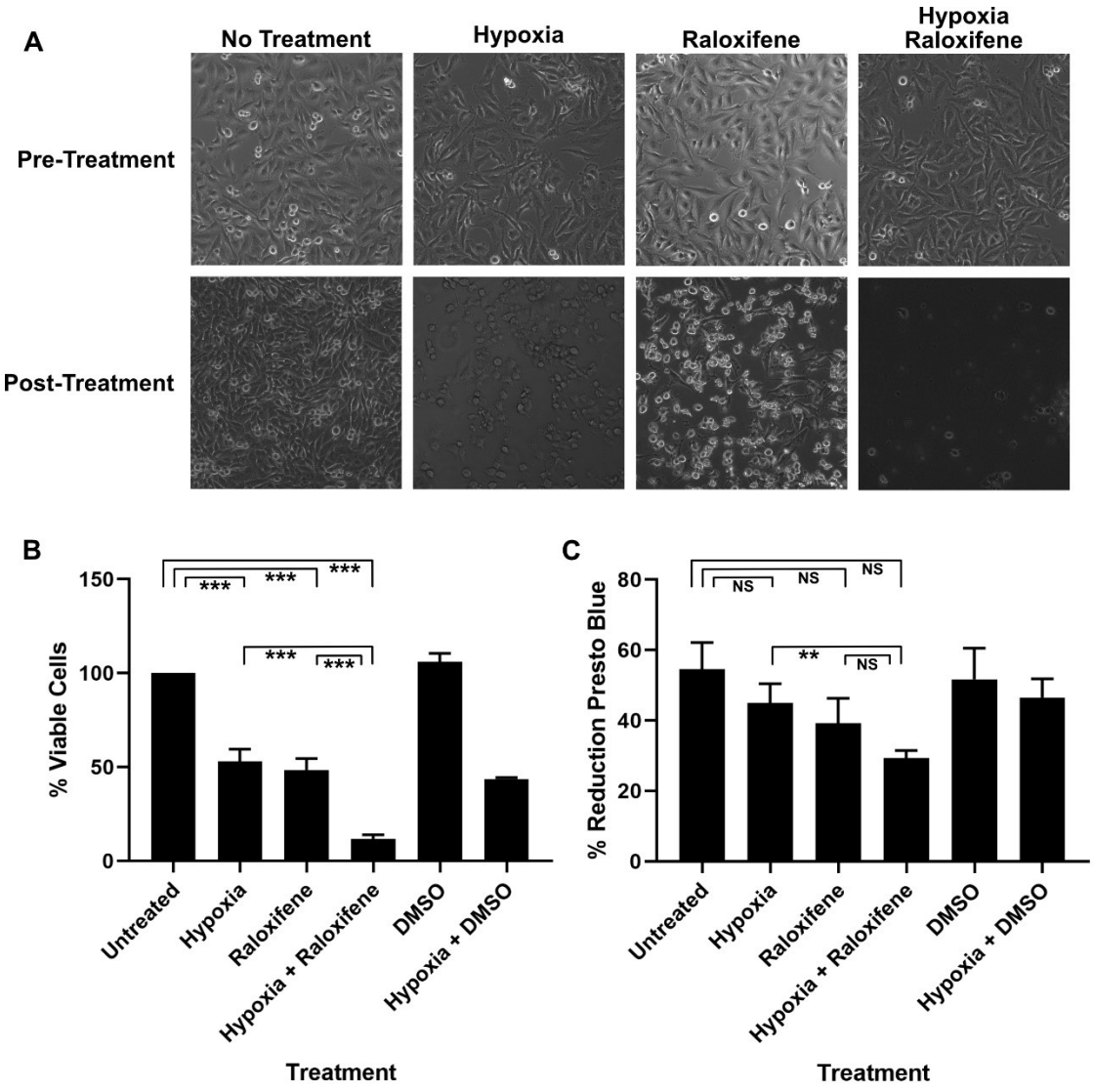

Figure 3.8. The combination of hypoxia and raloxifene results in synergistic astrocytoma cell death. (A) U251 cells before and after treatment visualized with light microscopy. Cells were incubated in hypoxia for 12 hours with or without a 1-hour pre-incubation in media containing raloxifene (40 μM). Raloxifene-treated cells were incubated for a total of 13 hours prior to visualization, without any hypoxic incubation. Untreated cells were incubated at 37 ºC for 13 hours in between imaging. **(B)** Quantification of data in (A) with addition of vehicle (DMSO) controls. Cell viability was assessed directly by counting the number of viable cells using a hemacytometer. **(C)** Quantification of Presto Blue assay data for cells treated identically to (A) and (B). Statistical analysis using the Holm Sidak method, performed on Prism8. Data presented

as mean ± SD (N=3 biological replicates for all experiments). ***p<0.001, **p<0.01, NS = not significant.

To asses the activation of apoptosis in our cells western blotting for levels of cleaved PARP (**Fig 3.9A,B**) and intact caspase 3 (**Fig 3.9C,D**) was carried out. Uncleaved caspase 3 was chosen instead of cleaved caspase 3 as initial cleaved caspase 3 antibodies were undetectable even in positive control treatments, and a working antibody for uncleaved caspase 3 was readily available from a neighboring lab. Individually, hypoxia and raloxifene resulted in increased levels of cleaved PARP, with 52.9 ± 15.4-fold and 9.7 ± 0.9-fold increase respectively ($p = 0.004$, 8×10^{-5}). However, due to high variability in the data, increase in cleaved PARP did not reach statistical significance compared to untreated cells despite a measured 63.7 ± 38.7-fold increase ($p = 0.05$) in combination treatment. There was also no statistically significant difference in fold change between combination treatment and hypoxia alone ($p = 0.68$) or raloxifene alone ($p= 0.07$). Evaluating caspase 3, the assumption was made that activation of apoptosis would result in a decrease in uncleaved caspase 3 as cleavage is required to initiate apoptosis. Individual treatment with hypoxia or raloxifene resulted in a 0.78 ± 0.14-fold and 0.55 ± 0.31-fold change respectively, with neither found to be a significant drop ($p = 0.05, 0.06$). Combination treatment, however, resulting in a 0.29 ± 0.04-fold change in uncleaved caspase 3, representing a significant decrease compared to untreated cells ($p = 9 \times 10^{-6}$). Contrary to cleaved PARP data, the decrease in caspase 3 seen with combination treatment was significantly different from the decrease from hypoxia alone ($p = 0.004$), but not different from the decrease with raloxifene alone ($p = 0.22$).

Activation of autophagy was assessed by western blotting against LC3I/LC3II (**Fig 3.10A,B**) and p62 (**Fig 3.10C,D**). LC3I is converted to LC3II at the initiation of autophagy, so measuring the ratio of LC3II to LC3I can be used to look for increased activation of autophagy. However, p62 is degraded during autophagy, hence it can be used to assess autophagic flux. The ratio of LC3II:LC3I was 0.39 ± 0.05 for untreated cells, 1.50 ± 0.21 for hypoxic treatment, 2.91 ± 0.88 for raloxifene treatment, and 3.57 ± 0.68 for combination treatment. Hypoxia or raloxifene alone, as well as combination treatment, all resulted in an increase in activation of autophagy over untreated cells ($p = 9 \times 10^{-4}$, 0.008, 0.001 respectively). Autophagic activation was statistically different between cells treated with combination treatment compared to

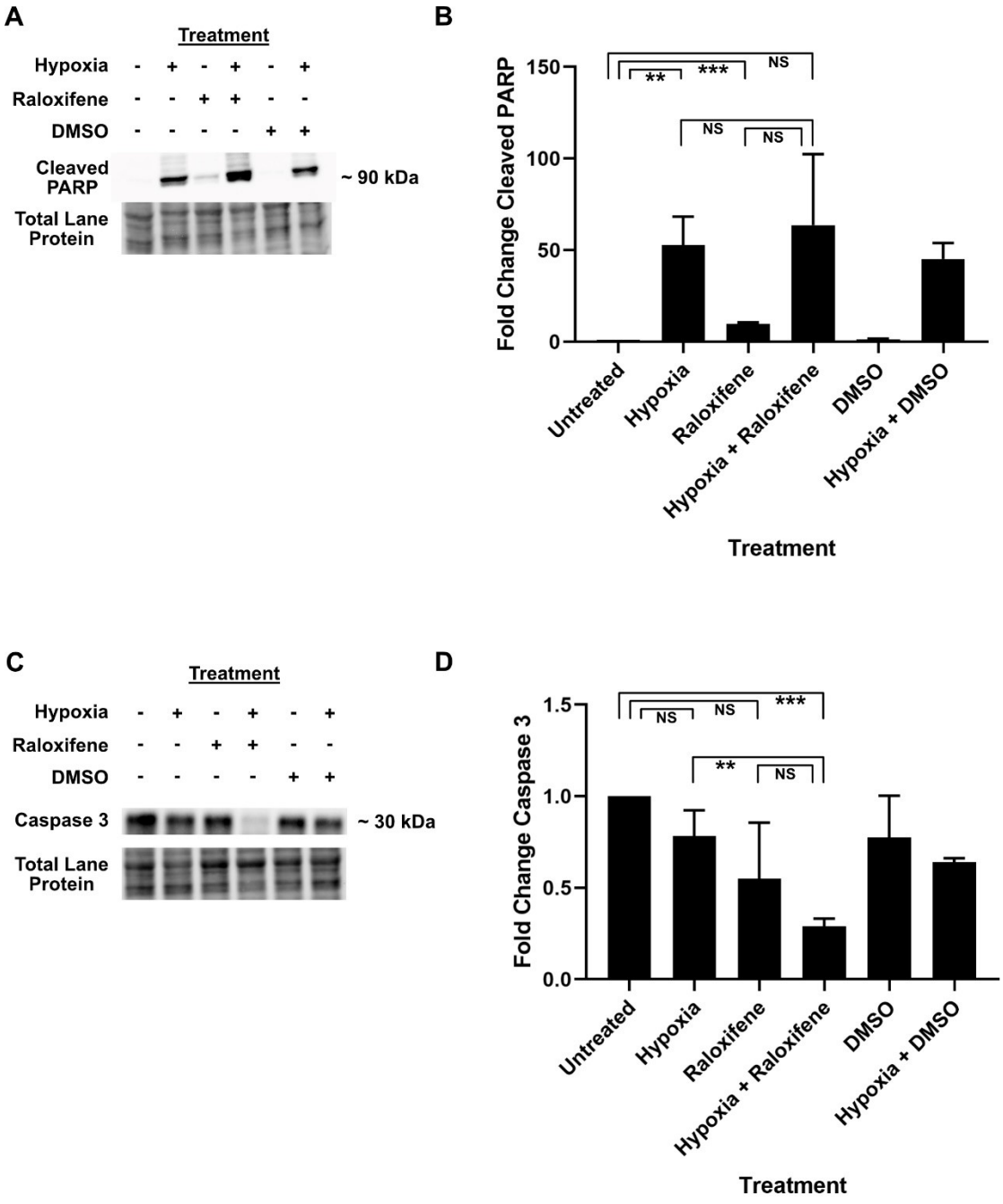

Figure 3.9. Apoptosis is activated in combination treatment. (A) Representative western blot against cleaved PARP in U251 cells. Cells were treated with raloxifene (40 μM, 13 hours), hypoxia (12 hours), or combination with DMSO used as vehicle control. Cells were lysed and protein was harvested immediately following release from hypoxia, or after 13 hours in cells that were not treated with hypoxia. **(B)** Quantification of cleaved PARP western blot data. **(C)** Representative western blot against caspase 3 in

U251 cells. Experimental protocol was identical to (A). **(D)** Quantification of caspase 3 western blot data. Statistical analysis using the Holm Sidak method, performed on Prism8. Data represented as mean ± SD (N=3 biological replicates for all experiments). ***p<0.001, **p<0.01, NS = not significant.

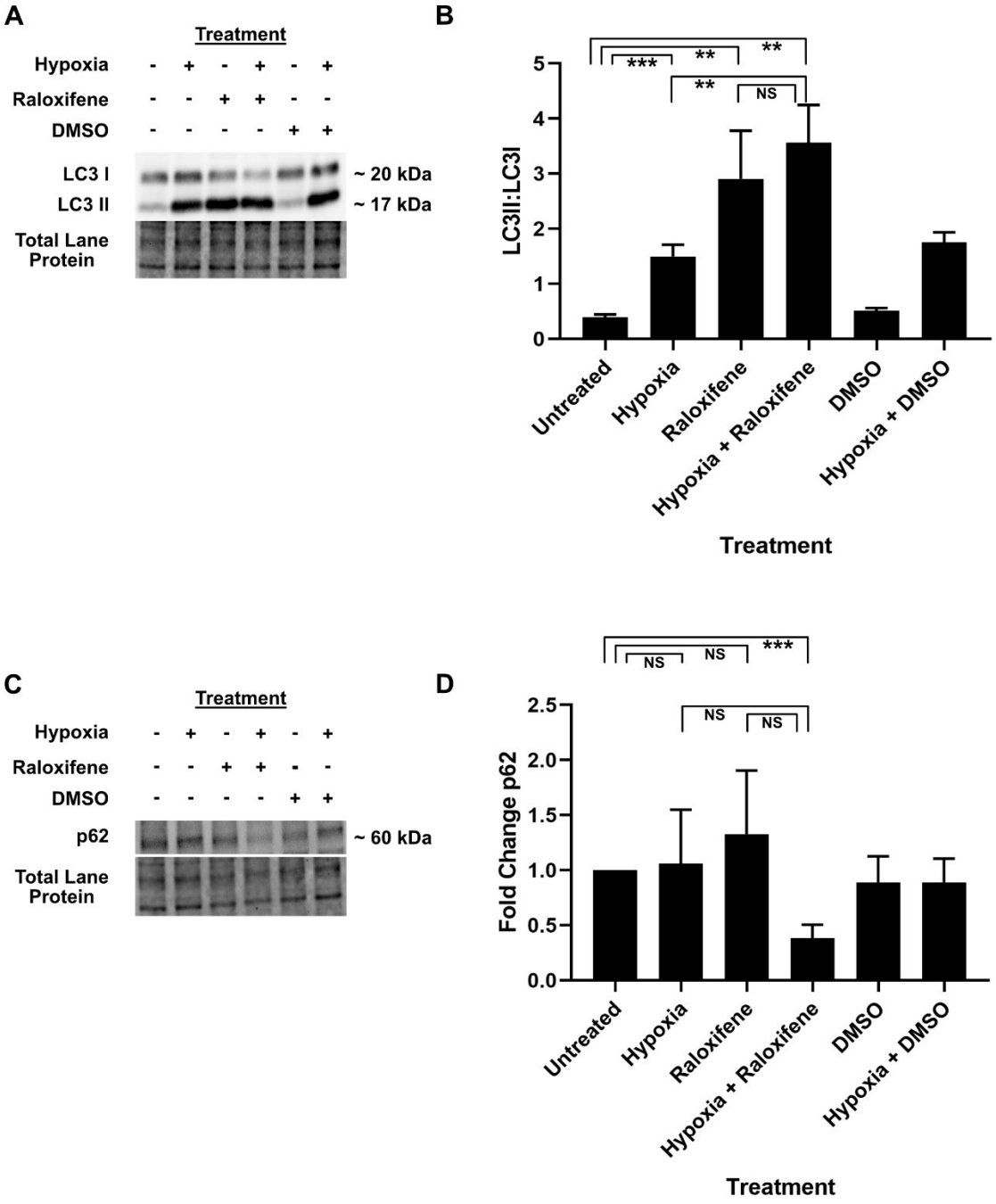

Figure 3.10. Autophagy is activated in combination treatment. **(A)** Representative western blot against LC3I and LC3II in U251 cells. Treatment was identical to cells in **Figure 3.9**. **(B)** Quantification of LC3 western blot data. **(C)** Representative western blot against p62 in U251 cells. **(D)** Quantification of p62 western blot data. Statistical analysis using the Holm Sidak method, performed on Prism8. Data presented as mean ±

SD (N=3 biological replicates for all experiments). ***p<0.001, **p<0.01, NS = not significant.

hypoxia alone ($p = 0.007$), but not raloxifene alone ($p = 0.36$), suggesting the effect may be primarily driven by raloxifene treatment. Raloxifene treatment demonstrated higher autophagic activation than DMSO (LC3II: LC3I 0.51 ± 0.05, $p = 0.009$), and combination treatment with raloxifene compared to DMSO followed the same trend (LC3II:LC3I 1.75 ± 0.18, $p = 0.01$) confirming the effect is from raloxifene and not DMSO. When measuring autophagic flux, neither hypoxia nor raloxifene treatment alone resulted in a decrease in p62 (1.05 ± 0.49-fold change, $p = 0.84$; 1.33 ± 0.58-fold change, $p = 0.38$); however, combination treatment did result in a statistically significant decrease in p62 (0.38 ± 0.12-fold change, $p = 9 \times 10^{-4}$). Once again, due to variability in triplicate values, there was no significant difference between autophagic flux in combination treatment compared to hypoxia alone ($p = 0.08$) or raloxifene alone ($p = 0.05$). Overall, western blot data was variable and although trends are detected confident interpretation of the results will require additional replicates.

CHAPTER 4: DISCUSSION

This project has investigated the role of stress granules in the survival of astrocytoma cells in a hypoxic environment. Stress granules were identified in human GBM tissue *in vivo*, and GBM was confirmed to have higher expression of SG-related mRNA than lower grade astrocytoma by review of TCGA data. A drug screen identified several currently marketed drugs that interfere with the formation and dissolution of SGs, and further screening of the initial drug hits identified the SERM raloxifene as an inhibitor of SG dissolution following induction of SGs by hypoxia. The number of cells containing SGs after recovery from hypoxia was higher in cells receiving raloxifene during hypoxia than in cells that did not receive the drug. In addition, rates of SG dissolution were much slower in the presence of raloxifene, as evidenced by the presence of SGs in up to 80% of cells at two hours in drug treated cells, compared to the relative absence of SGs at 30 minutes in cells treated with hypoxia alone. When cells were treated with raloxifene in the setting of chronic hypoxia, cell death rates increased synergistically compared to either treatment with hypoxia or raloxifene alone, suggesting there is an interaction between the two treatments that is itself detrimental to GBM cells. Finally, activation of both the apoptosis and autophagy pathways provides a potential mechanism for cell death under treatment conditions.

4.1 Stress Granules May Play a Role in Glioblastoma Pathogenesis

At the time of writing, there have been no published studies demonstrating the presence of SGs in human tissues *in vivo*. As SGs are a relatively recent discovery, most studies have been conducted in cell culture or in xenograft models using various non-primate organisms. In order to posit that SGs play a role in tumour cell survival and treatment resistance in GBM, it must first be established that they are present in these tissues *in vivo* and evidence must be provided for a correlation between tumour biology and SG expression and function. The current work provides some early evidence to support this assertion.

One of the first experiments conducted during this research was the staining of human tissues for the presence of SGs. As the research was conducted in conjunction with the Division of Neurosurgery, direct access to human tissue was possible. Tissue samples were taken directly from the OR at the time of tumour resection and embedded

in paraffin to allow for staining. Most of the tumour tissue stained for TIAR demonstrated diffuse staining, but some areas showed puncta within the cells, suggesting that some tumour regions were developing SG-like structures. As mentioned, this is the first example of SG-like structures detected in human tissues *in vivo* at the time of writing and their presence in human tissue allows for the possibility that they may be protective to tumour cells.

While this experiment showed the presence of SGs in tumour tissue and provides evidence for the formation of SGs in human GBM, it is unclear as to the trigger for SG production. Tumour tissue was placed in ice cold PBS after removal in the OR, and then embedded in paraffin and maintained in culture until fixation. The presence of SGs may be due to hypoxia within certain regions of tumour, nutrient starvation during culture, or any other number of stressors that the tissue might have been subject to between intraoperative removal and the final staining process. As mentioned, most of the tissue did not demonstrate granular TIAR staining suggesting that some stressor was acting locally in regions that did demonstrate granules. Nevertheless, demonstration of the ability of human GBM tissue to generate SG-like structures is a novel finding.

Definitive demonstration that SGs are forming in response to hypoxic stress in human GBM will require further experimentation. One possible protocol would involve subjecting tissue slices to hypoxia via incubation in the hypoxia chamber and staining for SGs as was done in cell culture. Ideally, one would like to demonstrate intra-tumoural hypoxia as a trigger for SG induction; immediate fixation of tumour tissue at the time of removal in the OR might provide a means of making this connection. However, it is difficult to predict how surgery might alter tumour tissue hypoxia or even SG dynamics. Intra-tumoural hypoxia might no longer be present once tumour resection has begun, and as it has been shown that hypoxia-induced SGs dissolve within 30 minutes, acquiring and fixing hypoxic tissue within 30 minutes of craniotomy might not be a reliable or reproducible possibility. Co-staining tissues for SG proteins and HIF or VEGF might help to correlate regions of relative hypoxia with SG formation and indirectly link the two processes in human GBM tissue.

It should be noted that in this experiment, tumour tissue was only stained for TIAR. Co-localization of two or more SG-specific markers would strengthen the

assertion that it is indeed SGs that have been identified in this tissue. Ideally, fluorescence in situ hybridization (FISH) to identify mRNA contained within granules should be done to definitively confirm SG presence, and future experiments will attempt this once the tissue slice culture and staining protocols have been optimized.

In addition to staining human tissue directly for SG components, a review of the TCGA database was conducted to provide evidence for SG functionality in human astrocytoma. Key mRNA involved in all stages of the SG life cycle are expressed in astrocytoma, and for many of the mRNA tested, increased expression is seen with increasing tumour grade. This demonstrates a correlation between SG function and increased tumour aggression, although the mechanism of this correlation is unclear. Higher grade tumours demonstrate increased growth rates and are therefore subject to higher levels of microenvironment-related stress, so it is not surprising that adaptive mechanisms are activated in proportion. However, given the proposed role of SGs in the regulation of mTOR and HIF signalling, increased SG cycling may in fact have a partially causative role in increased tumourigenicity. In any case, the presence of SGs in human GBM tissue and the increased expression of SG-related mRNA in high grade tumours identifies SGs as potential targets in GBM. Further studies should be done to characterize the role of SGs in GBM progression.

4.2 Interesting Avenues for Further Research Identified in the Drug Screen

The drug screen conducted focused on drugs that are already tested in humans and currently available. Under these circumstances, any drug shown to successfully inhibit either the formation or dissolution of SGs and have an impact on tumour cell survival in cell culture experiments could be immediately entered into a phase III study as safety and dosing trials have been previously conducted. Given the length of time typically required for a newly developed drug to be approved for use in humans, and the severity and rapid progression of GBM, a truncated timeline from testing to human use is an attractive notion. In addition, large scale drug screening may prove useful in elucidating mechanisms involved in SG metabolism by identifying patterns in drug classes inhibiting SG formation and dissolution, which is of particular interest as this field is relatively new. The Prestwick drug library has been cited in over 300 publications, and has previously

been used to repurpose drugs toward cancer treatment (Varbanov *et al.*, 2017) and specifically in identifying drugs with activity in GBM (Dong *et al.*, 2017).

In the initial screen, 98 drugs screened positive as inhibitors of SG formation. After removing candidates with a high probability of false positivity, 72 drugs remained as possible SG formation inhibitors. Of these drugs, three drug classes were highly represented. Various classes of antibiotic accounted for eight of the 72 hits, vitamins represented a further five hits, and six more positive hits were accounted for by cardiac glycosides. From a mechanistic perspective, the antibiotics and vitamins represent multiple different drug mechanisms and thus these classes are unlikely to provide insights into the dynamics of SG formation. The cardiac glycosides act to increase cardiac contractility by binding to and inhibiting the Na^+/K^+ ATPase, leading to increased intracellular concentrations of Na^+ and, consequently (in cardiac myocytes), increased intracellular Ca^{2+}. In GBM cells, the Ca^{2+} concentration would not be expected to change due to the lack of a sarcoplasmic reticulum, but the drugs may be affecting the concentration of Na^+. Interestingly, metolazone and torsemide, diuretics that act by blocking the Na/Cl cotransporter and Na/K/Cl symporter respectively, also showed a decrease in SG formation in the drug screen. Both of these drugs would act to decrease intracellular Na^+ concentrations, somewhat paradoxical to the activity of the cardiac glycosides. However, the Na^+/K^+ ATPase has been found to serve multiple functions apart from electrolyte homeostasis, including the regulation of multiple functions involved in cancer biology (Venugopal and Blanco, 2017), and GBM has been shown to express isoforms more highly involved in these oncogenic functions (Rotoli *et al.*, 2017), Thus, blockade of this channel may be interfering with SG formation through some mechanism unrelated to electrolyte balance. Cardiac glycosides are being investigated for their potential anti-tumour effects (Schneider *et al.*, 2017), and given the results of the present drug screen, the role of SGs in these findings may provide an interesting avenue for further investigation.

In the formation screen, the drug alexidine dihydrochloride screened positive as a potent inhibitor of SG formation. While most cells that screened positive as inhibitors had very low levels of SGs per cell on average, alexidine was the only drug that had no identified granules in any of the visualized cells. Treatment with alexidine in screening

conditions also caused a significant decrease in the number of viable cells compared to other drugs. The number of counted cells in control wells was averaged at roughly 1555 cells (SD 156 cells). After treatment with alexidine, only 217 cells were viable following hypoxia in the equivalent visualized area. Treatment with alexidine alone also resulted in a decrease in viable cell numbers (1788 counted cells vs an average of 2050 cells in untreated wells), although this was not statistically significant. Alexidine is a bisbiguanide compound commonly found in oral rinses that has been shown to induce apoptosis in cancer cells by compromising the mitochondrial membrane (Yip *et al.*, 2006). One mechanism through which this may be accomplished is inhibition of protein tyrosine phosphatase localized to the mitochondrion 1 (PTPMT1), the inhibition of which has been shown sufficient to induce apoptosis in cancer cells (Niemi *et al.*, 2013). Alexidine has not been studied in glioblastoma to date, and its potent inhibition of SG formation and marked cytotoxic effects in cancer cells in this drug screen represents an interesting prospect for ongoing research.

When investigating SG dissolution, 127 drugs screened positive as inhibitors. With the exclusion of potential false positives, 92 drugs remained as potential dissolution inhibitors. Calcium channel blockers accounted for five of the positive hits, and six anticholinergic drugs also prevented SG dissolution. However, 39% of hits (36 drugs) were accounted for by drugs involved in monoamine signalling (after removal of potential false positives). There were some paradoxical hits in this screen, with both dopamine agonists and antagonists being highly represented (five and eight drugs respectively). These results are interesting as acetylcholine and the monoamines are all highly active in the brain as neurotransmitters and neuromodulators, and release of many of these molecules is dependent on calcium influx at the axon terminal. The investigation on the role of monoamines in GBM metabolism is relatively new, and a recent review has summarized some of the most promising data (Caragher *et al.*, 2018). Most interesting are the conflicting findings that dopamine can enhance tumour cell proliferation by activating extracellular signal-regulated kinase (ERK), a downstream effector of EGFR (Li *et al.*, 2014), but also limits growth by inhibiting the activity of VEGF and thus angiogenesis (Basu *et al.*, 2004). Thus, research focusing on the role of VEGF suggests that dopamine agonism may be helpful in GBM treatment while studies investigating

dopamine's effects on ERK would favor dopamine antagonism to counter the proliferative actions of ERK activation. As both drug classes impair SG dissolution, the interaction of dopamine and SG metabolism may provide some sort of unifying mechanism for dopamine's activity in GBM, and further investigation is warranted.

4.2.1 Pyruvate Dampens Stress Granule Formation in Hypoxia

While conducting the drug screen, an interesting complication occurred which provided some insight into SG dynamics in hypoxia. Stress granules were reliably induced after two hours of hypoxic incubation in the Weeks laboratory at Dalhousie University. However, the same experimental protocol, when carried out in the Roberge laboratory at University of British Columbia, failed to produce SGs. After examining the protocol and materials more completely, a difference in culture media was detected. The DMEM in the Roberge lab contained pyruvate, while the DMEM in the Weeks lab did not. Upon purchasing media without pyruvate, the protocol was once again successful at inducing SGs in cell culture. To confirm the effect, pyruvate was added to the pyruvate-absent media, and once again, SGs did not form. Pyruvate has direct antioxidant effects through scavenging of peroxides and peroxynitrites, and indirectly by increasing flux through the hexose monophosphate pathway which leads to NADPH production and glutathione recycling (Liu *et al.*, 2011). In this way, pyruvate might serve to buffer oxidative stress caused by hypoxia and delay SG formation. While this work was not further investigated, it might have implications in the study of SG dynamics, and bears mentioning. In addition, this finding must be considered when analyzing the drug screen data for the drugs that screened positive as inhibitors of SG formation; care must be taken to differentiate between drugs that have prevented SG formation by simply buffering the oxidative stress experienced by cells (similar to pyruvate) and those that interfere with the biochemical processes leading to SG formation.

4.3 Raloxifene Prevents Dissolution of Hypoxia-Induced Stress Granules

Further testing of select drugs identified during the drug screen yielded a true positive result with raloxifene. Multiple drugs were tested and confirmed to be false positives, but raloxifene significantly impaired SG dissolution following hypoxic stress. Raloxifene, a SERM, is approved for use in estrogen receptor-positive breast cancer and post-menopausal osteoporosis. When administered to U251 cells prior to hypoxic stress,

raloxifene inhibited SG dissolution in a dose-dependent manner. When comparing rates of SG dissolution following release from hypoxic stress in the presence and absence of raloxifene, SGs dissolve within 30 minutes in the untreated condition, but persist beyond two hours in the presence of raloxifene.

An important distinction that must be made in these experiments is differentiation between inhibition of SG dissolution and induction of SG formation. During all experiments, raloxifene was added to the cultured cells which were then incubated for one hour to allow the drug to take effect prior to hypoxic incubation. Following release from hypoxia, cells were maintained in media containing raloxifene until they were fixed and stained, up to two hours in the dissolution rate experiments. In this experimental setting, either inhibition of SG dissolution or induction of SG formation by raloxifene would result in more SGs present following release from hypoxia. However, during the initial screen and in further testing, raloxifene alone failed to induce SGs in the absence of hypoxia (**Fig 3.6**), suggesting that raloxifene is not inducing SG formation but rather preventing the dissolution of hypoxia-induced SGs. Additionally, if some interaction between raloxifene and hypoxia is in fact responsible for inducing SG formation, one would expect a higher number of cells expressing SGs immediately following removal from hypoxia in the presence of raloxifene compared to hypoxia alone. This was not demonstrated in the dissolution experiments, with approximately 95% of cells in both groups expressing SGs following hypoxia (**Fig 3.7**). These experiments will be repeated using a metric of number of SGs per cell to confirm that the SG response is not more robust on a cellular level. This was not carried out in the current work due to the lack of reliable granule counting software, but development of a CellProfiler pipeline for this purpose is currently underway in the laboratory.

4.4 Raloxifene Increases Astrocytoma Cell Death in Experimental Conditions Mimicking Tumoural Hypoxia

The addition of raloxifene to astrocytoma cells in the setting of hypoxic stress had a marked cytotoxic effect. While both hypoxia and raloxifene alone resulted in an approximately 50% cell death rate, the combination killed close to 90% of cells. This represents a synergistic effect between raloxifene and hypoxia, suggesting an interaction between the two treatments is in part responsible for cell death. Increased death rates

were confirmed using the Presto Blue assay. As reduction of Presto Blue is non-linear with cell numbers (Sonnaert *et al.*, 2015), it is more difficult to determine synergy with this assay. Additionally, Presto Blue reduction is dependent on mitochondrial function, which can be impaired in hypoxia; this introduces a possible bias as cell viability may be underestimated in cells exposed to hypoxia. The experiment did, however, demonstrate a statistically significant increase in cell death with combined treatment over hypoxic treatment, with a trend to significance over isolated raloxifene treatment. Unfortunately, due to variability in the data and a small number or experimental replicates, significance was not reached between any treatment and untreated cells. More replicates are likely required to demonstrate statistically significant results.

Further testing should be conducted to confirm cell death rates in combination treatment. Counting cells by hand may be associated with some bias and is subject to human error; however, without access to more stringent cellomics-based assays, it provided the most accurate estimate of cell death rates in these experiments. Consensus between hand-counted cell numbers and Presto Blue strengthens this finding. Fluorescence-activated cell sorting (FACS) with annexin V and propidium iodide (PI) would not only confirm higher death rates in co-treated cells but would also differentiate between cells undergoing apoptotic versus necrotic death, providing some insight into the mechanisms of cell death, strengthening the western blotting results.

For cell death experiments, a raloxifene dose of 40 μM was chosen (IC_{50}), and cells were incubated in hypoxia for a period of 12 hours. This raloxifene dose was chosen as it provided a robust SG response in our cells, with between 50 and 60% of cells containing SGs at one hour post-hypoxia. Higher doses did result in a heightened response, but at these doses, close to 90% of cells contained granules, and this might have made detection of differences between varied treatment protocols difficult. This dose was also close to the screening dose of 30μM, which is a standard screening dose and therefore in keeping with protocols published in the literature. A hypoxic period of 12 hours was chosen to mimic more chronic hypoxic states in GBM *in vivo*, as well as for convenience running experiments. As previously mentioned, in GBM, hypoxia is usually fluctuating due to changes in the microenvironment resulting from angiogenesis and cell death; this pattern is difficult to replicate in a cell culture setting, so chronic hypoxia was

chosen as a proof of concept experimental design. True *in vivo* studies in mouse xenograft models will provide a more comprehensive analysis of intra-tumoural hypoxic stress and raloxifene treatment on tumour biochemistry.

4.5 Apoptosis and Autophagy May Contribute to Astrocytoma Cell Death with Combination Treatment

In these experiments, activation of apoptosis was investigated by western blotting for cleaved PARP and caspase 3. Intrinsic apoptosis is triggered by a number of microenvironmental stressors which all act to cause irreversible mitochondrial outer membrane permeabilization (MOMP) by inciting oligomerization of pro-apoptotic members of the B-cell lymphoma 2 (BCL2) family. MOMP leads to release of apoptogenic factors that typically exist in the intermembrane space, which activate the executioner caspases (caspase 3 and 7) via proteolytic cleavage. PARP is a family of proteins involved in a number of protective cellular processes (DNA repair and stability) that is cleaved by executioner caspases and thus inactivated during apoptosis. During apoptosis, one would expect to see a decrease in levels of caspase 3 (due to an increase in the cleaved "activated" form, detected by a different antibody) and an increase in cleaved PARP.

In order to assess activation of autophagy, western blotting was done against LC3 and p62. Autophagy is a system by which cells degrade cytosolic proteins and organelles for recycling of base components, but over-activation can lead to cell death (Denton *et al.*, 2012; Denton *et al.*, 2015). The process begins with formation of autophagosomes that engulf cytosolic components to be degraded. During this process, the cytosolic form of LC3 (LC3I) is conjugated to phosphatidylethanolamine (LC3II) which is incorporated into the autophagosome membrane. The autophagosome then fuses with a lysosome to form the autolysosome, where cytosolic products are degraded by the hydrolytic enzymes contained within. Sequestosome 1 (SQSTM1/p62) is a receptor that binds cargo and targets it to the developing autophagosome for degradation and is degraded itself in the process. If autophagy is active, one would expect to see an increase in the ratio of LC3II to LC3I concomitant with a drop in levels of p62. Often, LC3 is used to measure activation of autophagy, and p62 is used to measure autophagic flux as p62 only gets degraded if autophagy completes.

In these experiments, individual treatments resulted in an increase in cleaved PARP above untreated cells, but combination treatment failed to produce a significant increase in cleaved PARP. Somewhat paradoxically, levels of cleaved PARP between individual treatments and combination treatment were not statistically different. Individual and combination treatments resulted in statistically significant activation of autophagy, as determined by western blotting against LC3 isoforms, but only combination treatment caused a significant increase in autophagic flux when p62 levels were investigated. Autophagic activation did not differ between combination treatment and raloxifene treatment alone in these experiments and, paradoxically, autophagic flux did not differ when comparing combination treatment with each individual treatment independently. Overall, the western blotting data demonstrated a high degree of variability, partly owing to a low number of experimental replicates. This makes it hard to draw strong conclusions from this data, and further replicates will be required to lower the variability and strengthen the trends that are observed.

4.6 Selective Estrogen Receptor Modulators

The SERMs are a class of medications that have been designed to alter estrogen signalling in the cell through direct effects on the estrogen receptor. Depending on the cell or tissue type, and on the individual medication, SERMs can act as either estrogen agonists or antagonists (Dhingra, 2001). Tamoxifen was the first SERM to be discovered and remains widely used in estrogen receptor-positive breast cancer (Jaiyesimi *et al.*, 1995). Tamoxifen acts as an estrogen antagonist in breast tissue but due to its activity as an estrogen agonist in bone it has also been used to prevent and treat osteoporosis in post-menopausal women (Powles *et al.*, 1996). However, in pre-menopausal women, tamoxifen has the opposite effect, rather decreasing bone density. In addition, tamoxifen acts as an agonist in uterine and vascular tissues leading to increased risk of endometrial cancer and thromboembolic complications, respectively (Fisher *et al.*, 1994; Fisher *et al.*, 1998). This led to a search for SERMs with lower side effect profiles, and raloxifene was one of the drugs discovered in this process. As a SERM, raloxifene retains the beneficial effects of tamoxifen on breast tissues but demonstrates a reduced risk of endometrial cancer (Runowicz *et al.*, 2011). Consequently, current guidelines recommend either tamoxifen or raloxifene as prophylactic treatment for post-menopausal women at high

risk of developing breast cancer (Levine *et al.*, 2001; Moyer, 2013), although treatment of estrogen receptor-positive breast cancer is still managed primarily by tamoxifen. Raloxifene, however, is widely used in the prevention of osteoporotic fractures in post-menopausal women due to its lower side effect profile.

4.6.1 Estrogen Modulation in Glioblastoma

The initial drug screen identified raloxifene and clomiphene citrate as inhibitors of SG dissolution. Clomiphene is a non-steroidal SERM primarily used in the induction of ovulation through its actions on the estrogen receptor in the hypothalamus. Tamoxifen did not screen positive on the initial screen, but early testing with dose-response experiments has indicated an inhibitory effect on SG dissolution like the SERMS that were positive in the screen, suggesting its absence represents a false negative. False negatives might have occurred during the screen for a number of reasons, including pinning errors or drug breakdown within the library. The roles of sex hormones in aging and neurodegenerative disease is an active area of study, and although research is scarce, a role for estrogen signalling in astrocytoma has also been identified.

Estrogen signalling is transduced by nuclear estrogen receptors which are classified into two categories; estrogen receptor α or β (ERα/β). In cell culture or rat studies, activation of ERs has demonstrated neuroprotective effects in the setting of trauma or ischemia, as well as a number of other chemical or experimental insults (Segura-Uribe *et al.*, 2017). Sex hormones, including estrogens, have also been implicated in neurodegenerative disease and physiologic aging via their influence on mitochondria: as sex steroid levels decrease, mitochondrial function decreases, leading to the processes of physiologic or pathologic neurodegeneration (Gaignard *et al.*, 2017). However, despite this link, the use of SERMS in the treatment or prevention of neurodegenerative diseases has generally failed to prevent or reverse deterioration (Yang *et al.*, 2013; Henderson *et al.*, 2015; Fink *et al.*, 2018). Nevertheless, the possibility that estrogen signalling may be involved in complex neurological processes such as aging is established.

Although their functions in tumour biology remain unclear, estrogen receptors have also been found in astrocytomas (Tavares *et al.*, 2016). In general, ER expression tends to decrease with increasing dedifferentiation and malignancy, with the exception of

isoform ERβ5 which shows higher expression in astrocytoma compared to normal brain. In addition, expression of this isoform increases with increasing histological grade, as opposed to other isoforms which demonstrate a decrease in expression. As most isoforms decrease in higher grade tumours, it's possible that estrogen signalling may play a protective role in astrocytoma. In fact, Li and colleagues found that ERβ5 was induced by HIF signalling and acted to decrease signalling through the mTOR and MAPK pathways, providing further evidence for a protective effect of estrogen signalling (Li *et al.*, 2013). This work supports the hypothesis that the estrogen receptor may have a role in GBM treatment, although mechanistic links between raloxifene treatment and estrogen receptor activation or inhibition is lacking at this stage and should be investigated further.

The use of SERMs in the treatment of GBM is not a novel concept. In fact, tamoxifen was used as primary or rescue therapy prior to the widespread use of temozolomide (Mastronardi *et al.*, 1998; Parney and Chang, 2003). More recently, multiple temozolomide-resistant cell lines showed decreased viability when treated with tamoxifen (He *et al.*, 2015) further supporting a role for SERMS in GBM therapy. Raloxifene has also been tested in astrocytoma cell lines and sensitizes cells and GSCs to temozolomide therapy (Baritchii *et al.*, 2016). Interestingly, in the case of tamoxifen, its mechanism of action in GBM appears to be independent of the estrogen receptor. Early studies into the mechanism of tamoxifen's activity in astrocytoma demonstrated that inhibition of DNA replication occurred in the presence of estradiol flooding, and in ER negative astrocytoma cell lines (Pollack *et al.*, 1990), indicating ER signalling is not involved. Instead, tamoxifen appears to act in an off-target manner through inhibition of protein kinase C (PKC) dependent phosphorylation (O'Brian *et al.*, 1985). Raloxifene's mechanism of action in astrocytoma has not yet been elucidated.

4.7 Determining Raloxifene's Mechanism in Glioblastoma

The present work has shown that raloxifene prevents the dissolution of SGs in astrocytoma cells following hypoxic stress. In addition, raloxifene and hypoxia have a synergistic effect on astrocytoma cell death, suggesting that there is an interaction between the two treatments that enhances cell killing. Taken together, this would suggest that the prevention of SG dissolution may be responsible for this enhanced killing; however, this represents a correlation only, and does not prove that raloxifene's effects

on SG dissolution are responsible for increased cell death. It should also be noted that the exact mechanism of raloxifene's effects, both on SGs and cell death, is also unknown. Raloxifene may be acting through the estrogen receptor or, like tamoxifen, its action may be off target. Further work is required to elucidate these connections.

The first step in exploring raloxifene's mechanism of action in astrocytoma cells is to determine whether it is acting as an estrogen agonist or antagonist, or through some off-target mechanism. Repeating the raloxifene experiments while flooding the media with estradiol would provide some suggestion of raloxifene's mechanism. Abrogation of the observed SG and cell death responses would suggest that raloxifene is acting as an antagonist, and high levels of estradiol are reversing the effects by flooding the receptors and competitively inhibiting raloxifene's actions. If the response is heightened or unchanged, then raloxifene is likely acting as an ER agonist or off-target. Pharmaceutical inhibition of the ER would be expected to mimic the effects of raloxifene if raloxifene is acting in an antagonistic fashion. The compound PHTPP, a pyrazolo[1,5-a]pyrimidine, is a selective ERβ inhibitor (Compton *et al.*, 2004) and has been used to inhibit the receptor in studies involving the CNS (Naderi *et al.*, 2015) and astrocytes in particular (Ma *et al.*, 2016). To confirm if the effect is agonistic, cells can be treated with estradiol in the absence of raloxifene and rates of SG dissolution and cell death following hypoxic stress can be monitored. If raloxifene is acting as an ER agonist, one would expect that estradiol would mimic raloxifene's effects. Failure to demonstrate agonistic or antagonistic effects of raloxifene using these methods would suggest that raloxifene is acting through some off-target mechanism.

4.7.1 Raloxifene's Role in Cell Death

Understanding how raloxifene causes death in astrocytoma cells will be necessary to causally link SG effects with cell death. In my experiments, the combination of raloxifene and hypoxia activated apoptosis and autophagy to a higher degree than individual treatments. Although statistical significance was not reached when looking at changes in caspase 3 and cleaved PARP with combination treatment, trends were present, and a higher number of experiments will likely support activation of apoptosis. Autophagic flux was increased in combination treatment as evidenced by a significant drop in p62, despite the small number of experiments; however, due to a lack of

significant difference between combination treatment and either individual treatment, it is hard to attribute this to combination treatment. Activation of autophagy can contribute to cell death in certain circumstances (Denton *et al.*, 2015), but differentiation between autophagy-dependent cell death (ADCD) and cell death from other mechanisms can be difficult. In addition, as autophagy is known to be necessary for SG clearance, ADCD may be an unintentional result of increased autophagy in an attempt to clear persistent SGs under these experimental conditions rather than an independent process.

The definition of ADCD requires that the autophagic process or some components of the autophagic machinery are directly responsible for cell death (Galluzzi *et al.*, 2018). This implies that situations in which autophagy is activated alongside other mechanisms of cell death, or as a protective response in conditions of cellular stress that may precipitate apoptosis, may not be considered as examples of ADCD. In addition, autophagy may indirectly activate other pathways involved in cell death (Gump *et al.*, 2014; Dey *et al.*, 2016; Hou *et al.*, 2016); in these circumstances, autophagy is not directly responsible for cell death. Shen and Codogno proposed criteria for determining when cell death can be considered to be due to autophagy (Shen and Codogno, 2011) – cell death does not require apoptotic machinery, autophagic flux in increased, and autophagy suppression (pharmacologically and genetically) prevents cell death. My experiments suggest that apoptosis may be activated. Pharmacologically blocking apoptosis with benzoyl-Val-Ala-Asp-fluoromethyl ketone (zVAD), a broad-spectrum caspase inhibitor, could be used to block apoptosis and confirm the role of autophagy in cell death in these experiments. However, zVAD has also been shown to induce autophagy (Vandenabeele *et al.*, 2006) and may therefore be unreliable as a sole measure of autophagic cell death. Genetic knockdown of Bax and Bak, key activators of apoptosis, using either short interfering RNA (siRNA) or CRISPR-Cas9 (clustered regularly interspaced short palindromic repeats) would prove more reliable in this instance, albeit more time consuming. Autophagic flux has been confirmed in my experiments, as evidenced by an increase in LC3II and concomitant decrease in p62 under treatment conditions. Finally, chemical inhibition of autophagy using conventional inhibitors such as 3-methyladenine (3-MA, an inhibitor of autophagy nucleation) or bafilomycin-A (an inhibitor of lysosomal fusion) alone or in combination, or

siRNA/CRISPR knockout of key autophagy-related genes (ATGs), with subsequent rescue from cell death would fulfill the final criterion for confirmation of ADCD.

Analysis of the apoptosis data reveals some interesting trends. When considering individual treatments, both raloxifene and hypoxia elicited a significant increase in cleaved PARP without a concomitant drop in caspase 3 when compared to untreated cells. These results seem contradictory; caspase 3 is an executioner caspase that is responsible for the cleavage of multiple downstream proteins, including PARP. However, caspase 3 is not the only executioner caspase – multiple proteolytic enzymes, including caspase 7, have been found to cleave PARP resulting in cell death (Germain *et al.*, 1999; Bhaskara *et al.*, 2009; Chaitanya and Babu, 2009). Evaluation of caspase 7 levels was not conducted in these experiments and may provide a clearer explanation of apoptosis induction in individual treatment conditions. In addition, as already discussed, due to wide variability in the data and low replicates in western blotting experiments, statistical significance was not reached in some cases where clear trends are present. Further replications will be necessary to fully characterize caspase trends with combined treatment. Lastly, this work has only used western blotting to investigate apoptosis in treated astrocytoma cells. Other apoptosis-specific assays will need to be done to confirm or rule out activation of apoptosis. Galluzzi and colleagues provide a nice review of assays commonly used to identify apoptosis in cell culture (Galluzzi *et al.*, 2009).

Finally, only apoptosis and autophagy were investigated as possible mechanisms of cell death in this work – there exist multiple other mechanisms of cell death that could be contributing to astrocytoma cell death (Galluzzi *et al.*, 2018), and a thorough investigation into these potential mechanisms is warranted going forward. In a sufficiently toxic environment, direct necrosis may be responsible for a proportion of cell death observed. Differentiating necrosis from apoptosis can be accomplished using time-lapse microscopy (provided cells are visualised early during the cell death process), FACS, or electron microscopy (Krysko *et al.*, 2008). Necrosis can further be divided into accidental or regulated subtypes; necroptosis, parthanatos, and mitochondrial permeability transition-dependent regulated necrosis are distinct subtypes of regulated necrosis that can be triggered by oxidative stress, and can be identified based on the

molecular pathways that are affected (Galluzzi *et al.*, 2014). A full characterization of cell death processes exhibited in astrocytoma cells following combination treatment was not the goal of this project but may be pursued with subsequent experimentation.

4.7.2 Raloxifene's Role in Stress Granule Dissolution

In order to explore a causative link between inhibition of SG dissolution and increased astrocytoma cell death, a better understanding of the mechanisms of SG dissolution is needed. As previously mentioned, despite an abundance of literature on the mechanisms behind SG formation, little has been published exploring the way in which SGs dissolve. While this might make it more difficult to establish a causal link between raloxifene's effects on SG dissolution and astrocytoma cell death, it also represents an opportunity to elucidate the mechanisms of SG dissolution. In discovering how raloxifene inhibits SG dissolution, clues may be provided as to how SGs dissolve. Interestingly, although autophagy has been shown to have a role in SG clearance and autophagy inhibitors have been shown to delay SG dissolution, the current work demonstrated a persistence of SGs and activation of autophagy, indicating that raloxifene is not preventing SG dissolution by blocking autophagy, but rather via some other mechanism. Thus, further work to explain how raloxifene is exerting its effects may reveal new insights into the mechanisms of SG dissolution.

An important distinction must be made when interpreting the SG dissolution data in conjunction with the data demonstrating activation of autophagy. These experiments demonstrated a persistence of SGs for up to two hours following release from hypoxia; activation of autophagy was measured at 12 hours following release. Thus, these two phenomena are not temporally linked. Preliminary experiments showed activation of autophagy at two hours following hypoxic release, but not to the same extent as the 12-hour data, and not reproducibly. It may be that after release from hypoxia, normal SG clearance begins, but due to granule persistence through blockage of some other pathway, autophagy is not able to efficiently clear granules leading to overactivation of autophagy to a point where ADCD results. Staining of astrocytoma cells at 12 hours following release demonstrated an absence of SGs at this time point, further supporting this theory. Future experiments should clarify this by characterizing the time course of autophagic activation and SG dissolution to see if there is a correlation between the two processes.

The dynamic nature of SGs should be considered when SG persistence is noted following stress. The presence of SGs in the cytoplasm is in constant flux, and even statically visualized SGs are in fact in a balance between mRNP entry and exit on a time scale on the order of seconds (Kedersha *et al.*, 2000). Thus, one should view SG presence as an equilibrium between SG formation (canonically through phosphorylation of eIF2α) and SG dissolution (the mechanisms of which are still under investigation). As such, any process which tips the equilibrium either towards formation or away from dissolution will lead to SG persistence following stress. Indeed, Wippich and colleagues identified a number of compounds that caused SG persistence following arsenite-induced stress, and a handful of their tested compounds caused SG persistence by preventing complete eIF2α dephosphorylation following stress relief (Wippich *et al.*, 2013). Raloxifene alone did not induce the formation of granules, which would seem to suggest that it is delaying dissolution rather than inducing formation. However, there may exist some interaction between hypoxia and raloxifene that enhances the SG formation pathway. Examining phosphorylation status of eIF2α following release from hypoxic stress in the presence of raloxifene may clarify this ambiguity; if eIF2α is dephosphorylated (likely via CReP/GADD34) following release from stress, then raloxifene is likely acting to prevent SG clearance and dissolution.

In addition to investigating inefficiencies in reversing translational blocking, all the currently known players involved in SG dissolution should be investigated in this experimental model to see if treatment is influencing these pathways. Valosin-containing protein (an ATPase) and Syk (a tyrosine kinase) activate granulophagy, or the clearance of SGs by autophagy (Buchan *et al.*, 2013; Krisenko *et al.*, 2015). The exact mechanisms by which they activate autophagy are not yet known, but VCP function and Syk function can be independently tested to see if their functions are inhibited by raloxifene. A recent study found that VCP inhibition causes an increase in ubiquitylation of the transcription factor c-Myc and leads to increase in cellular levels (Heidelberger *et al.*, 2018); this may provide a means of measuring VCP function. Syk must be recruited to SGs in order to activate autophagy, a process that requires phosphorylation on two specific tyrosines. Measurement of phosphorylated syk by western blotting, and confirmation of syk localization to SGs using IF can be used to investigate syk function during raloxifene

treatment. Yet another group found that the protein zinc finger AN1-type containing 1 (ZFAND1) is responsible for the recruitment of proteosomal components and VCP to arsenite-induced SGs, and absence of the protein leads to lack of recruitment and persistent granules (Turakhiya *et al.*, 2018). Staining for colocalization of SG proteins and ZFAND1 following treatment would test the hypothesis that interference with this mechanism is responsible for persistent SGs here. Other authors have demonstrated a role for the molecular motor kinesin in the dissolution of SGs, with successful knockdown of kinesin-1 heavy chain or kinesin light chain (KLC) 1 delaying SG dissolution for up to two hours (Loschi *et al.*, 2009). Phosphorylation of the KLC is responsible for kinesin motor activity (Lindesmith *et al.*, 1997), and these authors describe a technique using radiolabelled ATP and autoradiography to identify levels of KLC phosphorylation. Conducting a similar experiment in our cells would help determine if dampening of kinesin activity has a role in delayed SG dissolution with combination treatment. The dual specificity tyrosine-phosphorylation-regulated kinase 3 (DYRK3) has been shown to prevent SG dissolution in its inactive form (Wippich *et al.*, 2013); Gockler and colleagues have described an in vitro assay for testing DYRK activity which could be used for investigating raloxifene's effect on the enzyme (Gockler *et al.*, 2009). Finally, the combination of raloxifene and hypoxia may be inhibiting the PQC response resulting in the incorporation of DRiPs into SGs, thus requiring autophagy for granule clearance. Labelling nascent peptide chains with O-propargyl-puromycin and assessing for localization in SGs following treatment would confirm that the granules formed in our conditions are aberrant granules, and that combination treatment is leading to increased protein misfolding and DRiP accumulation, leading to persistent SGs and activation of autophagy. If DRiP accumulation is not identified, this would strengthen the assumption that autophagy is being activated in a manner consistent with initiation of ADCD. Although a large number of individual processes have been identified contributing to clearance of SGs, many questions remain as the exact mechanisms of their dissolution following release from stress.

4.7.3 Linking Stress Granule Dissolution and Cell Death

A causal link can be established between the inhibition of SG dissolution and increased astrocytoma cell death if raloxifene's effects on SG dissolution can be

overcome despite the presence of the drug. This will require the forced dissolution of SGs with raloxifene present in the culture media. Autophagy is known to be involved in SG clearance, but as autophagy is already activated in these experiments, there must exist some other mechanism of SG dissolution that is targetable for these purposes. Investigation into other mechanisms associated with or responsible for SG dissolution, as outlined above, may provide some insight into the mechanism behind persistent granules in our experiments, and this would possibly allow for reversal of the process in the presence of raloxifene. Driving SG dissolution in the presence of raloxifene would result in a reduction of death rates if persistent SGs are a major contributing cause of cell death. However, both raloxifene and hypoxia alone are responsible for a large proportion of cell death and determining a threshold for significance in cell death reduction may prove difficult. If the only interaction between raloxifene and hypoxia responsible for synergistic cell death is the prevention of SG dissolution, then additive cell death would be expected; if both treatments kill roughly 50% of the cells, this would result in an overall death rate of 75% instead of the observed 90% with combination treatment found in these experiments, and would provide evidence for a link between inhibition of SG dissolution and increased death rates.

4.8 Limitations

There are limitations inherent to any study using cell lines for investigation of tumour biology or pharmacotherapy. Firstly, two-dimensional cultures of a single cell type fail to mimic the complex interplay between the multitude of cell types present within a tumour *in vivo*. The three-dimensional structure of tumours adds a level of complexity to true biological systems, specifically with regards to microenvironmental effects on tumour cells. In these experiments, we have attempted to recreate the hypoxia that may be experienced by tumour cells within certain tumoural microenvironments, but this system is imperfect, with an inability to recapitulate the cyclic hypoxia-reoxygenation present within tumours *in vivo*, and even inconsistency in the partial pressure of oxygen achieved with our incubation strategy. As a result of these shortcomings, many studies have shown positive results in cell culture studies that are not upheld with further *in vivo* or clinical testing.

This research used commercially available U251 human astrocytoma cell lines as a model for GBM. This cell line is widely used in the astrocytoma literature. It was developed in the 1960s in Sweden from patient-derived GBM, and has been maintained by the ATCC recently. Chronic *in vitro* subculture of human cell lines can result in genetic drift and cross-contamination with other cell types used in the same laboratory. Lee and associates suggested the superiority of using tumour stem cells as opposed to commercially available cell lines for experimentation by demonstrating higher rates of genotypic and phenotypic differences between serum cultured cells and their cells of origin compared to cultures derived from tumour stem cells (Lee *et al.*, 2006). Recent analysis of another common astrocytoma cell line (U87) showed that the DNA profile was markedly different from the original cell line but confirmed that is was a glioblastoma cell line (Allen *et al.*, 2016). Similar profiling of U251 cells confirmed similar findings in cells that had undergone long-term passage (Torsvik *et al.*, 2014). The lab is currently working on culturing primary GBM cells to confirm the present findings in a more reliable model.

The metric used to assess raloxifene's effect on SGs in this research was the number of cells containing SGs. This metric is widely used in the literature but may not be the best metric of the SG response. In our experiments, we used five SGs per cell as a threshold for whether or not a cell had mounted an SG response. This leaves room for quite a bit of variability in SG responses. Measuring the average number of SGs per cell may provide a better metric, but this is difficult to do without the correct software. Additionally, the number of SGs alone may not be appropriate, as granules coalesce and fuse into fewer large granules as the response progresses (Kedersha *et al.*, 2000). Therefore, a composite of average SGs per cell and average granule size would better measure granule response. A member of the lab (Elizabeth Castle) has developed a pipeline for Cell Profiler with the ability to measure these parameters, and experiments will be repeated with these metrics.

Finally, in these experiments, we measured SG response in combination treatments rather than SG function. The hypothetical role of SGs is dampening of global cellular translation and mRNA triage, with continued translation of important pro-survival transcripts. While one might assume that the presence of SGs would indicate

translational dampening, it has been demonstrated that translation can continue despite the presence of SGs (Loschi *et al.*, 2009). In order to demonstrate that observed granules are functioning as expected, western blotting for phosphorylated eIF2α should be done under experimental conditions. High levels of phosphorylation would provide evidence of decreased translation. Cellular protein synthesis can also be investigated with puromycin blotting. Given its aminonucleoside structure, puromycin is incorporated into elongating peptides after administration; subsequent blotting of total protein with anti-puromycin antibodies will provide a snapshot of active protein synthesis across treatment groups and could confirm that SGs are functional in our experiments.

4.9 Future Directions

This research provides the basis for many different avenues of further study into the role of stress granules in GBM. Many of the questions that remain to be answered have been addressed above; the exact mechanism of raloxifene's role in both stress granule dissolution and cell death and establishing a link between the two processes will be priorities going forward. Raloxifene was the first drug that exhibited a positive result on further testing following the screen, and the remaining drugs that screened positive on dissolution testing can also be further tested to confirm their effect. Specifically, as a high proportion of positively screened drugs were involved in monoamine biochemistry, investigating the link between these pathway and stress granules or GBM biology may prove interesting. Finally, the drug screen identified many drugs that potentially inhibit SG formation. Further testing should be done to determine if formation inhibition produces a similar effect to preventing SG dissolution.

Promising results with further *in vitro* testing will necessitate confirmation of positive results in *in vivo* studies. The next step will include mouse xenograft models of GBM to investigate the effects of raloxifene treatment in a physiologic model. Injection of commercially available astrocytoma cells (such as U251 cells, used in these experiments) or patient-derived GBM cells into mouse embryos has been used in a number of studies (Miyai *et al.*, 2017) and would be feasible going forward. A simple experimental protocol would consist of administration of raloxifene to one group of mice while giving only vehicle to a second group and comparing tumour growth rates and overall survival. At the time of death, tumour tissue could be removed and stained for

SG proteins to see if treated tumours exhibit a heightened SG response to normal intra-tumoural stressors compared to the untreated group. If positive, this would strengthen the level of evidence of a role for raloxifene and inhibition of SG dissolution in treatment of GBM. Finally, as raloxifene is an approved drug already tested and marketed in humans, clinical trials could begin at phase III without the need for safety (phase I) or dosing (phase II) trials.

This research serves as an initial proof of concept work by demonstrating a correlation between the chemical inhibition of SG dissolution and increased GBM cell death in experimental hypoxia. As mentioned, linking the observed outcomes may prove more difficult. In order to demonstrate a definitive role for SGs in GBM treatment, genetic knockdown or knockout of key players (eg VCP or ZFAND1 etc), using siRNA or CRISPR technologies respectively, should be done. Previous studies have used siRNA to successfully knock down VCP in cell culture (Fu *et al.*, 2016; Lin *et al.*, 2017), and this method has been used to study SG dynamics as well (Buchan *et al.*, 2013; Seguin *et al.*, 2014). Further, similar techniques can be used to target kinases involved in SG formation or key SG nucleating proteins to investigate SG formation inhibition in GBM cell survival.

4.10 Conclusions

This research has identified the SERM raloxifene as an inhibitor of SG dissolution. When GBM cells are treated with raloxifene and subject to hypoxic stress, similar to that experienced in the tumour microenvironment *in vivo*, the result is synergistic cell death when compared to hypoxia or raloxifene treatment alone. Activation of autophagy and apoptosis pathways are also observed, indicating the possibility of these mechanisms underlying cell death following treatment. This research provides a link between the inhibition of SG dissolution and GBM cell death in hypoxia, although further experimentation is needed to assign causality to this correlation. Provided is early evidence of a possible role for disruption of SG dynamics in GBM therapeutics. Further confirmatory experiments will allow early initiation of clinical trials as raloxifene is already approved for human use. Targeting SG dynamics in GBM may provide a novel therapeutic option for patients diagnosed with this uniformly fatal disease.

References

Adjibade P, St-Sauveur VG, Quevillon Huberdeau M, Fournier MJ, Savard A, Coudert L, Khandjian EW, Mazroui R (2015) Sorafenib, a multikinase inhibitor, induces formation of stress granules in hepatocarcinoma cells. Oncotarget 6:43927-43943.

Alberti S, Mateju D, Mediani L, Carra S (2017) Granulostasis: Protein Quality Control of RNP Granules. Frontiers in molecular neuroscience 10:84.

Allen M, Bjerke M, Edlund H, Nelander S, Westermark B (2016) Origin of the U87MG glioma cell line: Good news and bad news. Science translational medicine 8:354re353.

Amankulor NM, Holland EC (2011) Molecular Genetics and the Development of Targets for Glioma Therapy. In: Youmans Neurological Surgery, 6th Edition (JR Y, HR W, eds). Philadelphia, PA: Saunders/Elsevier.

Anderson P, Kedersha N (2008) Stress granules: the Tao of RNA triage. Trends in biochemical sciences 33:141-150.

Anderson P, Kedersha N (2009) Stress granules. Current biology : CB 19:R397-398.

Anderson P, Kedersha N, Ivanov P (2015) Stress granules, P-bodies and cancer. Biochimica et biophysica acta 1849:861-870.

Angara K, Borin TF, Arbab AS (2017) Vascular Mimicry: A Novel Neovascularization Mechanism Driving Anti-Angiogenic Therapy (AAT) Resistance in Glioblastoma. Translational oncology 10:650-660.

Appenzeller-Herzog C, Hall MN (2012) Bidirectional crosstalk between endoplasmic reticulum stress and mTOR signaling. Trends in cell biology 22:274-282.

Arcella A, Biagioni F, Antonietta Oliva M, Bucci D, Frati A, Esposito V, Cantore G, Giangaspero F, Fornai F (2013) Rapamycin inhibits the growth of glioblastoma. Brain research 1495:37-51.

Arimoto K, Fukuda H, Imajoh-Ohmi S, Saito H, Takekawa M (2008) Formation of stress granules inhibits apoptosis by suppressing stress-responsive MAPK pathways. Nature cell biology 10:1324-1332.

Ayyagari VN, Diaz-Sylvester PL, Hsieh TJ, Brard L (2017) Evaluation of the cytotoxicity of the Bithionol-paclitaxel combination in a panel of human ovarian cancer cell lines. PloS one 12:e0185111.

Bailey P, Cushing H (1926) A Classification of the Tumours of the Glioma Group on a Histogenic Basis With a Correlated Study of Prognosis. Montreal, CA: J. B. Lippincott Co.

Bao S, Wu Q, McLendon RE, Hao Y, Shi Q, Hjelmeland AB, Dewhirst MW, Bigner DD, Rich JN (2006) Glioma stem cells promote radioresistance by preferential activation of the DNA damage response. Nature 444:756-760.

Baritchii A, Jurj A, Soritau O, Tomuleasa C, Raduly L, Zanoaga O, Cernea D, Braicu C, Neagoe I, Stefan Florian I (2016) Sensitizer drugs for the treatment of temozolomide-resistant glioblastoma. Journal of BUON : official journal of the Balkan Union of Oncology 21:199-207.

Barker FG, 2nd, Simmons ML, Chang SM, Prados MD, Larson DA, Sneed PK, Wara WM, Berger MS, Chen P, Israel MA, Aldape KD (2001) EGFR overexpression and radiation response in glioblastoma multiforme. International journal of radiation oncology, biology, physics 51:410-418.

Basu S, Sarkar C, Chakroborty D, Nagy J, Mitra RB, Dasgupta PS, Mukhopadhyay D (2004) Ablation of peripheral dopaminergic nerves stimulates malignant tumor growth by inducing vascular permeability factor/vascular endothelial growth factor-mediated angiogenesis. Cancer research 64:5551-5555.

Beppu T, Kamada K, Yoshida Y, Arai H, Ogasawara K, Ogawa A (2002) Change of oxygen pressure in glioblastoma tissue under various conditions. Journal of neuro-oncology 58:47-52.

Bhaskara VK, Challa S, Panigrahi M, Babu PP (2009) Differential PARP cleavage: an indication for existence of multiple forms of cell death in human gliomas. Neurology India 57:264-268.

Bittencourt LFF, Negreiros-Lima GL, Sousa LP, Silva AG, Souza IBS, Ribeiro R, Dutra MF, Silva RF, Dias ACF, Soriani FM, Martins WK, Barcelos LS (2019) G3BP1 knockdown sensitizes U87 glioblastoma cell line to Bortezomib by inhibiting stress granules assembly and potentializing apoptosis. Journal of neuro-oncology.

Buchan JR, Kolaitis RM, Taylor JP, Parker R (2013) Eukaryotic stress granules are cleared by autophagy and Cdc48/VCP function. Cell 153:1461-1474.

Burri SH, Gondi V, Brown PD, Mehta MP (2018) The Evolving Role of Tumor Treating Fields in Managing Glioblastoma: Guide for Oncologists. American journal of clinical oncology 41:191-196.

Caragher SP, Hall RR, Ahsan R, Ahmed AU (2018) Monoamines in glioblastoma: complex biology with therapeutic potential. Neuro-oncology 20:1014-1025.

Cargnello M, Tcherkezian J, Roux PP (2015) The expanding role of mTOR in cancer cell growth and proliferation. Mutagenesis 30:169-176.

Chaitanya GV, Babu PP (2009) Differential PARP cleavage: an indication of heterogeneous forms of cell death and involvement of multiple proteases in the infarct of focal cerebral ischemia in rat. Cellular and molecular neurobiology 29:563-573.

Chakhoyan A, Guillamo JS, Collet S, Kauffmann F, Delcroix N, Lechapt-Zalcman E, Constans JM, Petit E, MacKenzie ET, Barre L, Bernaudin M, Touzani O, Valable S (2017) FMISO-PET-derived brain oxygen tension maps: application to glioblastoma and less aggressive gliomas. Scientific reports 7:10210.

Cherkasov V, Hofmann S, Druffel-Augustin S, Mogk A, Tyedmers J, Stoecklin G, Bukau B (2013) Coordination of translational control and protein homeostasis during severe heat stress. Current biology : CB 23:2452-2462.

Chheda MG, Wen PY, Hochberg FH, Chi AS, Drappatz J, Eichler AF, Yang D, Beroukhim R, Norden AD, Gerstner ER, Betensky RA, Batchelor TT (2015) Vandetanib plus sirolimus in adults with recurrent glioblastoma: results of a phase I and dose expansion cohort study. Journal of neuro-oncology 121:627-634.

Chinot OL, Wick W, Mason W, Henriksson R, Saran F, Nishikawa R, Carpentier AF, Hoang-Xuan K, Kavan P, Cernea D, Brandes AA, Hilton M, Abrey L, Cloughesy T

(2014) Bevacizumab plus radiotherapy-temozolomide for newly diagnosed glioblastoma. The New England journal of medicine 370:709-722.

Clarke HJ, Chambers JE, Liniker E, Marciniak SJ (2014) Endoplasmic reticulum stress in malignancy. Cancer cell 25:563-573.

Compton DR, Sheng S, Carlson KE, Rebacz NA, Lee IY, Katzenellenbogen BS, Katzenellenbogen JA (2004) Pyrazolo[1,5-a]pyrimidines: estrogen receptor ligands possessing estrogen receptor beta antagonist activity. Journal of medicinal chemistry 47:5872-5893.

Connock M, Auguste P, Dussart C, Guyotat J, Armoiry X (2019) Cost-effectiveness of tumor-treating fields added to maintenance temozolomide in patients with glioblastoma: an updated evaluation using a partitioned survival model. Journal of neuro-oncology 143:605-611.

Delgado-Lopez PD, Corrales-Garcia EM (2016) Survival in glioblastoma: a review on the impact of treatment modalities. Clinical & translational oncology : official publication of the Federation of Spanish Oncology Societies and of the National Cancer Institute of Mexico 18:1062-1071.

Denton D, Nicolson S, Kumar S (2012) Cell death by autophagy: facts and apparent artefacts. Cell death and differentiation 19:87-95.

Denton D, Xu T, Kumar S (2015) Autophagy as a pro-death pathway. Immunology and cell biology 93:35-42.

Der SD, Lau AS (1995) Involvement of the double-stranded-RNA-dependent kinase PKR in interferon expression and interferon-mediated antiviral activity. Proceedings of the National Academy of Sciences of the United States of America 92:8841-8845.

Dewhirst MW, Cao Y, Moeller B (2008) Cycling hypoxia and free radicals regulate angiogenesis and radiotherapy response. Nature reviews Cancer 8:425-437.

Dey A, Mustafi SB, Saha S, Kumar Dhar Dwivedi S, Mukherjee P, Bhattacharya R (2016) Inhibition of BMI1 induces autophagy-mediated necroptosis. Autophagy 12:659-670.

Dhingra K (2001) Selective estrogen receptor modulation: the search for an ideal hormonal therapy for breast cancer. Cancer investigation 19:649-659.

Dong J, Aulestia FJ, Assad Kahn S, Zeniou M, Dubois LG, El-Habr EA, Daubeuf F, Tounsi N, Cheshier SH, Frossard N, Junier MP, Chneiweiss H, Neant I, Moreau M, Leclerc C, Haiech J, Kilhoffer MC (2017) Bisacodyl and its cytotoxic activity on human glioblastoma stem-like cells. Implication of inositol 1,4,5-triphosphate receptor dependent calcium signaling. Biochimica et biophysica acta 1864:1018-1027.

Eller JL, Longo SL, Hicklin DJ, Canute GW (2002) Activity of anti-epidermal growth factor receptor monoclonal antibody C225 against glioblastoma multiforme. Neurosurgery 51:1005-1013; discussion 1013-1004.

Field KM, Simes J, Nowak AK, Cher L, Wheeler H, Hovey EJ, Brown CS, Barnes EH, Sawkins K, Livingstone A, Freilich R, Phal PM, Fitt G, Rosenthal MA (2015) Randomized phase 2 study of carboplatin and bevacizumab in recurrent glioblastoma. Neuro-oncology 17:1504-1513.

Fink HA, Jutkowitz E, McCarten JR, Hemmy LS, Butler M, Davila H, Ratner E, Calvert C, Barclay TR, Brasure M, Nelson VA, Kane RL (2018) Pharmacologic Interventions to Prevent Cognitive Decline, Mild Cognitive Impairment, and Clinical Alzheimer-Type Dementia: A Systematic Review. Annals of internal medicine 168:39-51.

Fisher B, Costantino JP, Redmond CK, Fisher ER, Wickerham DL, Cronin WM (1994) Endometrial cancer in tamoxifen-treated breast cancer patients: findings from the National Surgical Adjuvant Breast and Bowel Project (NSABP) B-14. Journal of the National Cancer Institute 86:527-537.

Fisher B, Costantino JP, Wickerham DL, Redmond CK, Kavanah M, Cronin WM, Vogel V, Robidoux A, Dimitrov N, Atkins J, Daly M, Wieand S, Tan-Chiu E, Ford L, Wolmark N (1998) Tamoxifen for prevention of breast cancer: report of the National Surgical Adjuvant Breast and Bowel Project P-1 Study. Journal of the National Cancer Institute 90:1371-1388.

Flavahan WA, Wu Q, Hitomi M, Rahim N, Kim Y, Sloan AE, Weil RJ, Nakano I, Sarkaria JN, Stringer BW, Day BW, Li M, Lathia JD, Rich JN, Hjelmeland AB (2013) Brain tumor initiating cells adapt to restricted nutrition through preferential glucose uptake. Nature neuroscience 16:1373-1382.

Fournier MJ, Gareau C, Mazroui R (2010) The chemotherapeutic agent bortezomib induces the formation of stress granules. Cancer cell international 10:12.

Franceschi E, Cavallo G, Lonardi S, Magrini E, Tosoni A, Grosso D, Scopece L, Blatt V, Urbini B, Pession A, Tallini G, Crino L, Brandes AA (2007) Gefitinib in patients with progressive high-grade gliomas: a multicentre phase II study by Gruppo Italiano Cooperativo di Neuro-Oncologia (GICNO). British journal of cancer 96:1047-1051.

Fu Q, Jiang Y, Zhang D, Liu X, Guo J, Zhao J (2016) Valosin-containing protein (VCP) promotes the growth, invasion, and metastasis of colorectal cancer through activation of STAT3 signaling. Molecular and cellular biochemistry 418:189-198.

Fujimura K, Sasaki AT, Anderson P (2012) Selenite targets eIF4E-binding protein-1 to inhibit translation initiation and induce the assembly of non-canonical stress granules. Nucleic acids research 40:8099-8110.

Fukumura D, Xu L, Chen Y, Gohongi T, Seed B, Jain RK (2001) Hypoxia and acidosis independently up-regulate vascular endothelial growth factor transcription in brain tumors in vivo. Cancer research 61:6020-6024.

Gaignard P, Liere P, Therond P, Schumacher M, Slama A, Guennoun R (2017) Role of Sex Hormones on Brain Mitochondrial Function, with Special Reference to Aging and Neurodegenerative Diseases. Frontiers in aging neuroscience 9:406.

Galanis E, Anderson SK, Lafky JM, Uhm JH, Giannini C, Kumar SK, Kimlinger TK, Northfelt DW, Flynn PJ, Jaeckle KA, Kaufmann TJ, Buckner JC (2013) Phase II study of bevacizumab in combination with sorafenib in recurrent glioblastoma (N0776): a north central cancer treatment group trial. Clinical cancer research : an official journal of the American Association for Cancer Research 19:4816-4823.

Gallouzi IE, Brennan CM, Stenberg MG, Swanson MS, Eversole A, Maizels N, Steitz JA (2000) HuR binding to cytoplasmic mRNA is perturbed by heat shock. Proceedings of the National Academy of Sciences of the United States of America 97:3073-3078.

Galluzzi L, Kepp O, Krautwald S, Kroemer G, Linkermann A (2014) Molecular mechanisms of regulated necrosis. Seminars in cell & developmental biology 35:24-32.

Galluzzi L et al. (2009) Guidelines for the use and interpretation of assays for monitoring cell death in higher eukaryotes. Cell death and differentiation 16:1093-1107.

Galluzzi L et al. (2018) Molecular mechanisms of cell death: recommendations of the Nomenclature Committee on Cell Death 2018. Cell death and differentiation 25:486-541.

Ganassi M, Mateju D, Bigi I, Mediani L, Poser I, Lee HO, Seguin SJ, Morelli FF, Vinet J, Leo G, Pansarasa O, Cereda C, Poletti A, Alberti S, Carra S (2016) A Surveillance Function of the HSPB8-BAG3-HSP70 Chaperone Complex Ensures Stress Granule Integrity and Dynamism. Molecular cell 63:796-810.

Gardner LB (2008) Hypoxic inhibition of nonsense-mediated RNA decay regulates gene expression and the integrated stress response. Molecular and cellular biology 28:3729-3741.

Germain M, Affar EB, D'Amours D, Dixit VM, Salvesen GS, Poirier GG (1999) Cleavage of automodified poly(ADP-ribose) polymerase during apoptosis. Evidence for involvement of caspase-7. The Journal of biological chemistry 274:28379-28384.

Ghosh S, Geahlen RL (2015) Stress Granules Modulate SYK to Cause Microglial Cell Dysfunction in Alzheimer's Disease. EBioMedicine 2:1785-1798.

Gilks N, Kedersha N, Ayodele M, Shen L, Stoecklin G, Dember LM, Anderson P (2004) Stress granule assembly is mediated by prion-like aggregation of TIA-1. Molecular biology of the cell 15:5383-5398.

Gockler N, Jofre G, Papadopoulos C, Soppa U, Tejedor FJ, Becker W (2009) Harmine specifically inhibits protein kinase DYRK1A and interferes with neurite formation. The FEBS journal 276:6324-6337.

Gogolla N, Galimberti I, DePaola V, Caroni P (2006) Staining protocol for organotypic hippocampal slice cultures. Nature protocols 1:2452-2456.

Gottschald OR, Malec V, Krasteva G, Hasan D, Kamlah F, Herold S, Rose F, Seeger W, Hanze J (2010) TIAR and TIA-1 mRNA-binding proteins co-aggregate under conditions of rapid oxygen decline and extreme hypoxia and suppress the HIF-1alpha pathway. Journal of molecular cell biology 2:345-356.

Grabocka E, Bar-Sagi D (2016) Mutant KRAS Enhances Tumor Cell Fitness by Upregulating Stress Granules. Cell 167:1803-1813.e1812.

Gump JM, Staskiewicz L, Morgan MJ, Bamberg A, Riches DW, Thorburn A (2014) Autophagy variation within a cell population determines cell fate through selective degradation of Fap-1. Nature cell biology 16:47-54.

Guzauskas GF, Pollom EL, Stieber VW, Wang BCM, Garrison LP, Jr. (2019) Tumor treating fields and maintenance temozolomide for newly-diagnosed glioblastoma: a cost-effectiveness study. Journal of medical economics:1-8.

Hainsworth JD, Ervin T, Friedman E, Priego V, Murphy PB, Clark BL, Lamar RE (2010) Concurrent radiotherapy and temozolomide followed by temozolomide and sorafenib in the first-line treatment of patients with glioblastoma multiforme. Cancer 116:3663-3669.

Halatsch ME, Gehrke EE, Vougioukas VI, Botefur IC, F AB, Efferth T, Gebhart E, Domhof S, Schmidt U, Buchfelder M (2004) Inverse correlation of epidermal growth factor receptor messenger RNA induction and suppression of anchorage-independent growth by OSI-774, an epidermal growth factor receptor tyrosine kinase inhibitor, in glioblastoma multiforme cell lines. Journal of neurosurgery 100:523-533.

Harding HP, Zhang Y, Bertolotti A, Zeng H, Ron D (2000a) Perk is essential for translational regulation and cell survival during the unfolded protein response. Molecular cell 5:897-904.

Harding HP, Novoa I, Zhang Y, Zeng H, Wek R, Schapira M, Ron D (2000b) Regulated translation initiation controls stress-induced gene expression in mammalian cells. Molecular cell 6:1099-1108.

Hartmann C, Hentschel B, Wick W, Capper D, Felsberg J, Simon M, Westphal M, Schackert G, Meyermann R, Pietsch T, Reifenberger G, Weller M, Loeffler M, von Deimling A (2010) Patients with IDH1 wild type anaplastic astrocytomas exhibit worse prognosis than IDH1-mutated glioblastomas, and IDH1 mutation status accounts for the unfavorable prognostic effect of higher age: implications for classification of gliomas. Acta neuropathologica 120:707-718.

He W, Liu R, Yang SH, Yuan F (2015) Chemotherapeutic effect of tamoxifen on temozolomide-resistant gliomas. Anti-cancer drugs 26:293-300.

Heberle AM, Prentzell MT, van Eunen K, Bakker BM, Grellscheid SN, Thedieck K (2015) Molecular mechanisms of mTOR regulation by stress. Molecular & cellular oncology 2:e970489.

Heddleston JM, Li Z, McLendon RE, Hjelmeland AB, Rich JN (2009) The hypoxic microenvironment maintains glioblastoma stem cells and promotes reprogramming towards a cancer stem cell phenotype. Cell cycle (Georgetown, Tex) 8:3274-3284.

Hegi ME, Diserens AC, Gorlia T, Hamou MF, de Tribolet N, Weller M, Kros JM, Hainfellner JA, Mason W, Mariani L, Bromberg JE, Hau P, Mirimanoff RO, Cairncross JG, Janzer RC, Stupp R (2005) MGMT gene silencing and benefit from temozolomide in glioblastoma. The New England journal of medicine 352:997-1003.

Heidelberger JB, Voigt A, Borisova ME, Petrosino G, Ruf S, Wagner SA, Beli P (2018) Proteomic profiling of VCP substrates links VCP to K6-linked ubiquitylation and c-Myc function. EMBO reports 19.

Heimberger AB, Hussain SF, Aldape K, Sawaya R, Archer GA, Friedman H, Reardon D, Friedman A, Bigner D, Sampson JH (2006) Tumor-specific peptide vaccination in newly-diagnosed patients with GBM. Journal of Clinical Oncology 24:2529-2529.

Henderson VW, Ala T, Sainani KL, Bernstein AL, Stephenson BS, Rosen AC, Farlow MR (2015) Raloxifene for women with Alzheimer disease: A randomized controlled pilot trial. Neurology 85:1937-1944.

Hentschel SJ, Lang FF (2003) Current surgical management of glioblastoma. Cancer journal (Sudbury, Mass) 9:113-125.

Holash J, Maisonpierre PC, Compton D, Boland P, Alexander CR, Zagzag D, Yancopoulos GD, Wiegand SJ (1999) Vessel cooption, regression, and growth in tumors mediated by angiopoietins and VEGF. Science (New York, NY) 284:1994-1998.

Hottinger AF, Aissa AB, Espeli V, Squiban D, Dunkel N, Vargas MI, Hundsberger T, Mach N, Schaller K, Weber DC, Bodmer A, Dietrich PY (2014) Phase I study of sorafenib combined with radiation therapy and temozolomide as first-line treatment of high-grade glioma. British journal of cancer 110:2655-2661.

Hou W, Xie Y, Song X, Sun X, Lotze MT, Zeh HJ, 3rd, Kang R, Tang D (2016) Autophagy promotes ferroptosis by degradation of ferritin. Autophagy 12:1425-1428.

International Agency for Research on Cancer (2007) WHO Classification of Tumours of the Central Nervous System, 4th Edition. Lyon, France: International Agency for Research on Cancer.

International Agency for Research on Cancer (2016) WHO Classification of Tumours of the Central Nervous System, 4th Revised Edition. Lyon, France: International Agency for Research on Cancer.

Ivan M, Kondo K, Yang H, Kim W, Valiando J, Ohh M, Salic A, Asara JM, Lane WS, Kaelin Jr WG (2001) HIFα targeted for VHL-mediated destruction by proline hydroxylase: implications for O_2 sensing. Science 292:464-468.

Ivanov PA, Chudinova EM, Nadezhdina ES (2003) Disruption of microtubules inhibits cytoplasmic ribonucleoprotein stress granule formation. Experimental cell research 290:227-233.

Jaiyesimi IA, Buzdar AU, Decker DA, Hortobagyi GN (1995) Use of tamoxifen for breast cancer: twenty-eight years later. Journal of clinical oncology : official journal of the American Society of Clinical Oncology 13:513-529.

Jaakkola P, Mole DR, Tian Y, Wilson MI, Gielbert J, Gaskell SJ, von Kriegsheim A, Hebestreit HF, Mukherji M, Schofield CJ, Maxwell PH, Pugh CW, Ratcliffe PJ (2001) Targeting of HIF-α to the von Hippel-Lindau ubiquitylation complex by O_2-regulated prolyl hydroxylation. Science 292:468-472.

Kawai T, Fan J, Mazan-Mamczarz K, Gorospe M (2004) Global mRNA stabilization preferentially linked to translational repression during the endoplasmic reticulum stress response. Molecular and cellular biology 24:6773-6787.

Kedersha N, Anderson P (2002) Stress granules: sites of mRNA triage that regulate mRNA stability and translatability. Biochemical Society transactions 30:963-969.

Kedersha N, Cho MR, Li W, Yacono PW, Chen S, Gilks N, Golan DE, Anderson P (2000) Dynamic shuttling of TIA-1 accompanies the recruitment of mRNA to mammalian stress granules. The Journal of cell biology 151:1257-1268.

Kedersha N, Stoecklin G, Ayodele M, Yacono P, Lykke-Andersen J, Fritzler MJ, Scheuner D, Kaufman RJ, Golan DE, Anderson P (2005) Stress granules and processing

bodies are dynamically linked sites of mRNP remodeling. The Journal of cell biology 169:871-884.

Kedersha NL, Gupta M, Li W, Miller I, Anderson P (1999) RNA-binding proteins TIA-1 and TIAR link the phosphorylation of eIF-2 alpha to the assembly of mammalian stress granules. The Journal of cell biology 147:1431-1442.

Kim EH, Song HS, Yoo SH, Yoon M (2016) Tumor treating fields inhibit glioblastoma cell migration, invasion and angiogenesis. Oncotarget 7:65125-65136.

Kim SH, Joshi K, Ezhilarasan R, Myers TR, Siu J, Gu C, Nakano-Okuno M, Taylor D, Minata M, Sulman EP, Lee J, Bhat KP, Salcini AE, Nakano I (2015) EZH2 protects glioma stem cells from radiation-induced cell death in a MELK/FOXM1-dependent manner. Stem cell reports 4:226-238.

Kim WJ, Back SH, Kim V, Ryu I, Jang SK (2005) Sequestration of TRAF2 into stress granules interrupts tumor necrosis factor signaling under stress conditions. Molecular and cellular biology 25:2450-2462.

Kimball SR, Horetsky RL, Ron D, Jefferson LS, Harding HP (2003) Mammalian stress granules represent sites of accumulation of stalled translation initiation complexes. American journal of physiology Cell physiology 284:C273-284.

Kirson ED, Gurvich Z, Schneiderman R, Dekel E, Itzhaki A, Wasserman Y, Schatzberger R, Palti Y (2004) Disruption of cancer cell replication by alternating electric fields. Cancer research 64:3288-3295.

Kirson ED, Dbaly V, Tovarys F, Vymazal J, Soustiel JF, Itzhaki A, Mordechovich D, Steinberg-Shapira S, Gurvich Z, Schneiderman R, Wasserman Y, Salzberg M, Ryffel B, Goldsher D, Dekel E, Palti Y (2007) Alternating electric fields arrest cell proliferation in animal tumor models and human brain tumors. Proceedings of the National Academy of Sciences of the United States of America 104:10152-10157.

Kong Z, Wang Y, Ma W (2018) Vaccination in the immunotherapy of glioblastoma. Human vaccines & immunotherapeutics 14:255-268.

Kreisl TN, Lassman AB, Mischel PS, Rosen N, Scher HI, Teruya-Feldstein J, Shaffer D, Lis E, Abrey LE (2009) A pilot study of everolimus and gefitinib in the treatment of recurrent glioblastoma (GBM). Journal of neuro-oncology 92:99-105.

Krisenko MO, Higgins RL, Ghosh S, Zhou Q, Trybula JS, Wang WH, Geahlen RL (2015) Syk Is Recruited to Stress Granules and Promotes Their Clearance through Autophagy. The Journal of biological chemistry 290:27803-27815.

Krysko DV, Vanden Berghe T, Parthoens E, D'Herde K, Vandenabeele P (2008) Methods for distinguishing apoptotic from necrotic cells and measuring their clearance. Methods in enzymology 442:307-341.

Lacroix M, Abi-Said D, Fourney DR, Gokaslan ZL, Shi W, DeMonte F, Lang FF, McCutcheon IE, Hassenbusch SJ, Holland E, Hess K, Michael C, Miller D, Sawaya R (2001) A multivariate analysis of 416 patients with glioblastoma multiforme: prognosis, extent of resection, and survival. Journal of neurosurgery 95:190-198.

Lassen U, Sorensen M, Gaziel TB, Hasselbalch B, Poulsen HS (2013) Phase II study of bevacizumab and temsirolimus combination therapy for recurrent glioblastoma multiforme. Anticancer research 33:1657-1660.

Lathia JD, Mack SC, Mulkearns-Hubert EE, Valentim CL, Rich JN (2015) Cancer stem cells in glioblastoma. Genes & development 29:1203-1217.

Lee EQ, Kuhn J, Lamborn KR, Abrey L, DeAngelis LM, Lieberman F, Robins HI, Chang SM, Yung WK, Drappatz J, Mehta MP, Levin VA, Aldape K, Dancey JE, Wright JJ, Prados MD, Cloughesy TF, Gilbert MR, Wen PY (2012) Phase I/II study of sorafenib in combination with temsirolimus for recurrent glioblastoma or gliosarcoma: North American Brain Tumor Consortium study 05-02. Neuro-oncology 14:1511-1518.

Lee J, Kotliarova S, Kotliarov Y, Li A, Su Q, Donin NM, Pastorino S, Purow BW, Christopher N, Zhang W, Park JK, Fine HA (2006) Tumor stem cells derived from glioblastomas cultured in bFGF and EGF more closely mirror the phenotype and genotype of primary tumors than do serum-cultured cell lines. Cancer cell 9:391-403.

Levine M, Moutquin JM, Walton R, Feightner J (2001) Chemoprevention of breast cancer. A joint guideline from the Canadian Task Force on Preventive Health Care and the Canadian Breast Cancer Initiative's Steering Committee on Clinical Practice Guidelines for the Care and Treatment of Breast Cancer. CMAJ : Canadian Medical Association journal = journal de l'Association medicale canadienne 164:1681-1690.

Li J, Zhu S, Kozono D, Ng K, Futalan D, Shen Y, Akers JC, Steed T, Kushwaha D, Schlabach M, Carter BS, Kwon CH, Furnari F, Cavenee W, Elledge S, Chen CC (2014) Genome-wide shRNA screen revealed integrated mitogenic signaling between

dopamine receptor D2 (DRD2) and epidermal growth factor receptor (EGFR) in glioblastoma. Oncotarget 5:882-893.

Li L, Quang TS, Gracely EJ, Kim JH, Emrich JG, Yaeger TE, Jenrette JM, Cohen SC, Black P, Brady LW (2010) A Phase II study of anti-epidermal growth factor receptor radioimmunotherapy in the treatment of glioblastoma multiforme. Journal of neurosurgery 113:192-198.

Li W, Winters A, Poteet E, Ryou MG, Lin S, Hao S, Wu Z, Yuan F, Hatanpaa KJ, Simpkins JW, Yang SH (2013) Involvement of estrogen receptor beta5 in the progression of glioma. Brain research 1503:97-107.

Li Z, Bao S, Wu Q, Wang H, Eyler C, Sathornsumetee S, Shi Q, Cao Y, Lathia J, McLendon RE, Hjelmeland AB, Rich JN (2009) Hypoxia-inducible factors regulate tumorigenic capacity of glioma stem cells. Cancer cell 15:501-513.

Lin YT, Prendergast J, Grey F (2017) The host ubiquitin-dependent segregase VCP/p97 is required for the onset of human cytomegalovirus replication. PLoS pathogens 13:e1006329.

Lindesmith L, McIlvain JM, Jr., Argon Y, Sheetz MP (1997) Phosphotransferases associated with the regulation of kinesin motor activity. The Journal of biological chemistry 272:22929-22933.

Liu-Yesucevitz L, Bassell GJ, Gitler AD, Hart AC, Klann E, Richter JD, Warren ST, Wolozin B (2011) Local RNA translation at the synapse and in disease. The Journal of neuroscience : the official journal of the Society for Neuroscience 31:16086-16093.

Liu J, Litt L, Segal MR, Kelly MJ, Pelton JG, Kim M (2011) Metabolomics of oxidative stress in recent studies of endogenous and exogenously administered intermediate metabolites. International journal of molecular sciences 12:6469-6501.

Lloyd RE (2013) Regulation of stress granules and P-bodies during RNA virus infection. Wiley interdisciplinary reviews RNA 4:317-331.

Loschi M, Leishman CC, Berardone N, Boccaccio GL (2009) Dynein and kinesin regulate stress-granule and P-body dynamics. Journal of cell science 122:3973-3982.

Ludwig K, Kornblum HI (2017) Molecular markers in glioma. Journal of neuro-oncology 134:505-512.

Ma DJ, Galanis E, Anderson SK, Schiff D, Kaufmann TJ, Peller PJ, Giannini C, Brown PD, Uhm JH, McGraw S, Jaeckle KA, Flynn PJ, Ligon KL, Buckner JC, Sarkaria JN (2015) A phase II trial of everolimus, temozolomide, and radiotherapy in patients with newly diagnosed glioblastoma: NCCTG N057K. Neuro-oncology 17:1261-1269.

Ma Y, Guo H, Zhang L, Tao L, Yin A, Liu Z, Li Y, Dong H, Xiong L, Hou W (2016) Estrogen replacement therapy-induced neuroprotection against brain ischemia-reperfusion injury involves the activation of astrocytes via estrogen receptor beta. Scientific reports 6:21467.

Mackenzie IR et al. (2017) TIA1 Mutations in Amyotrophic Lateral Sclerosis and Frontotemporal Dementia Promote Phase Separation and Alter Stress Granule Dynamics. Neuron 95:808-816.e809.

Martinez-Gonzalez A, Calvo GF, Perez Romasanta LA, Perez-Garcia VM (2012) Hypoxic cell waves around necrotic cores in glioblastoma: a biomathematical model and its therapeutic implications. Bulletin of mathematical biology 74:2875-2896.

Mastronardi L, Puzzilli F, Couldwell WT, Farah JO, Lunardi P (1998) Tamoxifen and carboplatin combinational treatment of high-grade gliomas. Results of a clinical trial on newly diagnosed patients. Journal of neuro-oncology 38:59-68.

Mateju D, Franzmann TM, Patel A, Kopach A, Boczek EE, Maharana S, Lee HO, Carra S, Hyman AA, Alberti S (2017) An aberrant phase transition of stress granules triggered by misfolded protein and prevented by chaperone function. The EMBO journal 36:1669-1687.

Mazroui R, Huot ME, Tremblay S, Filion C, Labelle Y, Khandjian EW (2002) Trapping of messenger RNA by Fragile X Mental Retardation protein into cytoplasmic granules induces translation repression. Human molecular genetics 11:3007-3017.

McEwen E, Kedersha N, Song B, Scheuner D, Gilks N, Han A, Chen JJ, Anderson P, Kaufman RJ (2005) Heme-regulated inhibitor kinase-mediated phosphorylation of eukaryotic translation initiation factor 2 inhibits translation, induces stress granule formation, and mediates survival upon arsenite exposure. The Journal of biological chemistry 280:16925-16933.

Mendiburu-Elicabe M, Gil-Ranedo J, Izquierdo M (2014) Efficacy of rapamycin against glioblastoma cancer stem cells. Clinical & translational oncology : official publication of the Federation of Spanish Oncology Societies and of the National Cancer Institute of Mexico 16:495-502.

Miyai M, Tomita H, Soeda A, Yano H, Iwama T, Hara A (2017) Current trends in mouse models of glioblastoma. Journal of neuro-oncology 135:423-432.

Moeller BJ, Dewhirst MW (2004) Raising the bar: how HIF-1 helps determine tumor radiosensitivity. Cell cycle (Georgetown, Tex) 3:1107-1110.

Moeller BJ, Cao Y, Li CY, Dewhirst MW (2004) Radiation activates HIF-1 to regulate vascular radiosensitivity in tumors: role of reoxygenation, free radicals, and stress granules. Cancer cell 5:429-441.

Morettin A, Paris G, Bouzid Y, Baldwin RM, Falls TJ, Bell JC, Cote J (2017) Tudor Domain Containing Protein 3 Promotes Tumorigenesis and Invasive Capacity of Breast Cancer Cells. Scientific reports 7:5153.

Moyer VA (2013) Medications to decrease the risk for breast cancer in women: recommendations from the U.S. Preventive Services Task Force recommendation statement. Annals of internal medicine 159:698-708.

Naderi V, Khaksari M, Abbasi R, Maghool F (2015) Estrogen provides neuroprotection against brain edema and blood brain barrier disruption through both estrogen receptors alpha and beta following traumatic brain injury. Iranian journal of basic medical sciences 18:138-144.

Nadezhdina ES, Lomakin AJ, Shpilman AA, Chudinova EM, Ivanov PA (2010) Microtubules govern stress granule mobility and dynamics. Biochimica et biophysica acta 1803:361-371.

Nagane M, Coufal F, Lin H, Bogler O, Cavenee WK, Huang HJ (1996) A common mutant epidermal growth factor receptor confers enhanced tumorigenicity on human glioblastoma cells by increasing proliferation and reducing apoptosis. Cancer research 56:5079-5086.

Neyns B, Sadones J, Joosens E, Bouttens F, Verbeke L, Baurain JF, D'Hondt L, Strauven T, Chaskis C, In't Veld P, Michotte A, De Greve J (2009) Stratified phase II

trial of cetuximab in patients with recurrent high-grade glioma. Ann Oncol 20:1596-1603.

Niemi NM, Lanning NJ, Westrate LM, MacKeigan JP (2013) Downregulation of the mitochondrial phosphatase PTPMT1 is sufficient to promote cancer cell death. PloS one 8:e53803.

O'Brian CA, Liskamp RM, Solomon DH, Weinstein IB (1985) Inhibition of protein kinase C by tamoxifen. Cancer research 45:2462-2465.

Ohgaki H, Dessen P, Jourde B, Horstmann S, Nishikawa T, Di Patre PL, Burkhard C, Schuler D, Probst-Hensch NM, Maiorka PC, Baeza N, Pisani P, Yonekawa Y, Yasargil MG, Lutolf UM, Kleihues P (2004) Genetic pathways to glioblastoma: a population-based study. Cancer research 64:6892-6899.

Omuro A et al. (2014) Phase II study of bevacizumab, temozolomide, and hypofractionated stereotactic radiotherapy for newly diagnosed glioblastoma. Clinical cancer research : an official journal of the American Association for Cancer Research 20:5023-5031.

Ostrom QT, Gittleman H, Stetson L, Virk SM, Barnholtz-Sloan JS (2015) Epidemiology of gliomas. Cancer treatment and research 163:1-14.

Osuka S, Van Meir EG (2017) Overcoming therapeutic resistance in glioblastoma: the way forward. The Journal of clinical investigation 127:415-426.

Paquette M, El-Houjeiri L, Pause A (2018) mTOR Pathways in Cancer and Autophagy. Cancers 10.

Parney IF, Chang SM (2003) Current chemotherapy for glioblastoma. Cancer journal (Sudbury, Mass) 9:149-156.

Patel AP, Tirosh I, Trombetta JJ, Shalek AK, Gillespie SM, Wakimoto H, Cahill DP, Nahed BV, Curry WT, Martuza RL, Louis DN, Rozenblatt-Rosen O, Suva ML, Regev A, Bernstein BE (2014) Single-cell RNA-seq highlights intratumoral heterogeneity in primary glioblastoma. Science (New York, NY) 344:1396-1401.

Pistollato F, Abbadi S, Rampazzo E, Persano L, Della Puppa A, Frasson C, Sarto E, Scienza R, D'Avella D, Basso G (2010) Intratumoral hypoxic gradient drives stem

cells distribution and MGMT expression in glioblastoma. Stem cells (Dayton, Ohio) 28:851-862.

Podszywalow-Bartnicka P, Wolczyk M, Kusio-Kobialka M, Wolanin K, Skowronek K, Nieborowska-Skorska M, Dasgupta Y, Skorski T, Piwocka K (2014) Downregulation of BRCA1 protein in BCR-ABL1 leukemia cells depends on stress-triggered TIAR-mediated suppression of translation. Cell cycle (Georgetown, Tex) 13:3727-3741.

Pollack IF, Randall MS, Kristofik MP, Kelly RH, Selker RG, Vertosick FT, Jr. (1990) Effect of tamoxifen on DNA synthesis and proliferation of human malignant glioma lines in vitro. Cancer research 50:7134-7138.

Powles TJ, Hickish T, Kanis JA, Tidy A, Ashley S (1996) Effect of tamoxifen on bone mineral density measured by dual-energy x-ray absorptiometry in healthy premenopausal and postmenopausal women. Journal of clinical oncology : official journal of the American Society of Clinical Oncology 14:78-84.

Razavi SM, Lee KE, Jin BE, Aujla PS, Gholamin S, Li G (2016) Immune Evasion Strategies of Glioblastoma. Frontiers in surgery 3:11.

Reichert M, Steinbach JP, Supra P, Weller M (2002) Modulation of growth and radiochemosensitivity of human malignant glioma cells by acidosis. Cancer 95:1113-1119.

Reifenberger G, Wirsching HG, Knobbe-Thomsen CB, Weller M (2017) Advances in the molecular genetics of gliomas - implications for classification and therapy. Nature reviews Clinical oncology 14:434-452.

Rich JN, Reardon DA, Peery T, Dowell JM, Quinn JA, Penne KL, Wikstrand CJ, Van Duyn LB, Dancey JE, McLendon RE, Kao JC, Stenzel TT, Ahmed Rasheed BK, Tourt-Uhlig SE, Herndon JE, 2nd, Vredenburgh JJ, Sampson JH, Friedman AH, Bigner DD, Friedman HS (2004) Phase II trial of gefitinib in recurrent glioblastoma. Journal of clinical oncology : official journal of the American Society of Clinical Oncology 22:133-142.

Rong Y, Durden DL, Van Meir EG, Brat DJ (2006) 'Pseudopalisading' necrosis in glioblastoma: a familiar morphologic feature that links vascular pathology, hypoxia, and angiogenesis. Journal of neuropathology and experimental neurology 65:529-539.

Rotoli D, Cejas MM, Maeso MD, Perez-Rodriguez ND, Morales M, Avila J, Mobasheri A, Martin-Vasallo P (2017) The Na, K-ATPase beta-Subunit Isoforms Expression in Glioblastoma Multiforme: Moonlighting Roles. International journal of molecular sciences 18.

Runowicz CD, Costantino JP, Wickerham DL, Cecchini RS, Cronin WM, Ford LG, Vogel VG, Wolmark N (2011) Gynecologic conditions in participants in the NSABP breast cancer prevention study of tamoxifen and raloxifene (STAR). American journal of obstetrics and gynecology 205:535.e531-535.

Sampson JH, Aldape KD, Archer GE, Coan A, Desjardins A, Friedman AH, Friedman HS, Gilbert MR, Herndon JE, McLendon RE, Mitchell DA, Reardon DA, Sawaya R, Schmittling R, Shi W, Vredenburgh JJ, Bigner DD, Heimberger AB (2011) Greater chemotherapy-induced lymphopenia enhances tumor-specific immune responses that eliminate EGFRvIII-expressing tumor cells in patients with glioblastoma. Neuro-oncology 13:324-333.

Schneider NFZ, Cerella C, Simoes CMO, Diederich M (2017) Anticancer and Immunogenic Properties of Cardiac Glycosides. Molecules (Basel, Switzerland) 22.

Seguin SJ, Morelli FF, Vinet J, Amore D, De Biasi S, Poletti A, Rubinsztein DC, Carra S (2014) Inhibition of autophagy, lysosome and VCP function impairs stress granule assembly. Cell death and differentiation 21:1838-1851.

Segura-Uribe JJ, Pinto-Almazán R, Coyoy-Salgado A, Fuentes-Venado CE, Guerra-Araiza C (2017) Effects of estrogen receptor modulators on cytoskeletal proteins in the central nervous system. Neural Regeneration Research 12:1231-1240.

Shelkovnikova TA, Dimasi P, Kukharsky MS, An H, Quintiero A, Schirmer C, Buee L, Galas MC, Buchman VL (2017) Chronically stressed or stress-preconditioned neurons fail to maintain stress granule assembly. Cell death & disease 8:e2788.

Shen HM, Codogno P (2011) Autophagic cell death: Loch Ness monster or endangered species? Autophagy 7:457-465.

Siegal T (2016) Clinical Relevance of Prognostic and Predictive Molecular Markers in Gliomas. In: Advances and Technical Standards in Neurosurgery, 2015/10/29 Edition (Schramm J, ed), pp 91-108: Springer International Publishing.

Silver DJ, Sinyuk M, Vogelbaum MA, Ahluwalia MS, Lathia JD (2016) The intersection of cancer, cancer stem cells, and the immune system: therapeutic opportunities. Neuro-oncology 18:153-159.

Singh SK, Hawkins C, Clarke ID, Squire JA, Bayani J, Hide T, Henkelman RM, Cusimano MD, Dirks PB (2004) Identification of human brain tumour initiating cells. Nature 432:396-401.

Slaine PD, Kleer M, Smith NK, Khaperskyy DA, McCormick C (2017) Stress Granule-Inducing Eukaryotic Translation Initiation Factor 4A Inhibitors Block Influenza A Virus Replication. Viruses 9.

Somasekharan SP, El-Naggar A, Leprivier G, Cheng H, Hajee S, Grunewald TG, Zhang F, Ng T, Delattre O, Evdokimova V, Wang Y, Gleave M, Sorensen PH (2015) YB-1 regulates stress granule formation and tumor progression by translationally activating G3BP1. The Journal of cell biology 208:913-929.

Sonnaert M, Papantoniou I, Luyten FP, Schrooten JI (2015) Quantitative Validation of the Presto Blue Metabolic Assay for Online Monitoring of Cell Proliferation in a 3D Perfusion Bioreactor System. Tissue engineering Part C, Methods 21:519-529.

Srivastava SP, Kumar KU, Kaufman RJ (1998) Phosphorylation of eukaryotic translation initiation factor 2 mediates apoptosis in response to activation of the double-stranded RNA-dependent protein kinase. The Journal of biological chemistry 273:2416-2423.

Stommel JM, Kimmelman AC, Ying H, Nabioullin R, Ponugoti AH, Wiedemeyer R, Stegh AH, Bradner JE, Ligon KL, Brennan C, Chin L, DePinho RA (2007) Coactivation of receptor tyrosine kinases affects the response of tumor cells to targeted therapies. Science (New York, NY) 318:287-290.

Stupp R, Mason WP, van den Bent MJ, Weller M, Fisher B, Taphoorn MJ, Belanger K, Brandes AA, Marosi C, Bogdahn U, Curschmann J, Janzer RC, Ludwin SK, Gorlia T, Allgeier A, Lacombe D, Cairncross JG, Eisenhauer E, Mirimanoff RO (2005) Radiotherapy plus concomitant and adjuvant temozolomide for glioblastoma. The New England journal of medicine 352:987-996.

Stupp R et al. (2015) Maintenance Therapy With Tumor-Treating Fields Plus Temozolomide vs Temozolomide Alone for Glioblastoma: A Randomized Clinical Trial. Jama 314:2535-2543.

Szaflarski W, Fay MM, Kedersha N, Zabel M, Anderson P, Ivanov P (2016) Vinca alkaloid drugs promote stress-induced translational repression and stress granule formation. Oncotarget 7:30307-30322.

Taal W et al. (2014) Single-agent bevacizumab or lomustine versus a combination of bevacizumab plus lomustine in patients with recurrent glioblastoma (BELOB trial): a randomised controlled phase 2 trial. The Lancet Oncology 15:943-953.

Takayama KI, Suzuki T, Fujimura T, Takahashi S, Inoue S (2018) Association of USP10 with G3BP2 Inhibits p53 Signaling and Contributes to Poor Outcome in Prostate Cancer. Molecular cancer research : MCR.

Taniuchi K, Nishimori I, Hollingsworth MA (2011) Intracellular CD24 inhibits cell invasion by posttranscriptional regulation of BART through interaction with G3BP. Cancer research 71:895-905.

Tavares CB, Gomes-Braga F, Costa-Silva DR, Escorcio-Dourado CS, Borges US, Conde-Junior AM, Barros-Oliveira Mda C, Sousa EB, Barros Lda R, Martins LM, Facina G, da-Silva BB (2016) Expression of estrogen and progesterone receptors in astrocytomas: a literature review. Clinics (Sao Paulo, Brazil) 71:481-486.

Terrasso AP, Silva AC, Filipe A, Pedroso P, Ferreira AL, Alves PM, Brito C (2017) Human neuron-astrocyte 3D co-culture-based assay for evaluation of neuroprotective compounds. Journal of pharmacological and toxicological methods 83:72-79.

Tews DS, Nissen A, Kulgen C, Gaumann AK (2000) Drug resistance-associated factors in primary and secondary glioblastomas and their precursor tumors. Journal of neuro-oncology 50:227-237.

Thedieck K, Holzwarth B, Prentzell MT, Boehlke C, Klasener K, Ruf S, Sonntag AG, Maerz L, Grellscheid SN, Kremmer E, Nitschke R, Kuehn EW, Jonker JW, Groen AK, Reth M, Hall MN, Baumeister R (2013) Inhibition of mTORC1 by astrin and stress granules prevents apoptosis in cancer cells. Cell 154:859-874.

Tian Q, Streuli M, Saito H, Schlossman SF, Anderson P (1991) A polyadenylate binding protein localized to the granules of cytolytic lymphocytes induces DNA fragmentation in target cells. Cell 67:629-639.

Tipping M, Eickhoff J, Ian Robins H (2017) Clinical outcomes in recurrent glioblastoma with bevacizumab therapy: An analysis of the literature. Journal of clinical neuroscience : official journal of the Neurosurgical Society of Australasia.

Torsvik A, Stieber D, Enger PO, Golebiewska A, Molven A, Svendsen A, Westermark B, Niclou SP, Olsen TK, Chekenya Enger M, Bjerkvig R (2014) U-251 revisited: genetic drift and phenotypic consequences of long-term cultures of glioblastoma cells. Cancer medicine 3:812-824.

Tourriere H, Chebli K, Zekri L, Courselaud B, Blanchard JM, Bertrand E, Tazi J (2003) The RasGAP-associated endoribonuclease G3BP assembles stress granules. The Journal of cell biology 160:823-831.

Turakhiya A, Meyer SR, Marincola G, Bohm S, Vanselow JT, Schlosser A, Hofmann K, Buchberger A (2018) ZFAND1 Recruits p97 and the 26S Proteasome to Promote the Clearance of Arsenite-Induced Stress Granules. Molecular cell 70:906-919.e907.

van den Bent MJ, Brandes AA, Rampling R, Kouwenhoven MC, Kros JM, Carpentier AF, Clement PM, Frenay M, Campone M, Baurain JF, Armand JP, Taphoorn MJ, Tosoni A, Kletzl H, Klughammer B, Lacombe D, Gorlia T (2009) Randomized phase II trial of erlotinib versus temozolomide or carmustine in recurrent glioblastoma: EORTC brain tumor group study 26034. Journal of clinical oncology : official journal of the American Society of Clinical Oncology 27:1268-1274.

Vandenabeele P, Vanden Berghe T, Festjens N (2006) Caspase inhibitors promote alternative cell death pathways. Science's STKE : signal transduction knowledge environment 2006:pe44.

Varbanov HP, Kuttler F, Banfi D, Turcatti G, Dyson PJ (2017) Repositioning approved drugs for the treatment of problematic cancers using a screening approach. PloS one 12:e0171052.

Venere M, Hamerlik P, Wu Q, Rasmussen RD, Song LA, Vasanji A, Tenley N, Flavahan WA, Hjelmeland AB, Bartek J, Rich JN (2014) Therapeutic targeting of constitutive PARP activation compromises stem cell phenotype and survival of glioblastoma-initiating cells. Cell death and differentiation 21:258-269.

Venugopal J, Blanco G (2017) On the Many Actions of Ouabain: Pro-Cystogenic Effects in Autosomal Dominant Polycystic Kidney Disease. Molecules (Basel, Switzerland) 22.

Vilas-Boas Fde A, da Silva AM, de Sousa LP, Lima KM, Vago JP, Bittencourt LF, Dantas AE, Gomes DA, Vilela MC, Teixeira MM, Barcelos LS (2016) Impairment of stress granule assembly via inhibition of the eIF2alpha phosphorylation sensitizes glioma cells to chemotherapeutic agents. Journal of neuro-oncology 127:253-260.

Wang J, Wakeman TP, Lathia JD, Hjelmeland AB, Wang XF, White RR, Rich JN, Sullenger BA (2010) Notch promotes radioresistance of glioma stem cells. Stem cells (Dayton, Ohio) 28:17-28.

Wang P, Lan C, Xiong S, Zhao X, Shan Y, Hu R, Wan W, Yu S, Liao B, Li G, Wang J, Zou D, Chen B, Feng H, Wu N (2017) HIF1alpha regulates single differentiated glioma cell dedifferentiation to stem-like cell phenotypes with high tumorigenic potential under hypoxia. Oncotarget 8:28074-28092.

Wang Z, Sun H, Yakisich JS (2014) Overcoming the blood-brain barrier for chemotherapy: limitations, challenges and rising problems. Anti-cancer agents in medicinal chemistry 14:1085-1093.

Weeks A, Agnihotri S, Lymer J, Chalil A, Diaz R, Isik S, Smith C, Rutka JT (2016) Epithelial Cell Transforming 2 and Aurora Kinase B Modulate Formation of Stress Granule-Containing Transcripts from Diverse Cellular Pathways in Astrocytoma Cells. The American journal of pathology 186:1674-1687.

Wek SA, Zhu S, Wek RC (1995) The histidyl-tRNA synthetase-related sequence in the eIF-2 alpha protein kinase GCN2 interacts with tRNA and is required for activation in response to starvation for different amino acids. Molecular and cellular biology 15:4497-4506.

Weller M et al. (2017) Rindopepimut with temozolomide for patients with newly diagnosed, EGFRvIII-expressing glioblastoma (ACT IV): a randomised, double-blind, international phase 3 trial. The Lancet Oncology 18:1373-1385.

Westphal M, Heese O, Steinbach JP, Schnell O, Schackert G, Mehdorn M, Schulz D, Simon M, Schlegel U, Senft C, Geletneky K, Braun C, Hartung JG, Reuter D, Metz MW, Bach F, Pietsch T (2015) A randomised, open label phase III trial with nimotuzumab, an anti-epidermal growth factor receptor monoclonal antibody in the treatment of newly diagnosed adult glioblastoma. European journal of cancer (Oxford, England : 1990) 51:522-532.

Wippich F, Bodenmiller B, Trajkovska MG, Wanka S, Aebersold R, Pelkmans L (2013) Dual specificity kinase DYRK3 couples stress granule condensation/dissolution to mTORC1 signaling. Cell 152:791-805.

Yang ZD, Yu J, Zhang Q (2013) Effects of raloxifene on cognition, mental health, sleep and sexual function in menopausal women: a systematic review of randomized controlled trials. Maturitas 75:341-348.

Yeomans A, Lemm E, Wilmore S, Cavell BE, Valle-Argos B, Krysov S, Hidalgo MS, Leonard E, Willis AE, Forconi F, Stevenson FK, Steele AJ, Coldwell MJ, Packham G (2016) PEITC-mediated inhibition of mRNA translation is associated with both inhibition of mTORC1 and increased eIF2alpha phosphorylation in established cell lines and primary human leukemia cells. Oncotarget 7:74807-74819.

Yip KW, Ito E, Mao X, Au PY, Hedley DW, Mocanu JD, Bastianutto C, Schimmer A, Liu FF (2006) Potential use of alexidine dihydrochloride as an apoptosis-promoting anticancer agent. Molecular cancer therapeutics 5:2234-2240.

Zagzag D, Amirnovin R, Greco MA, Yee H, Holash J, Wiegand SJ, Zabski S, Yancopoulos GD, Grumet M (2000) Vascular apoptosis and involution in gliomas precede neovascularization: a novel concept for glioma growth and angiogenesis. Laboratory investigation; a journal of technical methods and pathology 80:837-849.

Zurla C, Lifland AW, Santangelo PJ (2011) Characterizing mRNA interactions with RNA granules during translation initiation inhibition. PloS one 6:e19727.

Zustovich F, Landi L, Lombardi G, Porta C, Galli L, Fontana A, Amoroso D, Galli C, Andreuccetti M, Falcone A, Zagonel V (2013) Sorafenib plus daily low-dose temozolomide for relapsed glioblastoma: a phase II study. Anticancer research 33:3487-3494.

APPENDIX 1

Table A1.1. Top 100 screened drugs inhibiting SG dissolution.

Drug	Drug Class	Z Score
Chelidonine (+)	Monoamine Metabolism	47.59765484
Scoulerine	Monoamine Metabolism	40.01073732
Piperlongumine	Oxidative Stress	19.40302893
Lobeline alpha (-) hydrochoride	Monoamine Metabolism	17.04493294
Benzethonium chloride	Antimicrobial	10.62192853
Metergoline	Monoamine Metabolism	10.4904695
Nortriptyline hydrochloride	Monoamine Metabolism	10.42626503
Lobelanidine hydrochloride	Monoamine Metabolism	10.38074863
Benzamil hydrochloride	Electrolyte Homeostasis	9.980604543
Desipramine hydrochloride	Monoamine Metabolism	8.927833286
Eburnamonine (-)	Misc	8.637808122
Bepridil hydrochloride	Electrolyte Homeostasis	7.704900593
Berberine chloride	Misc	6.894867611
Dimethisoquin hydrochloride	Misc	6.689815786
Ifenprodil tartrate	Monoamine Metabolism	6.611121205
Promazine hydrochloride	Monoamine Metabolism	6.576654152
Methoxy-6-harmalan	Monoamine Metabolism	6.382238049
Hydrastine hydrochloride	Monoamine Metabolism	6.177186224
Homochlorcyclizine dihydrochloride	Monoamine Metabolism	6.026542715
Methyl benzethonium chloride	Antimicrobial	5.935330165
Thiethylperazine malate	Monoamine Metabolism	5.734660553
Clemastine fumarate	Monoamine Metabolism	5.565033382
Clomiphene citrate (Z,E)	Estrogen Receptor Modification	5.394916618
Dobutamine hydrochloride	Monoamine Metabolism	5.191094503
Methotrimeprazine maleat salt	Monoamine Metabolism	5.093076953
Raloxifene hydrochloride	Estrogen Receptor Modification	4.894554443
Lidoflazine	Electrolyte Homeostasis	4.885361329
Nicardipine hydrochloride	Electrolyte Homeostasis	4.817420624
Parbendazole	Antimicrobial	4.733216072
Trimipramine maleate salt	Monoamine Metabolism	4.651681997
Chlorprothixene hydrochloride	Monoamine Metabolism	4.613598509
Methiothepin maleate	Monoamine Metabolism	4.579628156
Protriptyline hydrochloride	Monoamine Metabolism	4.544257097
Thonzonium bromide	Misc	4.479818592
Doxepin hydrochloride	Monoamine Metabolism	4.365109114
Cloperastine hydrochloride	Monoamine Metabolism	4.295466207
Trifluoperazine dihydrochloride	Monoamine Metabolism	4.242039959
Pimethixene maleate	Monoamine Metabolism	4.180505381

Lanatoside C	Electrolyte Homeostasis	4.159356048
Oxyphenbutazone	Misc	4.132349383
Loracarbef	Antimicrobial	4.132349383
(S)-propranolol hydrochloride	Monoamine Metabolism	4.043332095
Maprotiline hydrochloride	Monoamine Metabolism	3.96816181
Albendazole	Antimicrobial	3.965134358
Imipramine hydrochloride	Monoamine Metabolism	3.913427966
GBR 12909 dihydrochloride	Monoamine Metabolism	3.798310047
Securinine	Monoamine Metabolism	3.734163865
Fluphenazine dihydrochloride	Monoamine Metabolism	3.657461469
Thioridazine hydrochloride	Monoamine Metabolism	3.620900314
Penbutolol sulfate	Monoamine Metabolism	3.531482693
Tetrandrine	Electrolyte Homeostasis	3.468699447
Dubinidine	Misc	3.464719728
Doxorubicin hydrochloride	DNA Damage	3.463026667
Palmatine chloride	Monoamine Metabolism	3.408986588
Netilmicin sulfate	Antimicrobial	3.353448119
Parthenolide	Misc	3.310854505
Acetopromazine maleate salt	Monoamine Metabolism	3.306460676
Trimeprazine tartrate	Monoamine Metabolism	3.2754048
Piperacetazine	Misc	3.264430832
Oxybutynin chloride	Anticholinergic	3.257486713
Paroxetine Hydrochloride	Monoamine Metabolism	3.248418972
Xylazine	Monoamine Metabolism	3.203934763
Econazole nitrate	Antimicrobial	3.195952136
Pimozide	Monoamine Metabolism	3.165184847
Spaglumic acid	Monoamine Metabolism	3.153159223
Perhexiline maleate	Misc	3.103650269
Guanabenz acetate	Monoamine Metabolism	3.049616826
Convolamine hydrochloride	Misc	2.998882938
Mecamylamine hydrochloride	Anticholinergic	2.99737897
(R)-Propranolol hydrochloride	Monoamine Metabolism	2.975124648
Diphenylpyraline hydrochloride	Anticholinergic	2.926040689
(-)-Quinpirole hydrochloride	Monoamine Metabolism	2.841598717
Corynanthine hydrochloride	Monoamine Metabolism	2.793831114
Quipazine dimaleate salt	Monoamine Metabolism	2.793831114
Monobenzone	Misc	2.761458449
Methapyrilene hydrochloride	Monoamine Metabolism	2.745229117
Hycanthone	Antimicrobial	2.711258765
Viomycin sulfate	Antimicrobial	2.708072786
Hydroquinine hydrobromide hydrate	Antimicrobial	2.691305201

Oxprenolol hydrochloride	Misc	2.685818464
Primaquine diphosphate	Antimicrobial	2.674719669
Fluspirilen	Monoamine Metabolism	2.632581438
Ethopropazine hydrochloride	Monoamine Metabolism	2.627744942
Dihydroergocristine mesylate	Monoamine Metabolism	2.588779289
Bromocryptine mesylate	Monoamine Metabolism	2.587276027
Midecamycin	Antimicrobial	2.564722817
6-Furfurylaminopurine	Misc	2.531379774
Clorgyline hydrochloride	Monoamine Metabolism	2.439495944
Disulfiram	Misc	2.418126954
Haloperidol	Monoamine Metabolism	2.406850349
Fendiline hydrochloride	Electrolyte Homeostasis	2.365235335
Sanguinarine	Oxidative Stress	2.349227947
Hydroxyzine dihydrochloride	Monoamine Metabolism	2.33919072
Proadifen hydrochloride	Misc	2.334673122
Procarbazine hydrochloride	DNA Damage	2.307494993
Chlorpheniramine maleate	Monoamine Metabolism	2.294084301
Seneciphylline	DNA Damage	2.281201552
Fenspiride hydrochloride	Monoamine Metabolism	2.236538424
Perphenazine	Monoamine Metabolism	2.215148067

Table A1.2. Screened drugs inhibiting SG formation.

Drug	Drug Class	Z Score
Alexidine dihydrochloride	PTPMT1 Inhibitor	6.6504
Strophanthidin	Cardiac Glycoside	5.4003
Clorsulon	Antimicrobial	5.045
Cycloheximide	Antimicrobial	5.0036
Quinethazone	Diuretic	4.6748
Proscillaridin A	Cardiac Glycoside	4.6146
Dorzolamide hydrochloride	Carbonic Anhydrase Inhibitor	4.5885
Digoxigenin	Cardiac Glycoside	4.5198
Iobenguane sulfate	Radiolabel	4.5102
Helveticoside	Steroid Glycoside	4.4479
Ethamivan	Respiratory Stimulant	4.2763
Trolox	Vitamin	4.1927
Emetine dihydrochloride	Antimicrobial	4.0495
Mitoxantrone dihydrochloride	Topoisomerase Inhibitor	3.7479
Butirosin disulfate salt	Antimicrobial	3.686
Tetrandrine	Electrolyte Homeostasis	3.5981
Niclosamide	Antimicrobial	3.4336
Avermectin B1	Antimicrobial	3.349
Ebselen	Antioxidant	3.3231
Dichlorphenamide	Carbonic Anhydrase Inhibitor	3.2699
Oxaprozin	NSAID	3.1862
Deoxycorticosterone	Corticosteroid	3.1743
Lanatoside C	Electrolyte Homeostasis	3.0706
Benzthiazide	Electrolyte Homeostasis	3.0697
Anisomycin	Antimicrobial	3.0262
Cephaeline dihydrochloride heptahydrate	Antimicrobial	3.0131
Cisapride	Monoamine Metabolism	3.0066
Piribedil hydrochloride	Monoamine Metabolism	3.0021
Flurandrenolide	Corticosteroid	2.9973
Paclitaxel	Microtubule Stabilizer	2.9053
Tocopherol (R,S)	Vitamin	2.882
Cyclizine hydrochloride	Monoamine Metabolism	2.8724
Cyclopenthiazide	Electrolyte Homeostasis	2.8699
Methazolamide	Carbonic Anhydrase Inhibitor	2.8695
Nizatidine	Antihistamine	2.838
Esculetin	Antioxidant	2.838
Sulfasalazine	Anti-inflammatory	2.8056
Amphotericin B	Antimicrobial	2.764
Calciferol	Vitamin	2.6919

Camptothecine (S,+)	Topoisomerase Inhibitor	2.6885
Aminocaproic acid	Amino Acid Derivative	2.661
Sertraline	Monoamine Metabolism	2.6584
Fluorocurarine chloride	Sympatholytic	2.6164
(+)-Isoproterenol (+)-bitartrate salt	Alpha Agonist	2.5902
(-)-Isoproterenol hydrochloride	Alpha Agonist	2.5606
Trichlormethiazide	Electrolyte Homeostasis	2.5405
Flumequine	Antimicrobial	2.5341
Betonicine	Plant Osmotic Solute	2.5284
Indapamide	Diuretic	2.4912
Methyl benzethonium chloride	Antimicrobial	2.4845
Mafenide hydrochloride	Antimicrobial	2.4654
Syrosingopine	Monoamine Metabolism	2.4362
Proxyphylline	Phosphodiesterase Inhibitor	2.4308
Ceftazidime pentahydrate	Antimicrobial	2.4212
Trimethylcolchicinic acid	Microtubule Inhibitor	2.4154
Vitamin K2	Vitamin	2.3664
Amrinone	Phosphodiesterase Inhibitor	2.3644
Metolazone	Electrolyte Homeostasis	2.3594
alpha-Santonin	Antimicrobial	2.3017
Memantine Hydrochloride	Monoamine Metabolism	2.3015
2-Aminobenzenesulfonamide	Carbonic Anhydrase Inhibitor	2.2715
Prenylamine lactate	Electrolyte Homeostasis	2.2708
Strophantine octahydrate	Cardiac Glycoside	2.2002
Digitoxigenin	Cardiac Glycoside	2.1937
Cefoxitin sodium salt	Antimicrobial	2.1829
Phenelzine sulfate	Monoamine Metabolism	2.1824
Kaempferol	Antioxidant	2.1722
Betulin	Impaired Cholesterol Synthesis	2.1561
Biotin	Vitamin	2.1478
Parthenolide	Microtubule Inhibitor	2.1371
Methylatropine nitrate	Anticholinergic	2.1299
Aminophylline	Phosphodiesterase Inhibitor	2.1257
Letrozole	Aromatase Inhibitor	2.1165
Bucladesine sodium salt	Phosphodiesterase Inhibitor	2.1114
Sanguinarine	Oxidative Stress	2.1033
Torsemide	Electrolyte Homeostasis	2.09
Cefmetazole sodium salt	Antimicrobial	2.0889
Gentamicine sulfate	Antimicrobial	2.0715
Hecogenin	Electrolyte Homeostasis	2.0711
Brinzolamide	Carbonic Anhydrase Inhibitor	2.0684

Methiothepin maleate	Monoamine Metabolism	2.0684
Methotrimeprazine maleat salt	Monoamine Metabolism	2.0373
Metoprolol-(+,-) (+)-tartrate salt	Beta Blocker	2.0034
Muramic acid, N-acetyl	Peptidoglycan	1.997
Spiperone	Monoamine Metabolism	1.9879
Flutamide	Anti-androgen	1.9851
Luteolin	Vitamin	1.9827
Amoxapine	Monoamine Metabolism	1.9822
Ciprofloxacin hydrochloride	Antimicrobial	1.9822
Clopamide	Electrolyte Homeostasis	1.9664
Colchicine	Microtubule Inhibitor	1.9586
Pindolol	Beta Blocker	1.9425
Napelline	Electrolyte Homeostasis	1.9423
Tolbutamide	Electrolyte Homeostasis	1.9422
Fendiline hydrochloride	Electrolyte Homeostasis	1.942
Tobramycin	Antimicrobial	1.9365
Nisoxetine hydrochloride	Monoamine Metabolism	1.9351
(±)-Nipecotic acid	Monoamine Metabolism	1.9174